Development and application of a non-point sources pollution model for hydrological processes and nutrient loadings in the Xitiaoxi catchment in South China

Dissertation

Zur Erlangung des Doktorgrades
der Mathematisch-Naturwissenschaftlichen Fakultät
der Christian-Albrechts-Universität zu Kiel
vorgelegt von

MSc. Guangju Zhao

Institute of the Conservation of Natural Resources, Department of Hydrology and Water Resources Management
Kiel University, Kiel, Germany

2011

Referentin: Prof. Dr. Nicola Fohrer

Koreferentin: Prof. Dr. Natascha Oppelt

Tag der mündlichen Prüfung: 8. February 2011

Zum Druck genehmigt: Kiel, 9. February 2011

gez. Prof. Dr. Lutz Kipp. Dekan

Summary

This dissertation describes the hydrology and non-point source pollution of the humid, subtropical Xitiaoxi catchment in the south-eastern China and comprises a hydrologic and nutrient dynamics simulation there. The study presents at first an interpretation of hydrological processes influenced by anthropological activities. Beyond that, it deals with nutrient cycles in both arable land with an intensive farming system and a natural forest dominated catchment.

The study catchment of the Xitiaoxi River is located upstream in the Taihu Basin in south-eastern China. The river is one of the major tributaries flowing into the Taihu Lake, contributing 27.7% of the water volume each year. Since it is influenced by sub-tropical summer monsoons with high rainfall, a large number of hydraulic structures (e.g. reservoirs and polders) have been constructed for flood control and water resources management. About 30% of the catchment is covered by arable land, which is cultivated by an intensive multi-cropping system with crop rotations of alluvial lowland summer rice and upland winter rapeseed or wheat. The major environmental problems consist of nutrient losses from agricultural land and urban sewage resulting in serious water pollution and complex hydrological processes influenced by human activities.

To better understand the hydrological processes in such a catchment, a raster-based distributed hydrological model based on the Xinanjiang model concept was developed for catchment runoff simulation in which flood polder regulation was integrated. The overland flow and channel flow are calculated by the kinematic wave equation. A simple bucket method is used for estimating outflow from polders. The model was applied to the Xitiaoxi catchment. To estimate the nutrient dynamics and identify the spatial and temporal characteristics of nutrient loads (nitrogen and phosphorus) on the catchment scale, the Xinanjiang-Nitrogen-Phosphorus (XAJ-NP) model was developed and implemented. The conceptual nutrient mobilization and transport model combines the Xinanjiang rainfall-runoff model, the **I**ntegrated **N**itrogen **CA**tchment (INCA) model and the **M**odified **U**niversal **S**oil **L**oss **E**quation (MUSLE). The model is implemented in the dynamic environmental modelling language PCRaster and calculates the water fluxes and nutrient loadings on a cell-by-cell basis on a daily time step. The nitrogen module includes the nitrogen cycle processes mineralization, leaching, fixation, volatilization, nitrification, denitrification and plant uptake. The phosphorus module simulates both dissolved phosphorus using the INCA model and particulate phosphorus with the soil erosion model. It is assumed that nutrient is mobilized by surface runoff and groundwater.

The hydrological model shows satisfactory results compared to observed values. The high values of the Nash-Sutcliffe index and correlation coefficients for both calibration and validation periods imply that the model is reliable. The polder operation simulation indicates that the polders can reduce the flood peaks. This process routine can slightly increase the accuracy of the discharge simulation. The nutrient simulation demonstrates that the model is capable of reproducing both the magnitude and the dynamics of the nutrient loads. As for nitrogen modelling, fertilization and atmospheric deposition are the main input components with input rates of 425-635 kg N ha^{-1} yr^{-1}, 22-25.8 kg N ha^{-1} yr^{-1}, respectively, while the N output mainly includes plant uptake, ammonium volatilization and leaching through runoff. The phosphorus simulation shows that an average of 127.4 t yr^{-1} of P is exported to the rivers and streams in the catchment. Spatial distribution of P loads indicates that the non-point source load from arable land has a dominant contribution with an export rate of 1.63 to 4.92 kg ha^{-1} yr^{-1}. P budget analysis indicates that average P input and output are 71.3 kg ha^{-1} yr^{-1} and 46.2 kg ha^{-1} yr^{-1} respectively. The total P utilization efficiency is 59.3%, leading to an average P surplus of 25.1 kg ha^{-1} yr^{-1} in the arable land of the Xitiaoxi catchment. In addition, the nutrient simulation also shows that point source pollution leads to large errors in the modelling results.

Zusammenfassung

Diese Doktorarbeit beschreibt die Hydrologie und diffuse Stoffeinträge im feuchten, subtropischen Einzugsgebiet des Xitiaoxi im Südosten Chinas und beinhaltet eine hydrologische- und nährstoffdynamische Modellierung. In der Arbeit werden zunächst hydrologische Prozesse abgebildet, die von anthropologischen Aktivitäten beeinflusst werden. Darüber hinaus werden Nährstoffkreisläufe von sowohl intensiv landwirtschaftlich genutzten Systemen als auch von einem natürlichen Waldeinzugsgebiet behandelt.

Das Forschungsgebiet des Xitiaoxi liegt im oberstromigen Teil des Taihu Einzugsgebietes im Südosten Chinas. Der Fluss führt dem Taihu Lake 27.7% des jährlichen Wasservolumens zu und ist damit einer seiner Hauptzuflüsse. Aufgrund des Einflusses des subtropischen Sommermonsuns mit seinen hohen Niederschlägen wurden für den Hochwasserschutz und die Wasserwirtschaft eine Vielzahl von wasserbaulichen Konstruktionen (z.B. Dämme und Polder) errichtet. Ungefähr 30% des Einzugsgebietes sind landwirtschaftliche Flächen, die in einem intensiven Mehrfacherntesystem mit Sommerreis in Auen, Winterraps im Hochland und Weizen Fruchtfolgen bewirtschaftet werden. Die größten Umweltprobleme sind die Wasserverschmutzung durch Nährstoffauswaschungen von landwirtschaftlichen Flächen und die von menschlichen Aktivitäten veränderten, komplexen hydrologischen Prozesse.

Um die hydrologischen Prozesse in solch einem Einzugsgebiet besser zu verstehen, wurde für die Abflussmodellierung ein rasterbasiertes, räumlich verteiltes hydrologisches Modell basierend auf dem Xinanjiang Modellkonzept entwickelt, in das die Regulation durch Hochwasserpolder integriert wurde. Der Oberflächenabfluss und die Gerinneströmung werden durch die kinematische Wellengleichung berechnet. Für den Abfluss aus Poldern wird eine einfache Einzellinearspeichermethode verwendet. Das Modell wurde im Einzugsgebiet des Xitiaoxi angewendet. Das Xinanjiang-Stickstoff-Phosphor (XAJ-NP) – Modell wurde entwickelt, um die Nährstoffdynamik abzuschätzen und die räumlichen und zeitlichen Charakteristika der Nährstofffrachten (Stickstoff und Phosphor) auf Einzugsgebietsebene zu identifizieren. Das konzeptionelle Nährstoffmobilisations- und Transportmodell kombiniert das Xinanjiang Niederschlags-Abflussmodell, das Integrierte Stickstoff Einzugsgebietsmodell (INCA) und die angepasste, allgemeine Bodenabtragsgleichung (MUSLE). Das Modell ist in der dynamischen, ökologischen Modellierungssprache PCRaster umgesetzt und berechnet die Wasserströme und Nährstofffrachten für jede Rasterzelle mit einem täglichen Zeitschritt. Das Stickstoffmodul berücksichtigt die Stickstoffkreislaufprozesse Mineralisation, Auswaschung, Fixierung, Ammonifikation, Nitrifikation, Denitrifikation und Pflanzenaufnahme. Das

Phosphormodul simuliert gelösten Phosphor mit dem INCA-Modellansatz und partikulär gebundenen Phosphor mit dem Bodenerosionsmodell. Es wird angenommen, dass die Nährstoffe durch Oberflächen- und Grundwasserabfluss mobilisiert werden.

Beim Vergleich mit gemessenen Werten erreicht das hydrologische Modell zufriedenstellende Ergebnisse. Hohe Werte für die Nash-Sutcliffe Indizes und die Korrelationskoeffizienten sowohl für den Kalibrierungs- als auch den Validierungszeitraum implizieren, dass das Modell zuverlässig ist. Die Simulation der Poldersteuerung zeigt, dass die Polder Hochwasserspitzen reduzieren können. Dieser Prozessroutine kann die Genauigkeit der Abflusssimulation leicht erhöhen. Die Nährstoffsimulation zeigt, dass das Modell sowohl die Größenordnung als auch die Dynamik der Nährstofffrachten reproduzieren kann. In der Stickstoffmodellierung sind die Düngung mit 425-635 kg N ha^{-1} a^{-1} und die atmosphärische Deposition mit 22-25.8 kg N ha^{-1} a^{-1} die Haupteintragskomponenten, während der Stickstoffaustrag hauptsächlich durch Pflanzenaufnahme, Ammonifikation und Auswaschung durch Abfluss geschieht. Die Phosphorsimulation legt dar, dass im Mittel eine Phosphormenge von 17.4 t a^{-1} zu den Bächen und Flüssen im Einzugsgebiet transportiert wird. Die räumliche Verteilung der Phosphorfrachten weist darauf hin, dass eine Fracht von 1.63 bis 4.92 kg ha^{-1} a^{-1} aus diffusen Quellen der landwirtschaftlichen Flächen stammt und dies einen dominierenden Anteil ausmacht. Die Analyse des Phosphorhaushaltes zeigt, dass der mittlere P Eintrag 71.3 kg ha^{-1} a^{-1} und der Austrag 46.2 kg ha^{-1} a^{-1} beträgt. Die gesamte P Nutzungseffizienz beträgt 59.3%, was zu einem mittleren P Überschuss von 25.1 kg ha^{-1} a^{-1} auf den landwirtschaftlichen Flächen des Xitiaoxi Einzugsgebietes führt. Darüber hinaus zeigt die Nährstoffsimulation, dass die Verschmutzung aus Punktquellen zu großen Fehlern in den Simulationsergebnissen führt.

Table of Contents

List of Figures

List of Tables

Chapter I Introduction

Water quantity and quality have become an increasing concern in many regions of China and other parts of the world. Agricultural non-point source pollution has been identified as the major contributor of water pollution (Canale and Effler, 1989; Edwards and Withers, 2008). Agricultural pollutants such as sediment, fertilizers, pesticides, salts and trace elements resulting from various activities cause the degradation of surface and ground water resources through soil erosion, chemical runoff and leaching (Donoso et al., 1999; Zalidis et al., 2002; Thorburn et al., 2003). Nutrient from diffuse non-point source pollution e.g. farmland fertilizer discharged into aquatic systems contribute main pollutants to surface water in a catchment, thereby causing serious ecological problems such as eutrophication, toxic algal blooms, oxygen depletion and loss of biodiversity. In addition, nutrient enrichment seriously degrades aquatic ecosystems and decreases the quality of water used for drinking, industry, agriculture, recreation, and other purposes (Potter et al., 2004; Farenga and Daniel, 2007, Ding et al., 2010).

Taihu Basin is one of the most developed regions in China with high population density, urbanization and economic development. The area covers only 0.4% of territory of China while contributing about 11% of Gross National Product (GNP) and more than 14% of China's gross domestic production (Qin et al., 2007). Since the 1980s, rapid development of local economy and increased population and urbanization has resulted in pollutants being produced and discharged into rivers and lakes. In recent years, frequent algal blooming has attracted much attention since it seriously affects the lake as a supply of drinking water. In the late May of 2007, Taihu Lake was overtaken by a major algae bloom, leaving approximately two million people without drinking water for at least one week (Qin et al., 2007).

Thus, due to the serious environmental problems mentioned above, the impacts of agricultural activities and water quality issues are investigated at the catchment scale. Consequently, there is an urgent need to improve the water quality condition and reduce pollutants discharged into surface water. Compared with point source pollution, the non-point source pollution is strongly associated with hydro-chemical processes, and thus hydrological models are commonly used to estimate the nutrient loadings, quantify the effects of agricultural activities on water quality and quantity. A variety of models have been developed to simulate hydrological processes, nutrient transport through surface runoff, interflow, and groundwater flow, as well as further in-stream nutrient transportation and mobilization on different scales. Examples include ANSWERS (Beasley et al., 1980), SWRRB (Williams et al., 1985), SWAT (Arnold et al., 1993), HSPF (Bicknell et al., 2001), AGNPS (Young et al., 1989), INCA (Whitehead et al., 1998a; 1998b)

and LASCAM (Viney et al., 2000) etc. These models are capable of simulating the nutrient cycles and providing accurate results; however, the values of a large number of parameters cannot be obtained from field data and must instead be determined through model calibration. A key constraint to model development and verification is that water quality, hydrological and ecological information is seldom collected simultaneously for sustained periods of time. Thus, the modeler must get along with data that have been routinely collected for regulatory or monitoring purposes. It is then necessary to develop a model with simpler structure and less data requirements and to calibrate the model with different methods (Breuer et al., 2008).

1.1 Statement of the problems

Water eutrophication is the major environmental problem of Taihu Lake (Figure 1.1a), and is mainly caused by nutrient losses from agricultural non-point sources in the catchment. According to the statistical data from the Management Bureau of Taihu Basin, Ministry of Water Resources, nitrogen pollution from the agricultural non-point sources accounted for 77% of the total nitrogen drained into Taihu Lake, and phosphorous pollution from the agricultural non-point sources accounted for 66% of the total amount (Wang et al., 2004b).

Figure 1.1: Environmental problems in the Taihu Basin (a) algae bloom in the Taihu Lake, (b) dominated arable land, (c) Instream water quality downstream of the Xitiaoxi River (d) an

example of polder in the Xitiaoxi catchment

The excessive fertilizer application in the arable lands resulted in large amount of nutrient accumulated in the soil and washed off by surface runoff or leached to groundwater (Figure 1.1b). The average nitrogen fertilizer appliation is 502 kg ha^{-1} in the north of Taihu Basin (located in Jiangsu Province), and 1125 kg ha^{-1} in the southern Taihu Basin (located in Zhejiang Province) (Wang et al., 2004b), much higher than the mean application rate (310 kg ha^{-1}) in China and the world average amount (120 kg ha^{-1}) in 2000 (Ju et al., 2004). Previous study indicates that the alternating water regime leads to high nitrogen transformation losses and low N uptake efficiencies by crops of 28-41% (Zhu and Wen, 1992). High annual N surpluses in the cropping system of 217-335 kg N ha^{-1} are leading to large-scale non-point source agricultural pollution of water bodies (Ma, 1992). The current level of nitrogen fertilization is far beyond the proper level and reduction of nitrogen fertilizer would be beneficial.

The point source pollution is still one important factor deteriorating the water bodies. Since the Taihu Basin is one of the most developed regions in China, high density of population and industry produces large amount of pollutants which are discharged into rivers and lakes (Figure 1.1c). In recent years, the government has paid more attention to the control of point source pollution. Regulations on point sources pollution control have been issued and measurements have been implemented continuously in the Taihu Basin. A large number of wastewater treatment plants have been constructed and commenced operation (Wang et al., 2004b). However, point sources pollution is still out of control in the small towns and villages in the Taihu Basin.

In addition, considerable hydraulic projects and other anthropogenic activities affect the natural river flow and aquatic ecosystems (Hu and Wang, 2009). Construction of hydraulic structures in the Taihu Basin dates backward to nearly a thousand years. Especially since 1960, a large number of hydraulic projects (e.g. reservoirs, dams and polders) are constructed for agricultural irrigation, floods control and power generation (Figure 1.1d). Nowadays, a flood drainage system has been established in the Taihu Basin which could drain floods northward to the Yangtze River, eastward to the Huangpu River, and southward to the Hangzhou Bay. Furthermore, Taihu Basin is a combination of smooth and rough topography, with 75% flat plains, 25% hilly and mountainous areas. The well developed drainage networks have uncertained flow directions during different seasons due to the human regulation and complex topography (Gao et al., 2010). Intensive human activities make rivers and channels have imbalanced environmental system which may lose the capability for self-purification and

pollution dilution.

1.2 Study area

The study area Xitiaoxi catchment, covering more than 2200 km^2, is located in the upstream of Taihu Lake in southeastern China (Figure 1.2). The catchment lies in the north part of Zhejiang Province, covering the whole Anji County. The Xitiaoxi River, with its length of 159 km, supplies 27.7% of the water volume of Taihu Lake.

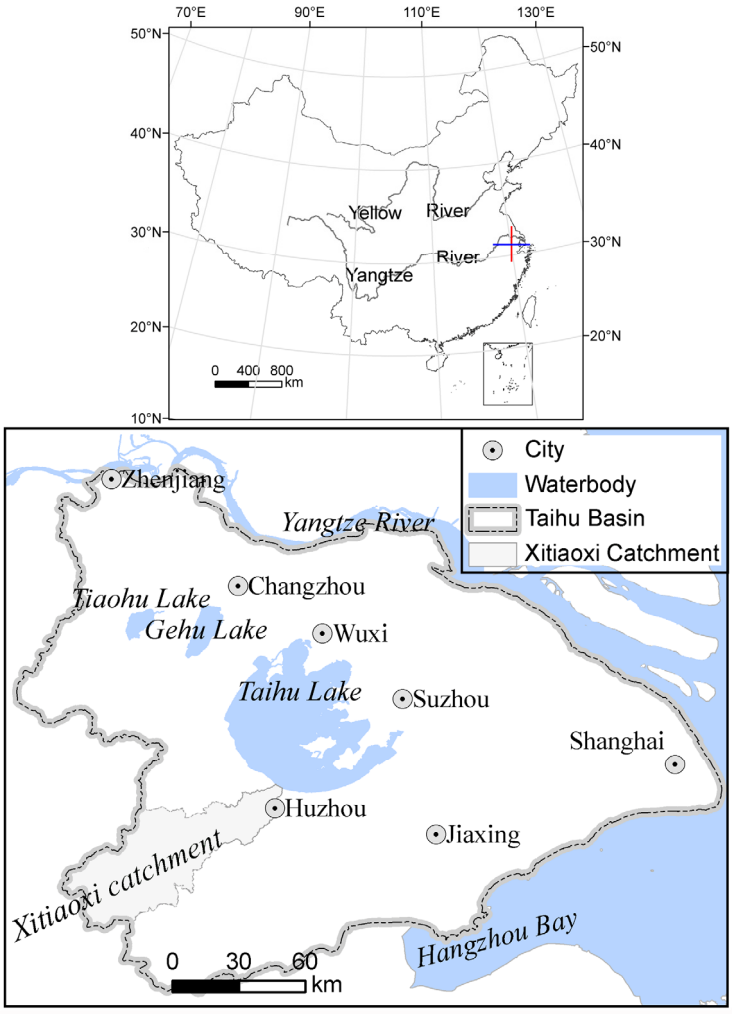

Figure 1.2: Location of the Xitiaoxi catchment (Gao and Lv, 2005)

The Xitiaoxi River, also known as “Western Tiaoxi River”, together with Eastern Tiaoxi River are two of the most important tributaries to Taihu Lake. As shown in Figure 1.3, high mountainous and hilly areas are distributed in the southwest with maximum elevation of 1585m (above mean sea level), whereas low alluvial plains lie in the northeastern parts with a well

developed drainage network. The river originates from the southwestern hilly region at Longwang Mountain, and the riverbed successively widens into a floodplain, where water flows in meandering river channels. In the upper reaches, water flows very fast due to the steep gradient, and the riverbed widens after several branches join into the main stream. During the course of its flow, there are several reservoirs in the upstream controlling the water flow during different seasons. The Xitiaoxi River combines with Eastern Tiaoxi River at Huzhou City, and then streams to the east as the "Tiaoxi River" to the Taihu Lake.

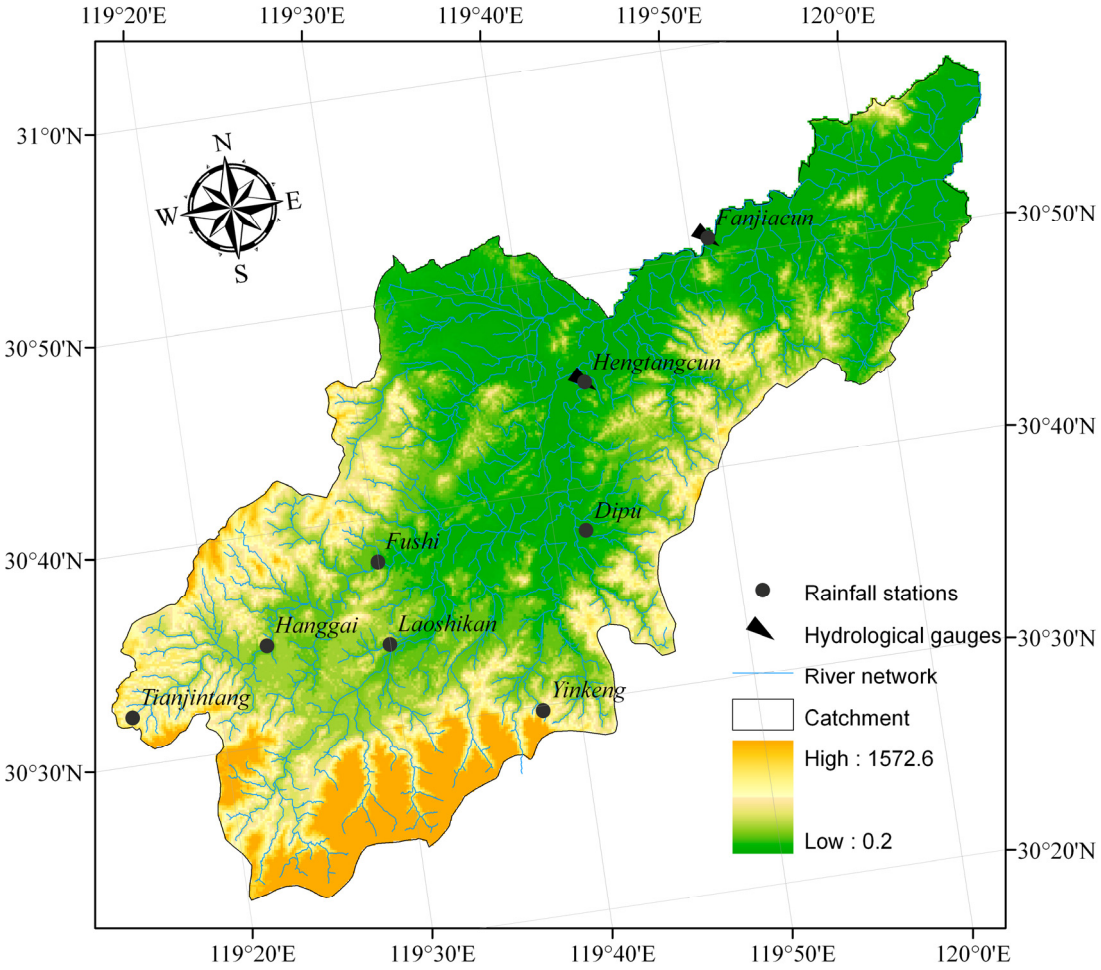

Figure 1.3: DEM and stream network in the Xitiaoxi catchment (Gao and Lv, 2005)

The catchment is characterized by a semitropical climate with mean annual precipitation of about 1385 mm, and most of the rainfall occurs between March and September (Xu et al., 2007). The distribution of river runoff in the Xitiaoxi catchment is mainly controlled by rainfall, which is dominated by the Asian summer monsoon. Figure 1.4 shows the streamflow at Hengtangcun gauge and precipitation at Anji station from 1995 to 2000. It clearly indicates the seasonal

dynamics of discharge and rainfall. However, it should be noted that there are some zero value discharge during the dry season at this station due to the upstream reservoirs operation. Two reservoirs (Fushi and Laoshikan) in the upper reaches of the catchment are used for irrigation, flood control and hydroelectricity generation. The reservoirs are refilled mainly in autumn and winter which lead to low water levels in the downstream part of the catchment. This may result in return flow from Taihu Lake into the river.

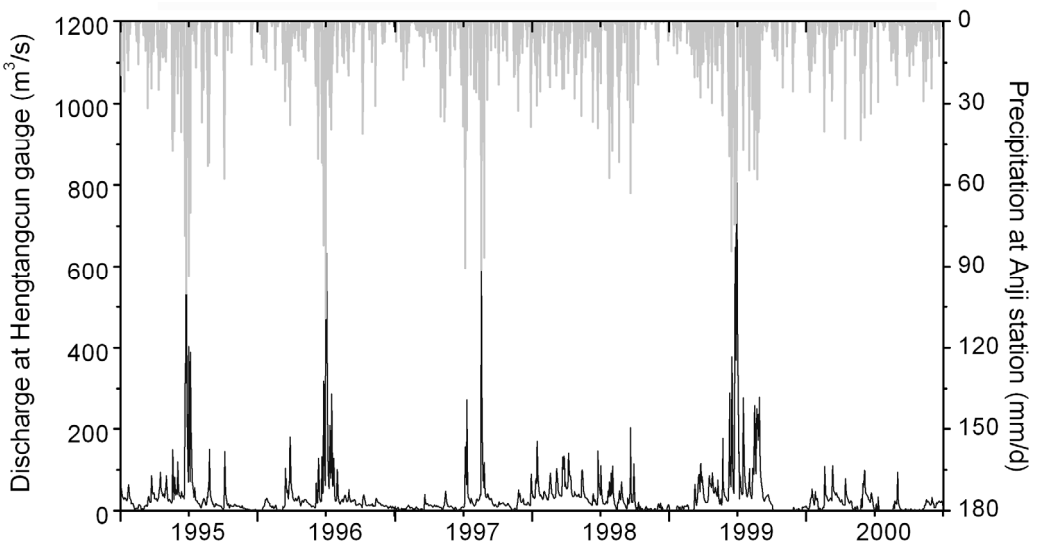

Figure 1.4: Discharge at Hengtangcun gauge and rainfall at Anji station in the Xitiaoxi catchment

Figure 1.5 denotes the satellite image obtained from Landsat 7 Enhanced Thematic Mapper (ETM) sensor (http://glcfapp.umiacs.umd.edu:8080/esdi/index.jsp) acquired on October 11, 2001. A combination of three multispectral bands 7, 4 and 2 is loaded as RGB image. As shown in the figure, a large area of the upstream hilly region is covered by forest accounting for 63.4% of the whole catchment, and about three quarters are planted with bamboo. The villages, urban area and arable lands are distributed in the flat alluvial plain. As for the agricultural land, about 25.6% of the catchment is paddy land, and a portion of about 4.1% of the area is farmland. Other minor land uses classes are residential area of 1.9% and grassland and surface water area of 5% (see Chapter IV, Figure 4.4). Red earth, skeleton soil and paddy soil are the main soil types, contributing about 82.4% of total area (Zhang et al., 2006) (see Chapter IV, Figure 4.4).

The Xitiaoxi catchment has an intensive multi-cropping system with alternating alluvial lowland summer rice - upland winter rapeseed or wheat rotations and integrated livestock breeding, fishery persisting over several centuries (Ellis and Wang, 1997). According to annual

statistics in 2005 (http://www.hustats.gov.cn), the agricultural crops mainly include rice (16,085 ha), rapes (5,268 ha), vegetables (6,034 ha), beans (3,224 ha) and sweet potato (2,006 ha) etc. The agricultural practices are strongly associated with the local climate conditions (i.e. precipitation and temperature). Rice is planted from mid of June, and is harvested in October. Rape is planted from the end of October and harvested between the end of May and the beginning of June in the subsequent year.

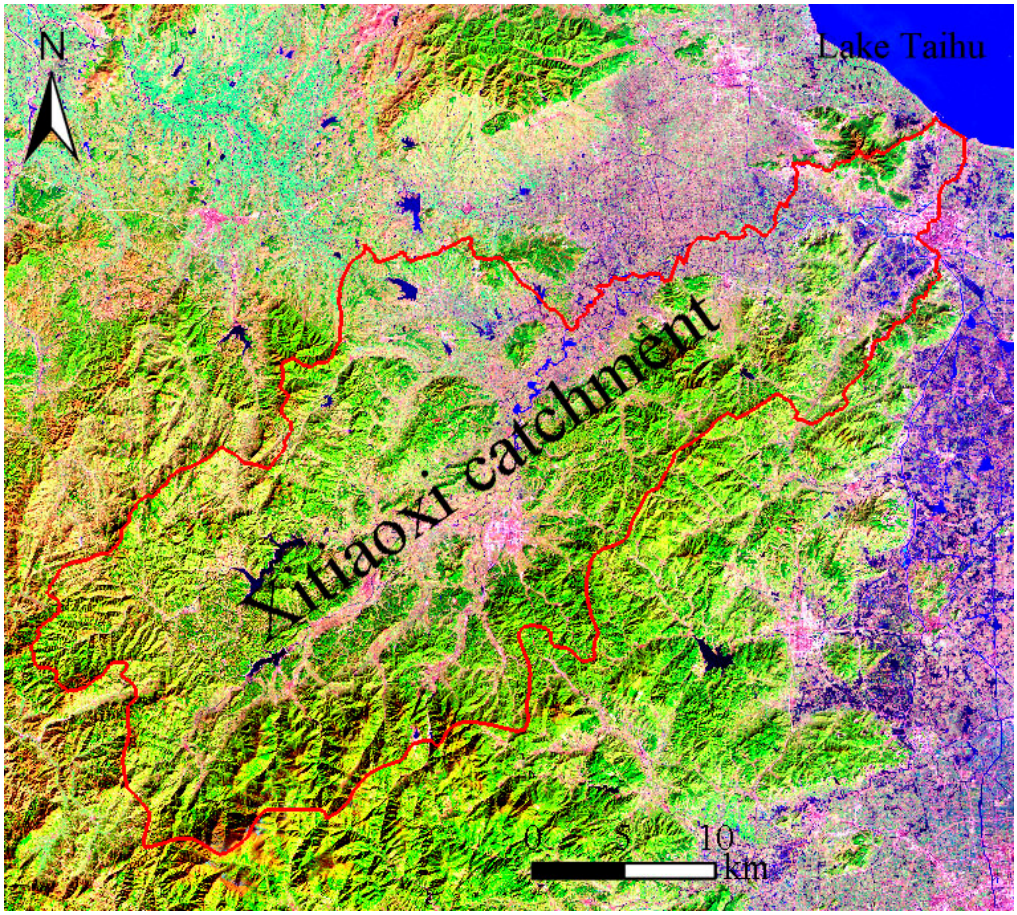

Figure 1.5: Landsat image of the Xitiaoxi catchment (ETM, Oct, 11, 2001)

1.3 Objectives and outline

This research project aims to develop a raster-based Xinanjiang model by using PCRaster, an environmental dynamic modelling language for rainfall-runoff simulation (PCR-XAJ model), and to develop a dynamic nutrient model for prediction of both nitrogen and phosphorus transportation and mobilization (XAJ-NP model) based on the Integrated (INCA) model concept at a catchment scale.

The thesis is cumulatively organized as stand-alone manuscripts that are published or awaiting publication in international peer-reviewed journals. These papers are reproduced here unmodified except for cross-references.

Chapter II focuses on the development and application of a simple raster-based hydrological model for streamflow prediction in a humid catchment with polder systems. The aim of this chapter is to develop a simple distributed rainfall-runoff model: the PCR-XAJ model by using PCRaster to simulate the runoff for the purpose of water resources management and environmental planning. The model employed the mechanism of runoff generation based on the Xinanjiang model (Zhao et al., 1980) for pervious areas. Impervious areas (open water bodies and urban area) are treated separately. In addition, a simple method for flood polder operation based on pumping regulation was employed to analyze the effects of the polder systems on simulated flood peaks (Pressed, Water Resources Mangement).

Chapter III mainly discusses the impact of spatial data resolution on the discharge simulation, describing how the aggregation of the input data (mainly including land use and DEM) influences the hydrological modelling. In order to estimate the impact of the spatial data resolution on simulated catchment discharge, the available data set of 25 m resolution was aggregated using standard GIS functions to create grid based data sets with increasing grid size from 50 m to 1 km. Thereafter, the PCR-XAJ hydrologic model was applied to investigate the impacts of the spatial data aggregation (Pressed, Advances in Geosciences).

Chapter IV presents the development and application of a nitrogen simulation model in a data scarce catchment in south China. The objectives of this chapter are to develop a simple nutrient transport model named Xinanjiang-Nitrogen (XAJ-N) model by integration of hydrology, soil erosion and nitrogen dynamics at the watershed scale and to apply the XAJ-N model for understanding the characteristics of nitrogen cycle in the Xitiaoxi catchment. The XAJ-N model is implemented with the environmental modelling language PCRaster and estimates the water fluxes and nutrient loadings on a cell-by-cell basis in daily time step. The model includes the nitrogen cycling processes of mineralization, leaching, fixation, volatilization, nitrification, denitrification and plant uptake. The model performance was verified by comparing simulated and measured daily discharge and nutrient loadings. Due to the scarce observed data, the simulation results were also validated using an internal mass balance method and values from literature (Pressed, Agricultural Water Mangement).

Chapter V concentrates on the application of a nutrient model for sediment yield and

phosphorus load estimation in a data scarce catchment in south China. In this chapter, the new developed Xinanjiang-Phosphorus (XAJ-P) model simulates several key processes by integration of PCR-XAJ hydrological model and INCA-P model. The model describes the mobilization of suspended solids (SS), particulate phosphorus (PP) and dissolved phosphorus (DP) in the soil store and/or groundwater store, and transportation through different pathways. A case study was undertaken to estimate the nutrient dynamics and identify the spatial and temporal characteristics of phosphorus loading in the Xitiaoxi catchment (Accepted, Journal of Environmental Sciences-China).

Chapter VI consisting of summary and conclusion draws attentions to the achievements of the developed nutrient model applied for non-point source pollution identification in the agricultural catchment, as well as to general conclusions related to the integration of hydrological models with nutrient processes.

Chapter II Application of a simple raster-based hydrological model for streamflow prediction in a humid catchment with polder systems

G.J. Zhao, G. Hörmann, N. Fohrer, J.F. Gao, H.P. Li, P. Tian

Water Resources Management, Volume 25 (2011), Pages 661-676

Submitted, 10.11.09, Accepted, 20.09.10.

Abstract

The hydrological processes are controlled by many factors such as topography, soil, climate and land management practices. These factors have been included in most hydrological models. This study develops a raster-based distributed hydrological model for catchment runoff simulation integrating flood polders regulation. The overland flow and channel flow are calculated by kinematic wave equations. A simple bucket method is used for outflow estimation of polders. The model was applied to Xitiaoxi catchment of Taihu Lake Basin. The accuracy of the model was satisfactory with Nash-Sutcliffe efficiencies of 0.82 during calibration period and 0.85 for validation at Hengtangcun station. The results at Fanjiacun station are slightly worse due to the tidal influence of Taihu Lake with high values of root mean square errors. A model sensitivity analysis has shown that the ratio of potential evapotranspiration to pan evaporation (K), the outflow coefficients of the freewater storage to groundwater (KG) and interflow (KSS) and the areal mean tension water capacity (WM) were the most sensitive parameters. The simulation results indicate that the polder systems could reduce the flood peaks. Additionally, it was confirmed that the proposed polders operation method improved the accuracy of discharge simulation slightly.

Keywords: Distributed hydrological model; The PCRaster-Xinanjiang (PCR-XAJ) model; Polder systems; Daily discharge; Xitiaoxi catchment

2.1 Introduction

In recent decades, numerous distributed hydrological models involving various ranges of complexity were developed for rainfall-runoff simulation. The majority of spatial distributed physically-based models such as KINEROS (Smith et al., 1995), SHE (Abbott et al., 1986), TOPKAPI model (Todini and Ciarapica, 2001; Liu et al., 2005) combining the land use, soil or

topography information, compute water balance at a highly detailed spatial and temporal resolution. Although this type of models is capable of explicit spatial representation of hydrological components and accounting for spatial variability of hydrological process, the application is not without limitations due to their complex structure, a huge number of parameters and large data requirements (Beven, 2001; Du et al., 2007).

On the other hand, the conceptual distributed or semi-distributed hydrological models are less complex and low requirement in terms of the driving data (Uhlenbrook et al., 2004). Examples of such models include TOPMODEL (Beven and Kirby, 1979), HBV model (Bergström, 1976), Xinanjiang model (Zhao et al., 1980) and ARNO model (Todini, 1996). However, due to the lack of direct physical meaning of the parameters, most of the conceptual models are limited in the estimate of sediment erosion and contaminant transport within a watershed as well as prediction of the effects of land-use change or climate-related changes (Ciarapica and Todini, 2002; Du et al., 2007). Recently, much attention has been given to developing and applying conceptual based distributed models which can incorporate the merits of the conceptual rainfall-runoff models and overcome the deficiencies of physically-based models (Robinson and Sivapalan, 1995; Koren et al., 2003; Chen et al., 2007; Yao et al., 2009, Zhang and Werner, 2009).

Advances in remote sensing, geographic information systems and computer technology have made distributed hydrological models attractive for discharge simulation (Wang et al., 2004a; Liu et al., 2005; Du et al., 2007). Recent research indicates that hydrological models loosely or tightly coupled with GIS techniques have become popular (Pullar and Springer, 2000). The SWAT model (Neitsch et al., 2002; Arnold and Fohrer, 2005), integrated within different GIS software, has been widely applied in many cases (Fohrer et al., 2005; Schuol et al., 2008). However, the model is complex, data intensive and time consuming to adjust or modify for regional variations. In contrast, a public domain GIS tool, PCRaster (Van Deursen, 1995; Wesseling et al., 1996) was used to develop a few simple models, e.g. LISEM (De Roo et al., 1996), LISFLOOD model (De Roo et al., 2000) and BEACH (Sheikh et al., 2009) for water resources and environmental management. These models confirm that the GIS tools are powerful and flexible for runoff simulation in a human influenced catchment (Bates and De Roo, 2000; Hessel et al., 2003).

Polders are used to protect flood plains by river dikes, which can reduce the flood peaks and flood risk. To simulate and predict the capping effects of the polder systems during flood events, several hydrodynamic models were applied (Huang et al., 2007; Förster et al., 2008). Most of

these models use the hydrodynamic modeling approach to simulate the flood inundation in the polder caused by dike breach events (Hesselink et al., 2003; Bates et al., 2005). However, only few studies calculated the water balance by using hydrological models including polder systems in the catchment scale. The LISFLOOD model (Van der Knijff and De Roo, 2008) employs a polder routine based on the weir equation of Poleni formula. While this method is useful for outflow estimation in the polder, it may not be appropriate for the polders regulated by pumping stations.

The objective of this study is to develop a simple distributed rainfall-runoff model: the PCR-XAJ model, to simulate the runoff for the purpose of planning and management of environment and water resources over large geographical regions. The model employed the mechanism of runoff generation based on the Xinanjiang model (Zhao et al., 1980) for pervious areas. Impervious areas (open water bodies and urban area) are treated separately. In addition, a simple method for flood polder operation based on pumping regulation was employed to analyze the effects of the polder systems on simulated flood peaks. The model was applied to Xitiaoxi catchment with an area of more than 2200 km^2, a humid region in southeastern China.

2.2 Description of the rainfall-runoff model

The PCR-XAJ model is implemented within PCRaster and conceptually based on the Xinanjiang model. PCRaster is a dynamic modelling system for the construction of iterative spatial-temporal environmental models. It facilitates a clear understanding of model structure and provides a sequence of internal GIS functions for spatial maps computation. Recent research indicates that the Xinanjiang model has been justified for incorporating grid scale resolution of 1 km, which is capable of using more detailed information, such as topography and land cover (Li et al., 2004b; Lu et al., 2008; Yao et al., 2009). Thus, in the present PCR-XAJ model, a grid size of 200×200 m is selected for water balance simulation.

The precipitation and evaporation were the main forcing variables for runoff calculation. The actual evaporation is calculated based on the concept of one layer evaporation method in the Xinanjiang model (Zhao, 1992). The mechanism of runoff generation and separation in the Xinanjiang model was employed in the pervious areas (i.e. paddies, forests and arable land).

2.2.1 Runoff generation

In the PCR-XAJ model, runoff generation on different land surfaces is calculated for each cell

described as below:

Pervious area

The Xinanjiang model is a well-known lumped watershed model and has been widely used for humid regions in China. The model describes watershed heterogeneity using a parabolic curve of field capacity (FC) (Zhao et al., 1980):

$$\frac{f}{F} = 1 - (1 - \frac{\mathrm{WM'}}{\mathrm{WMM}})^b \tag{1}$$

Where f/F represents the fraction of the basin with water storage capacity, $\mathrm{WM'}$ is the tension water capacity at a point, which varies from zero to a maximum WMM. The f/F versus $\mathrm{WM'}$ curve is shown in Figure 2.1. The parameter b is the exponent of the curve, which controls the spatial variability of $\mathrm{WM'}$ that increases with large values of b and becomes uniform when $b = 0$. For the grid-based Xinanjiang model, we assumed that the parabolic curve was regarded as an accumulative function or statistical description of the spatial heterogeneity for all pixels (Liu et al., 2009).

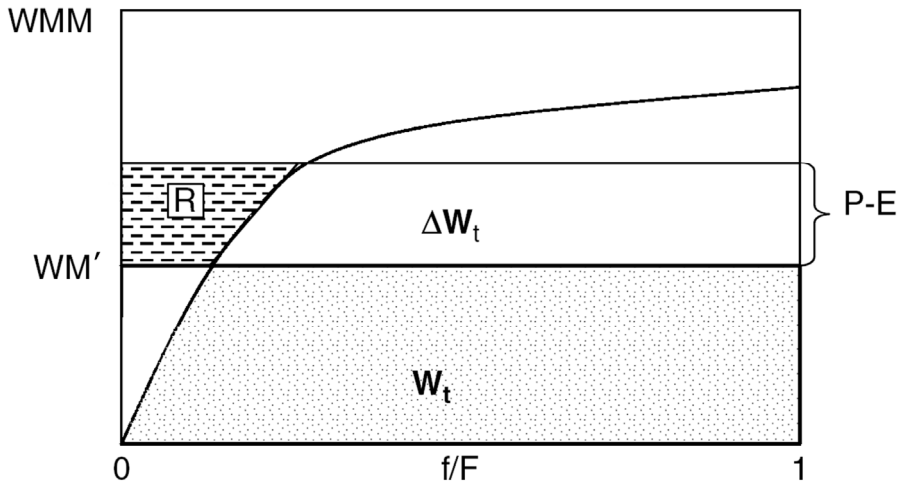

Figure 2.1: Soil water content distribution curve. WMM is maximum of soil water content in a watershed; WM' is field capacity at a point in the watershed; R is runoff yield at time t; Δw_t is soil moisture storage deficit at time t; W_t is watershed-average soil moisture storage at time t.

The total water storage WM is obtained integrating $1 - f/F$ between $\mathrm{WM'} = 0$

and WMM , obtaining:

$$\mathrm{WM} = \mathrm{WMM}/(1+b) \tag{2}$$

W_t , the soil moisture storage at time t , is the integral of $1-f/F$ between zero and the actual value of the water level in the cell:

$$W_t = \int_0^{Wt^*}(1-\frac{f}{F})d(\mathrm{WM}') = WM\cdot\left[(1-(1-\frac{\mathrm{WM}'}{\mathrm{WMM}})^{1+b}\right] \tag{3}$$

Thus, the critical point W_t^* corresponding to watershed average soil moisture storage W_t is:

$$W_t^* = \mathrm{WMM}\cdot\left[(1-(1-\frac{\mathrm{WM}}{\mathrm{WMM}})^{1/(1+b)}\right] \tag{4}$$

Runoff occurs when soil moisture reaches W_t^*. If the effective rainfall amount in a time interval $(t, t+1)$ is $P_t - E_t$ (Figure 2.1), then runoff yield in the time interval R_t can be calculated as follows:

If $P_t - E_t + WM_t^* < WMM$

$$R_t = P_t - E_t - WM + W_t + WM\cdot[1-(P_t - E_t - WM_t^*)/WMM]^{1+b} \tag{5}$$

Else,

$$R_t = P_t - E_t - WM + W_t \tag{6}$$

Where W_t is the initial soil moisture (tension water) in the unsaturated zone and can be calculated by the following water balance equation

$$W_t = W_{t\text{-}1} + P_t - E_t - R_t \tag{7}$$

In the Xinanjiang model, the total runoff R_t is separated into three components: surface runoff RS , interflow RI , and groundwater RG . Further details of the derivation of the three components are given in Zhao (1992).

Impervious areas

The open water bodies (e.g. lakes and reservoirs) and urban areas are treated as impervious areas. For a pixel representing these areas, the model assumes that the seepage will not be considered, which means that the water from rainfall will not infiltrate into the soil but flows out directly to surface runoff. Thus, the surface flow in the impervious areas equals to difference between precipitation and evaporation.

Polders routines

The polders, distributed in the flood plain, are enclosed by embankments and form artificial hydrological entities. The polders connect with outside streams through man-operated structures, and the pumping stations regulate the water levels. These artificial hydrological entities are used for agricultural irrigation and flood control, which is a great challenge for water flux calculation. Due to the unavailability of polder operations data, the polders are assumed to be buckets for outflow calculation. According to local investigation, the pumping stations only work during flood periods. Thus, we assume that the water will flow out of the polder without pumping stations regulation until it reaches maximum drainage volume. The water balance in the polder is calculated as follows:

$$\begin{aligned} W &= W_t + R_t \\ W_{out} &= R_t && if \quad R_t \le W_m \\ &= W_m \\ &= Q_{dr} \cdot T && if \quad R_t > W_m \\ W_{t+1} &= W - W_{out} \end{aligned} \tag{8}$$

where W_{t+1} and W_t are the water storage in the polders at time $t+1$ and t, W_{out} is the outflow from the polders, W_m is the maximum drainage volume of the polder which equals to the product of pumping capacity Q_{dr} and running time of pumping station in one day T.

2.2.2 Overland flow and channel flow

Numerous practical models apply the dynamic wave equations to calculate overland flow, but these equations are highly nonlinear and do not have analytical solutions. Under a set of simplifying assumptions, many studies employ the kinematic wave theory to model overland

flow (Eagleson, 1970; Singh and Woolhiser, 1996; Du et al., 2007). In the present study, both the overland flow routing of runoff and channel routing are calculated by the one-dimensional kinematic wave equations, which has been developed in PCRaster as the first physically-based routing method (Van der Knijff and De Roo, 2008). However, the kinematic wave may not be applicable in featureless areas; further study should implement other routing methods to expand the capabilities for the flat region. The interflow and groundwater are modeled by a simple linear storage.

2.3 Model applications

2.3.1 Study area and data

The Xitiaoxi catchment, covering more than 2200 km^2, is located in the upper reaches of Taihu Lake Basin in south China (Figure 2.2). In the Xitiaoxi catchment 63.4% of the mountainous areas in the upper reaches are covered with forest. About three quarters of this area are bamboos. About 25.6% of the catchment is paddy land, which is mostly located in the low alluvial plains. A portion of about 4.1% of the area is farmland. Other minor land uses classes are residential area of 1.9% and grassland and surface water area of 5%. Two reservoirs (Fushi and Laoshikan) in the upper reaches of the catchment are used for irrigation, flood control and hydroelectricity generation. The reservoirs are refilled mainly in autumn and winter which lead to low water levels in the downstream portion of the catchment. This may result in return flow from Taihu Lake to the river.

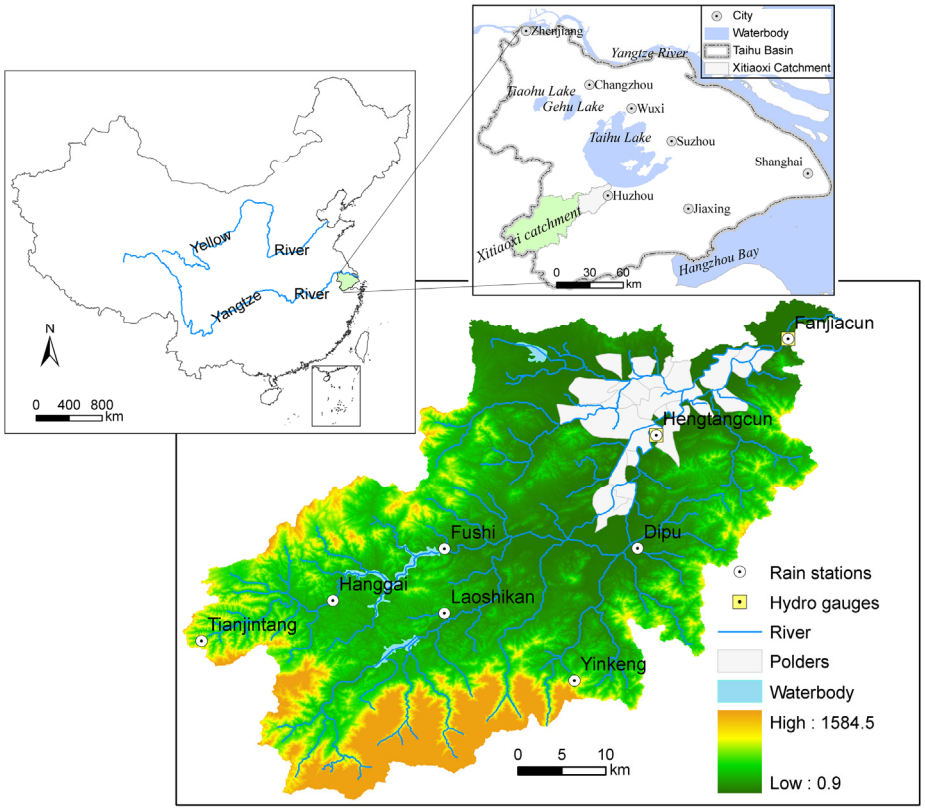

Figure 2.2: Location of the study area and rainfall gauges (Li et al., 2004a)

The catchment is characterized by a semitropical climate with mean annual precipitation of about 1385 mm, and most of the rainfall occurs between March and September (Xu et al., 2007). The distribution of river runoff in the Xitiaoxi catchment is mainly controlled by rainfall (Figure 2.3), which is dominated by the Asian summer monsoon.

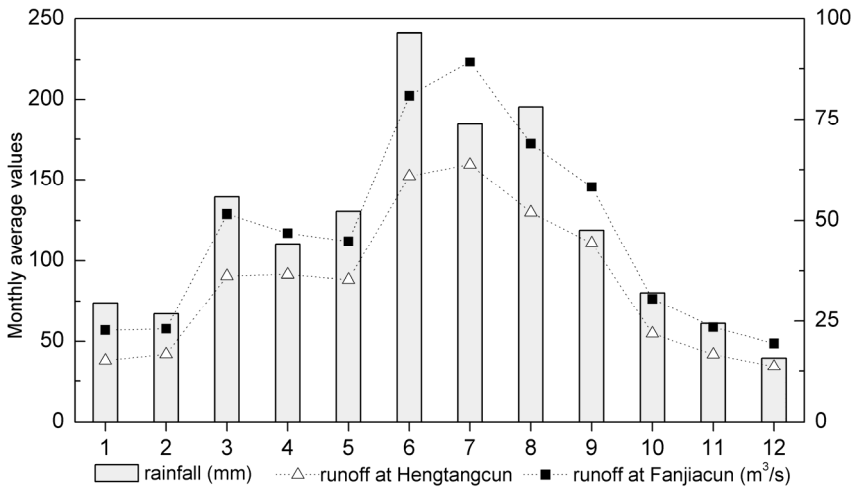

Figure 2.3: Monthly precipitation and discharge at two stations in Xitiaoxi catchment

(1979-2001)

There are 75 polders in the catchment, and 29 of them lie in the upper reaches of Fanjiacun station with total area of 138 km^2 (Figure 2.2). The height of the dykes varies from 9 m to 18 m above mean sea level (a.m.s.l.), and the pumping capacities in the polders are mostly between 0.3 m^3/s and 4 m^3/s, except the polder Wangxiangxiaoyun with 13.99 m^3/s (Huzhou Hydrology Bureau). In this study, we only present the effects of the upstream 29 polders operation on the simulated discharge. The total pumping capacity is 66.4 m^3/s, and the outflow is estimated by above proposed approach.

The Anji Hydrology Bureau provided detailed meteorological and hydrological data collected from 1979 to 2001 for the Xitiaoxi catchment. Daily precipitation data sets within the Xitiaoxi catchment consist of 8 rainfall gauging stations (Figure 2.2). Also streamflow gauging stations with continuous daily streamflow records are situated at Fanjiacun and Hengtangcun. In order to obtain the rainfall input of each cell and consider the spatial variability of precipitation and its effect on basin response such as the soil moisture distribution, the Xitiaoxi catchment was divided into 8 sub-basins by using the Thiessen polygon method.

The satellite images from Enhanced Thematic Mapper (ETM) sensor were used for extracting the land use maps (http://glcfapp.umiacs.umd.edu:8080/esdi/index.jsp). The images (30m spatial resolution for band 1, 2, 3, 4, 5, and 7 plus 120 m and 15 m spatial resolution for band 6 and PAN-band, respectively) acquired on October 11 2001 were classified using an unsupervised classification method. Digital elevation model (DEM) at 25×25 m horizontal resolution (see Figure 2.2) for the catchment was obtained from the Anji Bureau of Agriculture. The DEM was used to derive hydrologic parameters of the catchment such as slope and local drainage direction (LDD). To avoid producing a large number of pixels for the catchment, a grid size of 200×200 m was selected for continuous daily simulation. All the spatial data (land use, DEM) were resampled to the same resolution for runoff modeling.

The spatial distribution of Manning's roughness coefficient of each overland flow cell is determined based on the values published in the literature for an appropriate land cover (Chow et al., 1988; Du et al., 2007). The Manning's roughness coefficient is linearly interpolated based on the stream order grid between 0.11 $m^{-1/3}s$ for the lowest order and 0.035 $m^{-1/3}s$ for the highest order.

Model calibration and validation for the whole catchment were carried out at both Hengtangcun (1308 km^2) and Fanjiacun (1914 km^2) stations. Most parameters were preset by referring to

literature (Zhao, 1992) or calibrated by means of simple trial-and-error method. These parameters are all easy to determine because most of the parameters have approximate values in humid or semi-humid regions in south China (Zhao, 1984). The model efficiencies according to the Nash-Sutcliffe efficiency (1970), the correlation coefficient (R^2) and the root mean square error (RMSE) were calculated at a daily resolution to evaluate the hydrological model performance. There were 22 years (1978-1999) of continuous daily streamflow records for both stations. After the initial "warm-up" period, 10 years of continuous daily discharge was used each for calibration (1980-1989) and validation (1990-1999).

Sensitivity analysis was carried out to evaluate and quantify the effect of the parameter variations on model output. The sensitivity is calculated as the ratio between the relative changes of model output and the relative change of a parameter. To avoid the disadvantages of the conventional variation by a fixed percentage of the initial parameter value, Lenhart et al. (2002) suggested an alternative approach by a fixed percentage of the valid parameter range. However, it is difficult to define a valid range for some parameters in the Xinanjiang model. Thus, a fixed percentage of the calibrated parameter value is preferable. The sensitivity is analyzed by the relative changes of annual streamflow to the variation of the calibrated parameter value.

2.3.2 Results and discussion

Model calibration and validation

Table 2.1 shows model efficiencies for calibration and validation at two gauges in the Xitiaoxi catchment. The results illustrate a good correlation between measured and simulated daily discharge for both calibration and validation at Hengtangcun station. This is demonstrated by the correlation coefficient ($R^2 = 0.83$) and Nash-Suttcliffe efficiency (NS = 0.82) values during the calibration period. For validation, the NS and R^2 values were calculated to be 0.85 and 0.86 respectively, indicating good agreement between observed and simulated discharges. Comparably, the simulated results at Fanjiacun station are slightly worse than at Hengtangcun station. The correlation efficiencies for daily discharge are 0.83 for calibration and 0.82 for validation. The NS values of 0.79 during the two periods, though relatively lower, the simulation results are still acceptable. The RMSE of the discharge at Fanjiacun is almost 40% higher than that at Hengtangcun, as can be seen in Table 1. This is caused by the reservoirs operation and the return flow from Taihu Lake during the dry season.

Table 2.1 Model performance in Xitiaoxi catchment

Station	Used for	Period	NS	R^2	RMSE (m^3/s)
Hengtangcun	calibration	1980-1989	0.82	0.83	24.62
	validation	1990-1999	0.85	0.86	24.23
Fanjiacun	calibration	1980-1989	0.79	0.83	34.03
	validation	1990-1999	0.79	0.82	36.95

Figure 2.4 shows the hydrographs of the observed and modeled discharges at the Hengtangcun and Fanjiacun stations. Both of them illustrate that some peaks of the modeled values are much higher than the measured discharge, while the simulated values are lower after the flood peaks. This may be attributed to the two reservoirs, which are located in the upper reaches of the catchment. The reservoirs are used for flood control during the rainy season. As illustrated in Figure 2.4, the reservoirs clearly reduce and delay the flood peaks for extreme hydrological events. In the dry season, the reservoirs are refilled and occasionally release the water for irrigation.

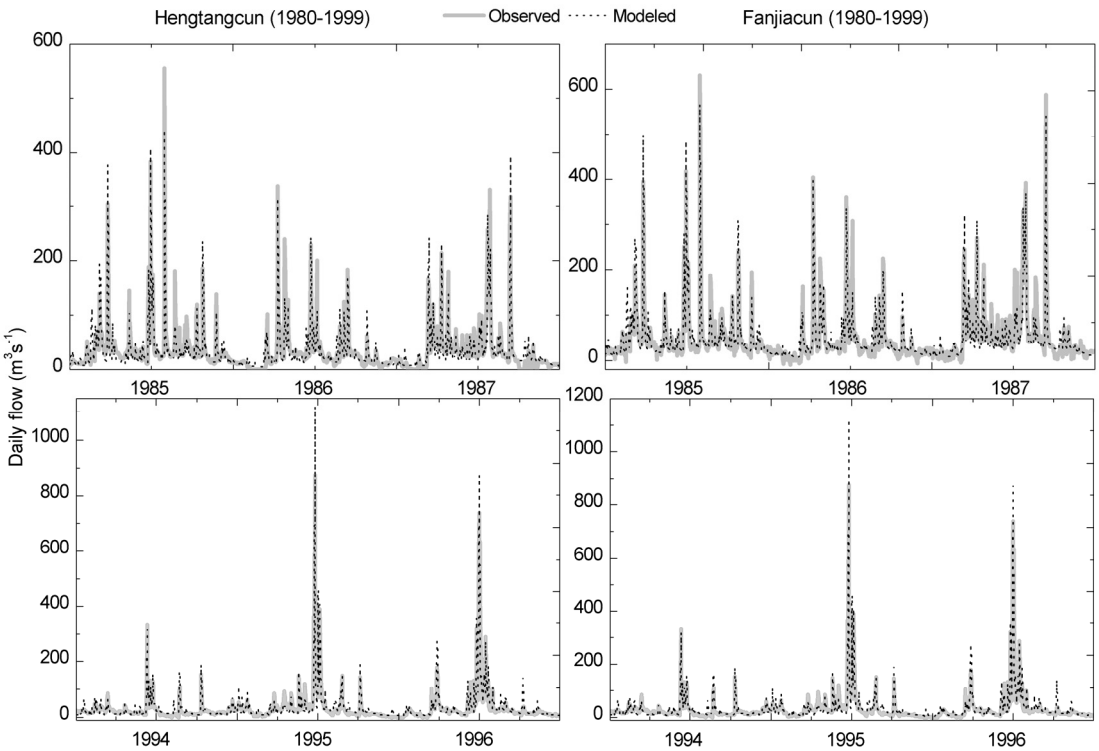

Figure 2.4: Flow hydrographs during the calibration period and validation time

Figure 2.5 shows the measured and simulated flow duration curves (FDC) for both stations from 1980 to 1999. Both FDC curves indicate that the simulated low streamflow has a great deviation compared to the observed discharge (Figure 2.5a and b). For Hengtangcun station, it clearly shows that evident deviation occurs above 70 percentage of time flow between observed and modeled discharge (Figure 2.5c). About 3% of observed discharge is zero, which mostly happens in the dry season. In contrast, the distinctions between the modeled and observed low flow at Fanjiacun station are more significant. The return flow from Taihu Lake leads to observed negative discharge at Fanjiacun station (Figure 2.5d), which can explain the high values of RMSE.

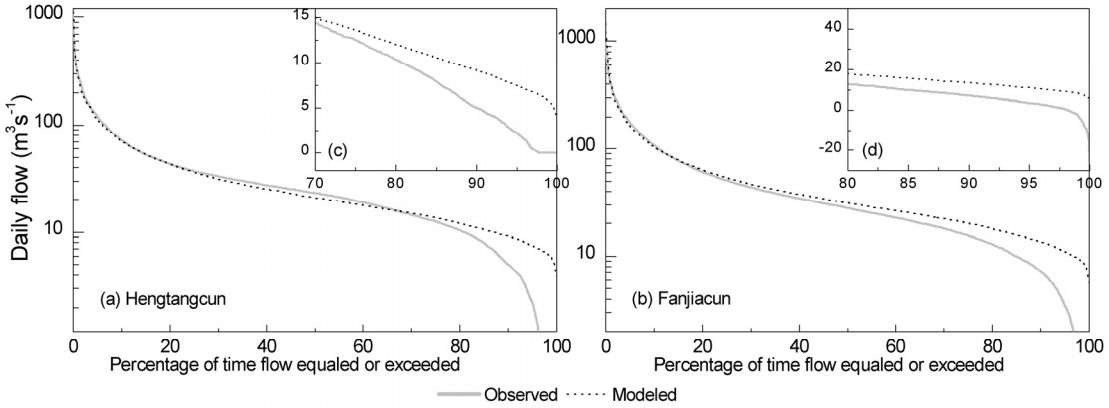

Figure 2.5: Flow duration curves at two stations in the Xitiaoxi catchment from 1980 to 1999

Sensitivity analysis

Table 2.2 shows the calibrated parameter values and their sensitivity ranks based on the criteria defined by Lenhart et al. (2002). There are four parameters with high sensitivity. The annual streamflow is particularly sensitive to the ratio of potential evapotranspiration to pan evaporation (K), which controls the water balance. A 20% change in parameter K results in approximately 8% streamflow changes. The sum (0.7-0.8) of the outflow coefficients of the freewater storage to groundwater (KG) and interflow (KSS) determines the flow rate from freewater storage and their ratio represents the proportion going to interflow and groundwater flow, respectively (Zhao, 1992). Previous studies (Zhao, 1992; Chen et al., 2007) indicate that WM is mainly dependent on climatic dryness or wetness, which varies from 80 mm in the humid region to 170 mm in the semi-arid area. An approximate value of 120 mm for the regions in the south of the Yangtze River Basin is recommended by Zhao (1984), therefore, we chose 110 mm for parameter WM in the present study.

Comparably, the parameters SM and KKG are of medium sensitivity. SM is the areal mean of the free water capacity of the surface soil layer, which represents the maximum possible deficit of free water storage. Surface runoff is sensitive to the value of this parameter. KKG, the recession constant of groundwater storage, usually lies in a range between 0.99 and 0.998 (Zhao, 1992). The parameters b, Ex and KKSS are insensitive to the model predictions. In the grid-based Xinanjiang model, the spatial heterogeneity is regarded as an accumulative function represented by the parabolic curve. This may lead to the model output generally insensitive to the parameter b.

Table 2.2 Parameters in the runoff generation and separation components of the model

Parameter	Definition	Range[a]	Value[b]	Rank
K	Ratio of potential evapotranspiration to pan evaporation	Calibrated according to water balance	1.02	III
b	Exponent of the tension water capacity parabolic curve	0.1 for small catchments (<10 km^2); 0.2-0.3 for medium-sized catchments (≤300 km^2); 0.3-0.4 for large catchments (thousands km^2)	0.4	I
WM	Areal mean tension water capacity (mm)	80-170 mm and varies from humid areas to semi-arid areas	110	III
SM	Areal mean free water capacity of the surface soil	5-45 mm	40	II
Ex	Exponent of the free water capacity curve	0.5-2.0	1.4	I
KG	Outflow coefficients of the free water storage to groundwater	KG + KSS = 0.7-0.8	0.45	III
KSS	Outflow coefficients of the free water storage to interflow		0.25	III
KKG	Recession constant of groundwater storage	0.95-0.995	0.98	II
KKSS	Recession constant of lower interflow storage	0.5-0.9 in humid regions	0.5	I

[a] After Zhao (1992), [b] parameters values determined by calibration.

I --small to negligible; II --medium; III --high; IV --very high

Polder operation impacts

The mechanism of the polder operation is that the pumping station does not control the low outflow of the polder but only affects the flood peaks. Therefore, four flood events (from 1989 to 1993) were selected to evaluate the effects of the polder operation on simulated discharge. Figure 2.6 and Figure 2.7 show the simulation results at Hengtangcun and Fanjiacun stations.

As shown in Figure 2.6, there were no evident distinctions among the simulated discharge with different running time of the pumping station at Hengtangcun station. Only seven polders with total pumping capacity of 11.55 m^3/s are located in the upper reaches of Hengtangcun station. This may explain why the polder operation did not evidently influence the discharge of this gauging station.

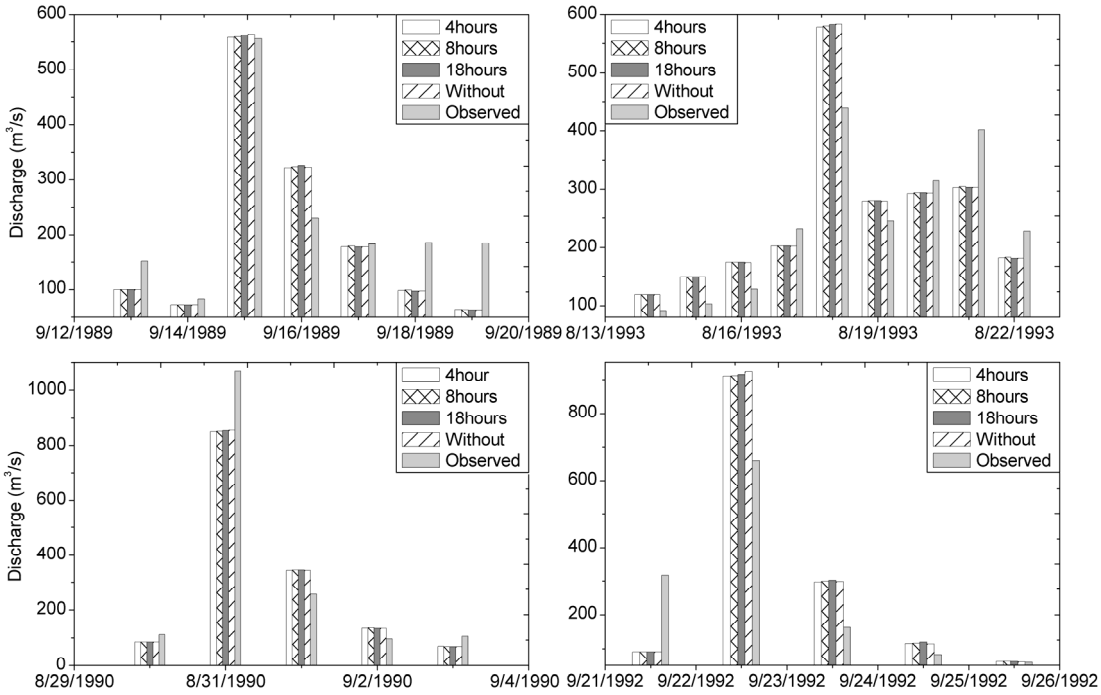

Figure 2.6: Effects of pumping stations running time at polders on simulated discharge at Hengtangcun

Figure 2.7 shows the impacts of the polder operation on simulated discharge at Fanjiacun station. It can be clearly seen that the flood peaks are slightly higher with increasing running time of the pumping station. Comparably, the simulation with decreased running time tended to give time-lagged predictions and resulted in flood detention. Once the outflow reaches maximum drainage volume, the pumping station runs for a fixed period and produced its peak runoff. The shorter the running time of the pumping station, the lower the peaks become. In general, storage effects of the polder systems delay and cap the flood peaks. This was also confirmed by other researchers (De Roo, 2003; Förster et al., 2008). In addition, Figure 2.7 reveals that the distinctions of flood peaks between 4 hours running time and that without polder systems varies from 42 m^3/s to 57 m^3/s, which is not effective. Although polders operation can cap the flood peaks and produce time-lagged flood wave, significant discrepancies still exist between simulated and observed peaks in some events. As mentioned

above, the total pumping capacity of the upstream polders is 66.4 m^3/s. In contrast, the reservoirs operation made large contribution to the significant discrepancies. Thus, an efficient model to simulate the outflow of reservoirs is necessary to improve the simulation results in the future.

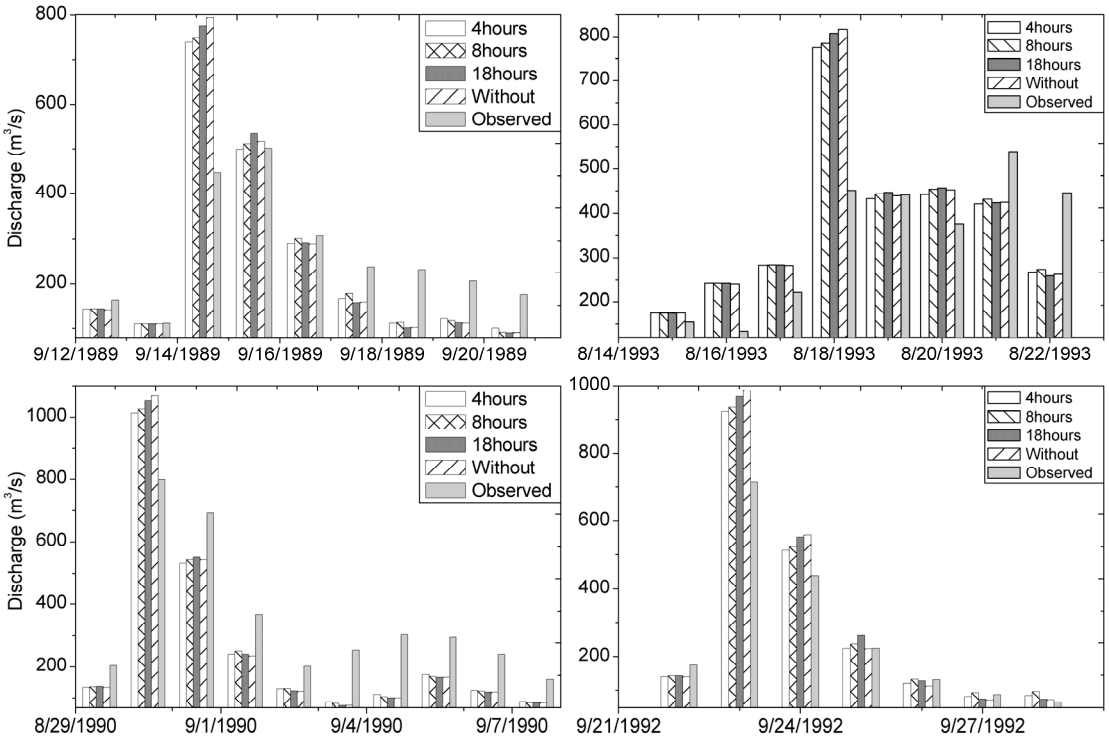

Figure 2.7: Effects of pumping stations running time at polders on simulated discharge at Fanjiacun

Runoff simulation challenges in Xitiaoxi catchment

Although the simulation results show a satisfactory fit between observed discharge and modeled runoff, there are still some discrepancies, resulting in high values of RMSE, and this can be attributed to the operation of the reservoirs and the return flow from Taihu Lake.

Figure 2.8 shows the simulated and observed outflows from two reservoirs between 1983 and 1984. Both hydrographs indicate that the modeled discharge is much higher at flood peaks than the regulated reservoir outflow. Most flow records show a pronounced reduction in flood magnitude as a consequence of dam operation. It also can be clearly seen that the reservoirs release the floodwater over an extended period of time to protect agricultural and urban areas in the lower reaches. The results indicate that reservoirs produce substantial alterations to the low

flow regime. This may explain the discrepancies between the simulated low flow and the much higher peaks at the two stations. In addition, the observed discharge series at Fanjiancun indicate that the negative discharge occurs frequently from September to the following February. An average of 8.8 days with negative observed discharge per year was found in the measured streamflow records from 1980 to 1999. However, due to the scarce available data from the two reservoirs, an appropriate method to simulate the outflow of the reservoirs could not be implemented in present model.

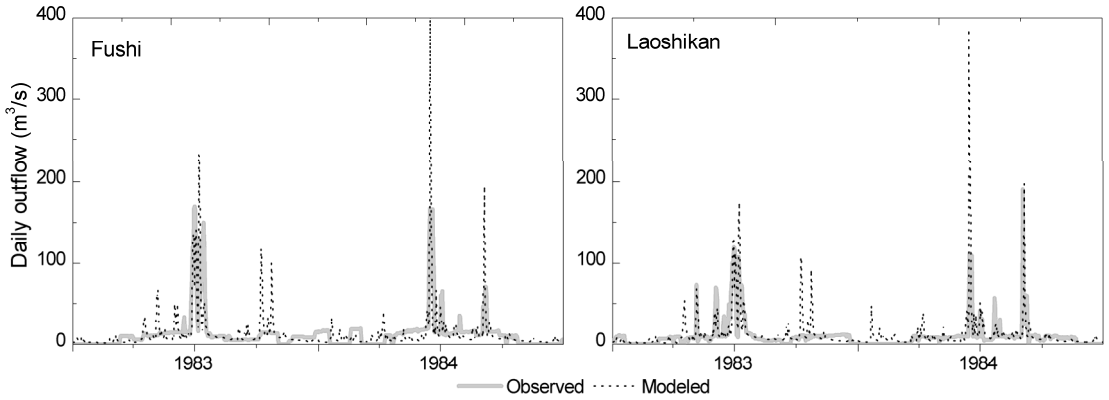

Figure 2.8: Comparison the regulated and simulated outflow from two reservoirs in the upper reaches of the Xitiaoxi catchment

2.4 Conclusions

In this study, we developed a raster-based Xinanjiang model, the PCR-XAJ model, to calculate the daily streamflow for a humid catchment with polder systems. The hydrological model has been tested in the Xitiaoxi catchment in south China. The simulation results presented a good agreement with the observed values. The Nash-Sutcliffe index is 0.82 for the calibration period and 0.85 for the validation period at Hengtangcun station. For Fanjiacun station, the results were slightly worse, which may be caused by return flow from Taihu Lake in the lower reaches of Xitiaoxi catchment. However, some disagreements between observed and simulated data were evident through the high value of RMSE, especially at Fanjiacun station. In addition, considering such a large area of a complex catchment with reservoirs, polder systems and return flow, the model predictions are still encouraging. The simulation results demonstrate that the model was capable of reproducing both the magnitude and the dynamics of the daily discharge. Furthermore, it is evident that during the wet season, rainfall primarily controls the runoff hydrographs of the catchment.

In the present paper, a simplified polder operation method was introduced to calculate the outflow in polder systems. The results imply that the polder operation can reduce the flood peaks and the proposed method can slightly improve the accuracy of the discharge simulation.

The distributed hydrological model has been used as a basic tool for finding a reasonable solution of regional hydrological problems associated with flood forecasting and water resources planning, optimal allocation and management. Based on the results of the present study, the model can be extended to other catchments in humid regions.

Acknowledgements

This study was supported by the 'Studies and Research in Sustainability' program from Deutscher Akademischer Austausch Dienst (DAAD), and was funded by the Program for Key Science & Technology Projects (2008ZX07101-014 and 2008ZX07526-007). The authors would express their gratitude to the Nanjing Institute of Geography and Limnology, Chinese Academy of Sciences (CAS) for data collection. Great thanks are also extended to the anonymous reviewers for their very helpful comments and valuable suggestions.

Chapter III Impacts of spatial data resolution on simulated discharge, a case study of Xitiaoxi catchment in south China

G. J. Zhao, G. Hörmann, N. Fohrer, J. F. Gao

Advances in Geosciences, Volume 21 (2009), Pages 131-137
Submitted 22.01.09, Accepted 28.04.09, Published 12.08.09

Abstract

In this paper we analyse the effects of different spatial input data resolution on water balance simulation using a simple distributed hydrological model: PCR-XAJ model. A data set consisting of land use and digital elevation model at 25m resolution of Xitiaoxi catchment in south China is used for investigation. The model was first calibrated and validated at 50m cell size, thereafter an aggregation of the digital elevation model (DEM) and land use maps at 100m, 200m, 300m, 500m and 1km are applied to evaluate the effects of spatial data resolution on simulated discharge. The simulation results at a grid size of 50m show a good correlation between measured and simulated daily flows at Hengtangcun station with Nash-Suttcliffe efficiency larger than 0.75 for both calibration and validation periods. In contrast, the model performs slightly worse at Fanjiacun station. The increasing grid size affects the characteristics of the slope and land use aggregation and causes important information loss. The aggregation of input data does not lead to significant errors up to a grid of 1km. Model efficiencies decrease slightly with cell size increasing, and more significantly up to the grid size of 1km.

Keywords: spatial resolution, PCR-XAJ model, simulated discharge, model efficiency, spatial aggregation

3.1 Introduction

Advanced techniques in remote sensing, geographic information systems and computer have been widely applied to distributed hydrological models in recent years. Thereby a number of large spatial data sets are employed in spatial distributed hydrological modeling. Different spatial resolution of input data can represent the heterogeneity of landscape to some extent, which may have a significant impact on the simulation results (Blöschl et al., 1997). Thus, an appropriate spatial resolution for hydrological modeling should be considered carefully (Grayson and Blöschl, 2000).

There are numerous studies in literature which investigated the effects of using different spatial resolution data on the results of hydrological modeling (Blöschl, 2001). Considerable research on how grid size affects the topographic characteristics, wetness index and outflow has been carried out with TOPMODEL (Beven and Kirkby, 1979; Quinn et al., 1991; Moore et al., 1993; Bormann, 2006; Wu et al., 2008). In general, spatial input data with higher resolution led better simulation results. However, the smaller the grid size, the higher is the amount of spatial information. Reduction of the grid size also means much more computational time and a tremendous increase in the work for data collection and processing. Although some authors reported that grid size can directly affect the simulation results, most research focused on the topological indices variation and their effects on discharge and sediments based on TOPMODEL. Only a few studies analyzed the impacts of spatial data resolution by using other models (Wechsler, 2007), such as the SWAT model (Chaplot, 2005; Chaubey et al.; 2005; Haverkamp et al, 2005) and the Agricultural Nonpoint Source Pollution (AGNPS) (Vieux and Needham, 1993).

The objective of this paper is to develop a raster-based hydrological model: the PCR-XAJ model and assess the effects of different spatial data resolution on discharge simulation. The Xitiaoxi catchment, a humid semitropical catchment, was selected for this study. The PCR-XAJ model calculates the water balance in both the mountainous and flat sub catchments.

3.2 Study area

The Xitiaoxi catchment is located in the upper reaches of Tai Lake basin (Figure 3.1), in south China. It covers more than 2200 km^2. In the Xitiaoxi catchment 63.4% of the mountains in the upper reaches areas are covered with forest. About three quarters of this area is bamboos. About 25% of the catchment is paddy land, which lies in the low alluvial plains. A portion of about 4% of the area is fallow land, 1.8% is covered by urban area and the other land uses are grassland and bare land. Two reservoirs (Fushi and Laoshikan) located in the upper reaches of the catchment are primarily used for flood control in rainy season. There are 75 polders in the lower reaches of the Xitiaoxi catchment, which are enclosed by embankments and form artificial hydrological entities.

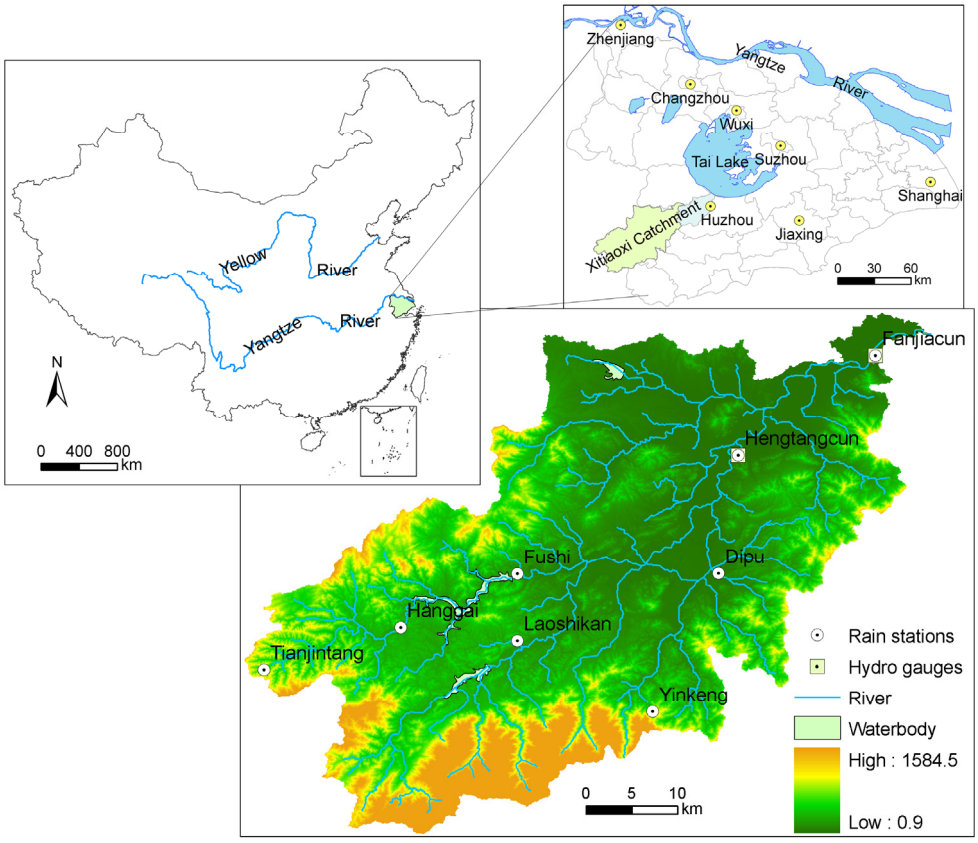

Figure 3.1: Location of the study area and rainfall gauges (Li et al., 2004a)

The catchment is characterized by a semitropical climate with mean annual rainfall of about 1465 mm. The distribution of river runoff in the Xitiaoxi catchment is mainly controlled by rainfall (Fig. 2), which is dominated by the Asian summer monsoon.

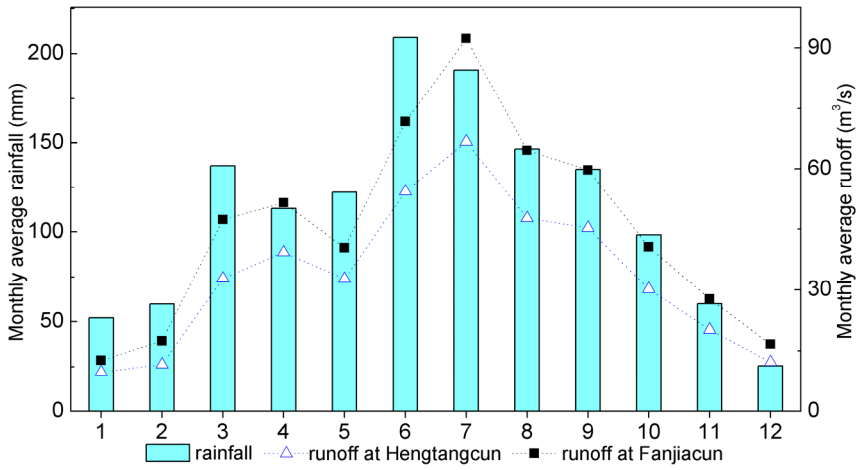

Figure 3.2: Monthly precipitation and discharge at two stations in Xitiaoxi catchment (1979-1988)

Detailed climate and hydrological data collected from 1978 to 1988 for the Xitiaoxi catchment are provided by Huzhou Hydrological Bureau, Zhejiang Province. Daily precipitation data sets are available for 8 rain gauging stations within the Xitiaoxi catchment (Figure 3.1). Among these stations, the Fanjiacun station and Hengtangcun station are also the streamflow gauging stations with continuous streamflow records. The land use and land cover maps for the year 2001 and DEM at 25×25 m horizontal resolution for the catchment are provided by Huzhou Bureau of surveying and mapping, Zhejiang Province.

To estimate the impact of the spatial data resolution on simulated catchment discharge, the available data set of 25m resolution was aggregated using standard GIS functions to create grid based data sets of increasing grid size: 50m, 100m, 200m, 300m, 500m and 1km. Thereafter, the spatial data sets (e.g. land use, channel) were systematically aggregated applying the same aggregation methods. Subsequently, the PCR-XAJ model was applied to investigate the impacts of data aggregation.

3.3 Hydrological modelling

The simple raster-based PCR-XAJ model is so called because it is implemented within PCRaster and conceptually based on Xinanjiang model (Wesseling et al., 1996). Figure 3.3 shows its structure. The model simulation is based on grid calculation. Once the grid size is fixed, all the maps will be calculated at this scale for daily step. As shown in Figure 3.3, DEM and river channels are used to create a local drainage direction map according to the D8 algorithm (O'Callaghan and Mark, 1984), which calculates the water flow directions. The actual evapotranspiration is calculated based on the concept of one layer evaporation method in Xinanjiang model (Zhao, 1992). Precipitation and evaporation time series are interpolated with inverse-distance weighting (IDW) to predict daily discharge. The land uses were reclassified in four types i.e. paddy, water-body, urban area and forests for runoff calculation. As a simplification, the relatively small areas of grassland and bare land are assumed to behave in a similar way as forests regarding runoff formation. The runoff generation component of the Xinanjiang model (Zhao, 1992) is used to estimate the surface runoff and groundwater in the catchment for each grid. Both the overland flow and channel flow are calculated by kinematic wave equation. The polders and reservoirs are considered as points in the simulation (van der Knijff and de Roo, 2008).

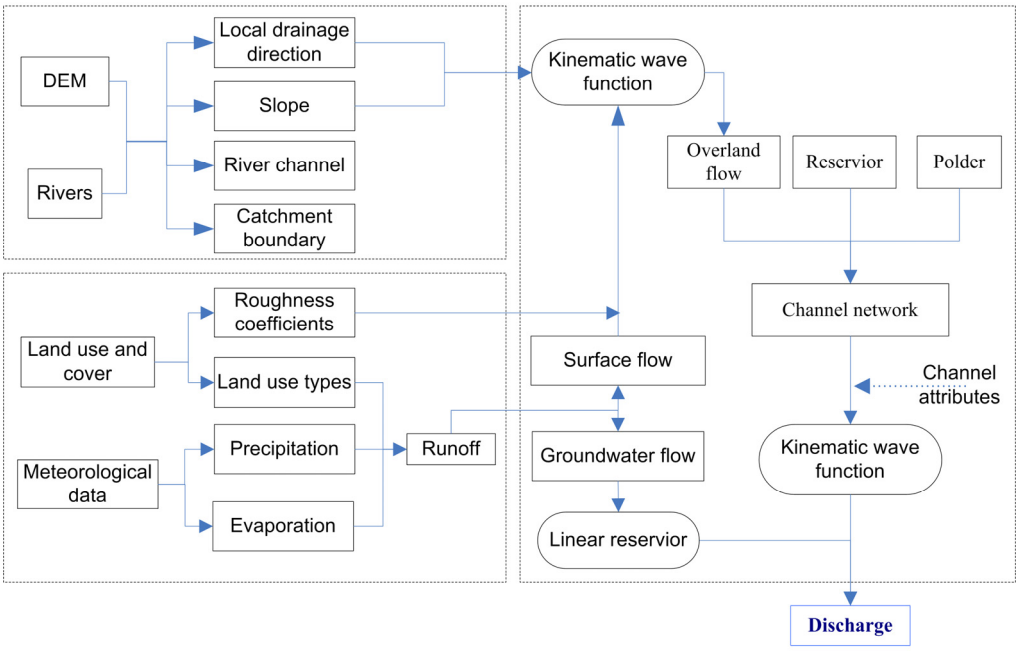

Figure 3.3: Structure of the PCR-XAJ model

The Xinanjiang model has been widely applied in humid and semi-humid areas in south China (Zhao, 1992) .The Xinanjiang model is a well-known lumped model, characterized by the concept of runoff generation on repletion of storage, which means that runoff is not generated until the soil moisture content of the aeration zone reaches maximum capacity, and thereafter runoff equals the rainfall excess without further loss (Su et al., 2003). The runoff is separated into two components: the surface runoff and groundwater, according to their generating levels in the vertical profile. More details were described by Zhao et al. (1980, 1992).

The model was calibrated and validated for the whole catchment at both Hengtangcun (1307.6 km^2) and Fanjiacun (1913.5 km^2) stations at the 50m grid size due to a limitation in the number of computational units by using PCRaster. Calibration period at Hengtangcun station is from 1979 to 1983, Fanjiacun from 1980 to 1983, and the validation periods are both between 1984 and 1988. For all different grid sizes (100m, 200m, 300m, 500m, 1km) derived from the original data sets, continuous water balance simulations from 1978 to 1988 were performed without a recalibration of the simple model. All the spatial data (DEM, land uses and their derivative data such as slope, Manning's roughness) were adapted to the same resolution correspondingly.

3.4 Results and discussion

3.4.1 Model performance

The model efficiencies according to the Nash-Suttcliffe index (NS) (1970), the correlation coefficient (R^2) and the root mean square errors (RMSE) were calculated at daily resolution to evaluate the hydrological model performance.

Figure 3.4 shows the hydrographs of the measured and simulated discharge at Hengtangcun and Fanjiacun stations. Both of them illustrate that some peaks of the modeled values are much higher than the measured discharge, while the simulated values are lower after the peaks. This may be caused by the two reservoirs which are located in the upper reaches of the catchment. The reservoirs are used for irrigation during dry season and flood control during rainy season. This also explains some missing peaks in the modeled data during dry season.

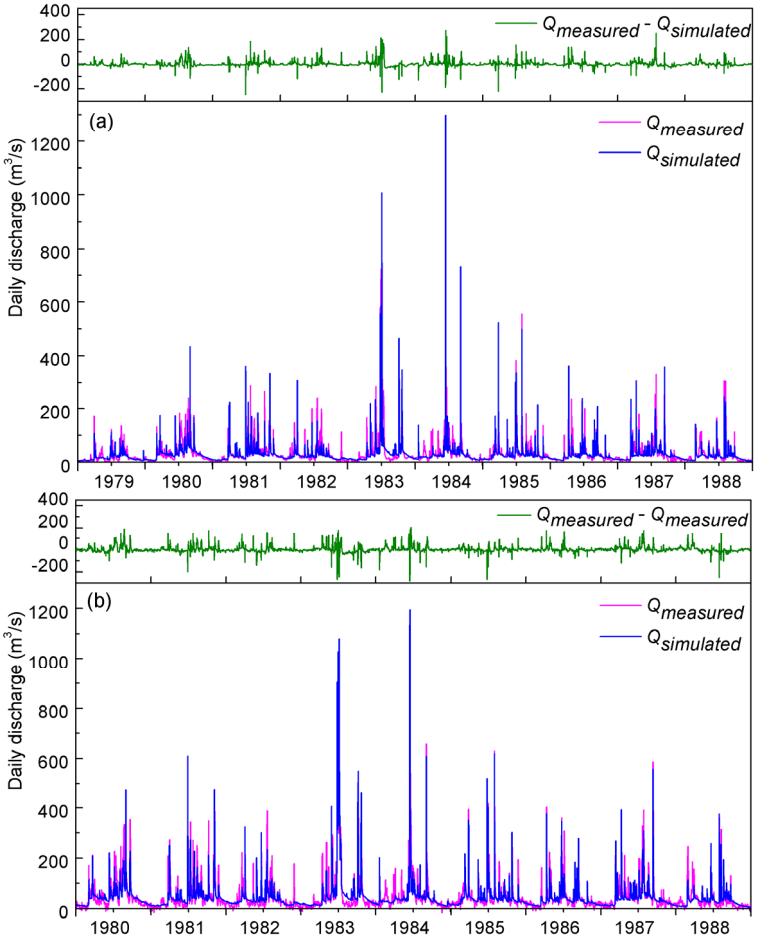

Figure 3.4: Comparison of daily measured and modeled discharge in Xitiaoxi Catchment (a: Hengtangcun station; b: Fanjiacun station)

Table 3.1 shows model efficiencies for calibration and validation at the two gauges. The calibration results show a good correlation between measured and simulated daily flows at Hengtangcun station. This is demonstrated by the correlation coefficient (R^2 = 0.82) and Nash-Suttcliffe simulation efficiency (NS = 0.77) values. For validation, the NS was found to be 0.81 and R^2 0.86, which is in a very good agreement with the observed discharge, and the RMSE is much lower than that for the calibration period. Comparably, the simulated results at Fanjiacun station are slightly worse than at Hengtangcun station. The correlation efficiencies for daily discharge are of moderate quality (0.71 for calibration, 0.76 for validation). The NS values of 0.62 and 0.67 during the two periods, though relatively lower, are acceptable as these values are larger than 0.5 (Santhi et al., 2001a). However, the values of the RMSE are much higher during the two periods at Fanjiacun station.

Table 3.1 Model performance in Xitiaoxi catchment

Station	Used for	Period	NS	R^2	RMSE (m^3/s)
Hengtangcun	calibration	1979-1983	0.77	0.82	27.31
	validation	1984-1988	0.81	0.86	18.32
Fanjiacun	calibration	1980-1983	0.62	0.71	37.51
	validation	1984-1988	0.67	0.76	33.97

The polders connect with outside streams through man-operated devices, and the water fluxes are adjusted manually. These artificial hydrological entities are used for agricultural irrigation and flood control, which is a great challenge for water flux calculation in hydrological simulation. Additionally, the return flow from Tai Lake leads to some negative discharge values at Fanjiacun station, which can not be estimated by our hydrological model. Over the years 1980 to 1988, there is a negative discharge occurring at an average of 15.2 days per year. This may causes the higher RMSE in Fanjiacun station.

The model efficiencies at Fanjiacun station are slightly worse; however, the simulation results demonstrate that the simple hydrological model can successfully simulate water balance at regional scale in the wet subtropical area based on Xinanjiang concepts.

3.4.2 Effects of spatial resolution changes on simulated discharge

The evaluation results, shown in Figure 3.5, reveal that model efficiencies do not decrease significantly for most of the grid sizes at both gauges. Up to a grid size of 500m the model

efficiencies remain almost constant. At a grid size of 1km the simulation results change evidently at Hengtangcun station. As shown in Figure 3.5, the correlation coefficient (R^2) during the validation period for the 1km grid size (0.68) is much lower than that for 500m (0.76). In contrast, the model efficiencies at Fanjiacun station decrease slightly with increasing grid size, but the changes are not obvious (Figure 3.5). In general, the increasing resolution of spatial input data can slightly improve the model results. The comparable results were also found by other researchers (Booij, 2005; Bormann, 2006). Additionally, our simulation results indicate that the effects of spatial resolution in the hilly region are more sensitive than in flat region. This may attribute to the slope smooth.

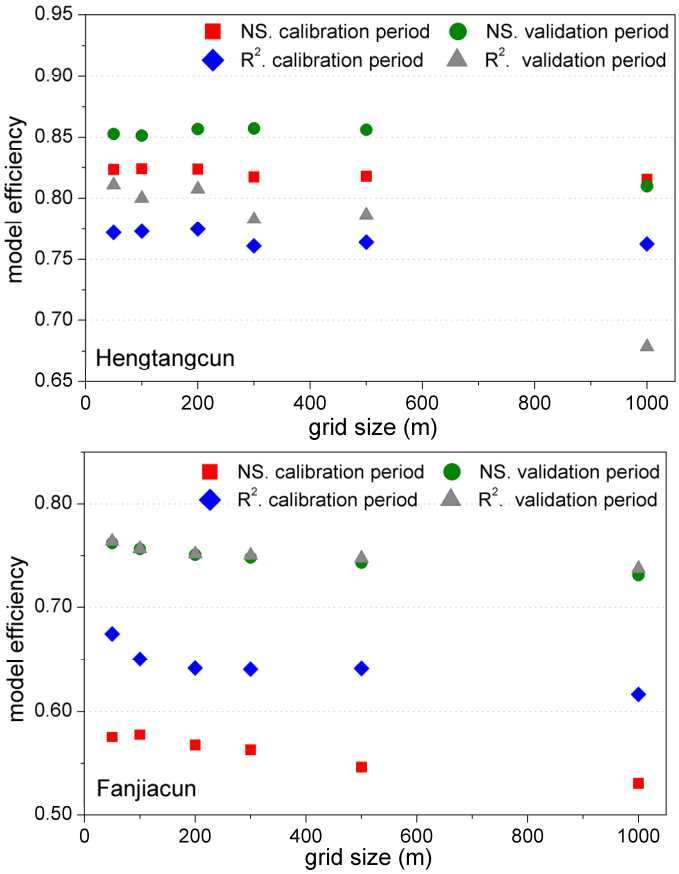

Figure 3.5: Model efficiencies with different spatial resolution at two gauging stations in Xitiaoxi catchment

Figure 3.6 reveals the annual runoff deviations between simulated and observed discharge in dry (1985), normal (1980) and wet (1983) years. It can be obviously seen that the simulated runoff is near 10% lower than the observed values at all grid size in 1983 at Hengtangcun station (Figure 3.6a). In contrast, significant deviations only occur at 1km grid size in the other

two years (Figure 3.6a), and similar results can also be found at Fanjiacun station (Figure 3.6b). In general, annual runoff deviations do not change significantly up to a grid size of 1km in both sub catchments.

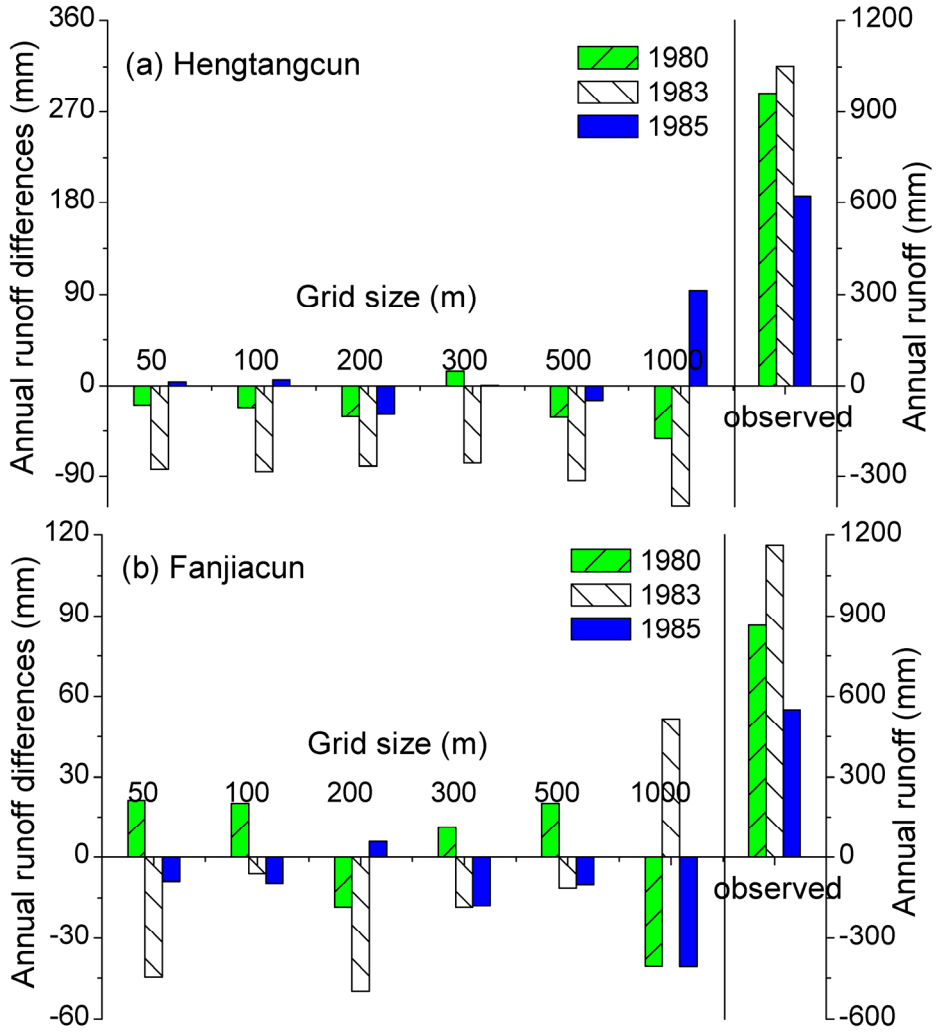

Figure 3.6: Annual runoff deviations with different spatial resolution in dry (1985), normal (1980) and wet year (1983) at two stations

The above analysis indicates that both the model efficiencies and simulated runoff changed with increasing grid size, which may be caused by the slope smoothness and land use aggregation. Increasing the grid size leads to a smoothed surface of elevation and therefore to a decreased mean slope as well as the standard deviation of the slope (Figure 3.7). Comparably, the slope and standard deviation in Hengtangcun sub catchment decrease much more significantly with grid size increasing. Consistent with previous finding from Chaubey et al. (2005), our research confirmed that a finer data resolution resulted in higher slope.

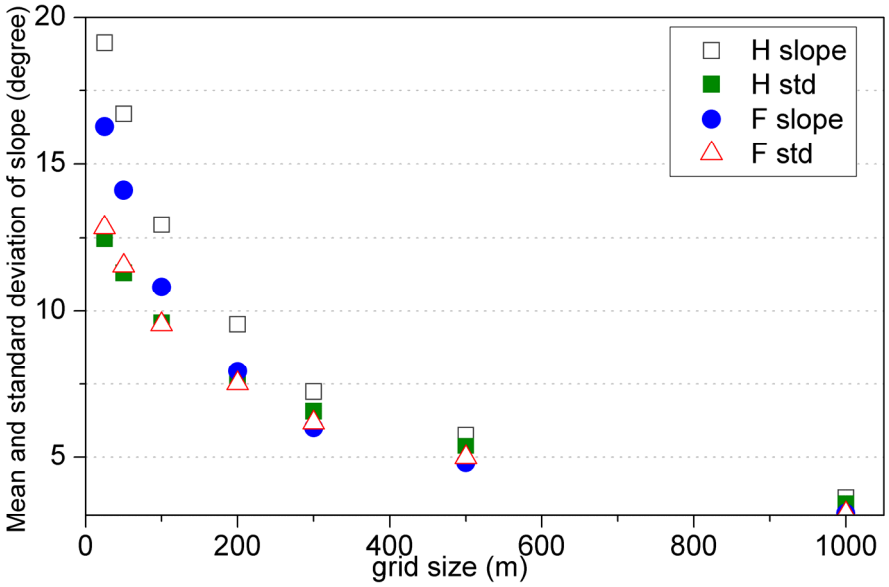

Figure 3.7: Mean and standard deviation of slope in two sub catchments (H: Hengtangcun, F: Fanjiacun; std: standard deviation)

The effects of aggregation on the land use fractions are shown in Figure 3.8. It indicates that the aggregations do not play an important role up to a grid size of 1km in Hengtangcun sub catchment. Significant deviations for paddy and urban area, especially forest were found at the 1km level which may have an influence on the model efficiencies (Figure 3.8a). For Fanjiacun sub catchment, significant changes in land use fractions can be observed for paddy land at almost all grid sizes (Figure 3.8b). In addition, the changes in most land use types are more significant at 1km grid size, which is consistent with the model efficiencies and annual runoff changes.

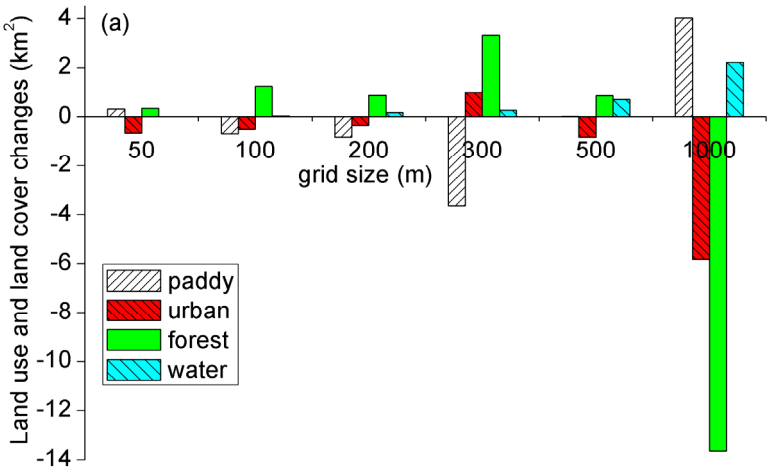

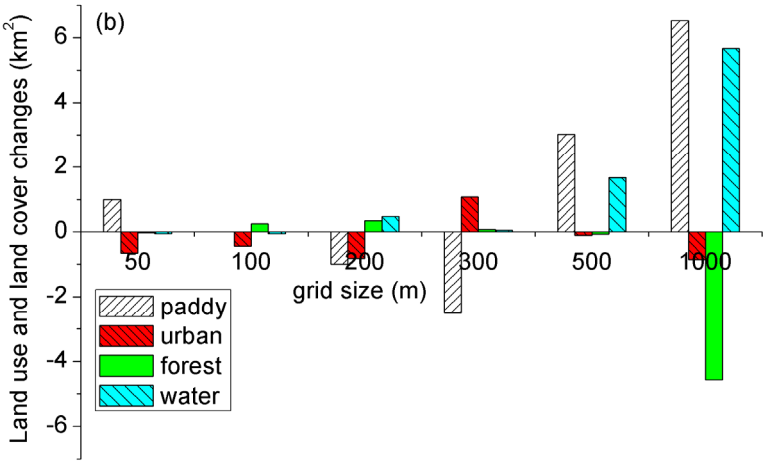

Figure 3.8: Land use changes with different spatial resolution in two sub catchments (a: Hengtangcun; b: Fanjiacun)

Although the slope smoothness and land use aggregation influence the simulation results and model efficiencies, other catchment properties (e.g. roughness coefficients, channel width) can additionally contribute to that. Thus, simulations results are related to all spatial data sets, and the data aggregation therefore would affect all the spatial data sources. However, one difficult issue is to quantify the effects of these factors on simulation results. Bormann (2006) proposed a correlation analysis between statistics of input data and simulated annual water fluxes. He found that predominantly the correlation between catchment properties and simulated water flows varies from catchment to catchment, and catchment specific properties determine correlations between properties and fluxes, but do not influence the effect of data aggregation.

3.5 Conclusions

In this study, the PCR-XAJ model was applied in Xitiaoxi catchment for different spatial resolutions of all spatial input data. The simulation results present a good agreement with the observed values. The Nash-Sutcliffe index of 0.77 for calibration and 0.81 for validation period at Hengtangcun station is satisfactory. For Fanjiacun station, the results are slightly worse, which may be caused by the polders and return flow from Tai Lake in the lower reaches of Xitiaoxi catchment.

Hydrological simulation for two sub catchments was implemented for evaluation the effects of spatial data resolution. The results show that an aggregation of input data does not lead to significant errors up to a grid size of 1km. Land use aggregation causes significant information loss from a grid size of 500m to 1km, which leads to a large deviation in water balance

simulation. Both mean slope and standard deviation decrease significantly with cell size increase in two sub catchments.

In general, this study shows that the higher the input data available, the better the simulation results can be obtained, but the trends are not always obvious. The model efficiencies do not get significantly worse up to spatial resolution at 1km cell size and the results also depends on the watershed response of interest.

Acknowledgements

This study was funded by the 'Studies and Research in Sustainability' program (Deutscher Akademischer Austausch Dienst, DAAD). The authors would express their gratitude to the Nanjing institute of Geography and Limnology, Chinese Academy of Sciences (CAS) for providing the data. The authors would like to express their gratitude to two anonymous reviewers for their valuable comments that helped to improve the quality of our paper.

Chapter IV Development and application of a nitrogen simulation model in a data scarce catchment in south China

G. J. Zhao, G. Hörmann, N. Fohrer, H.P. Li, J. F. Gao, K. Tian

Agricultural Water Management, Volume 98 (2011), Pages 619-631

Submitted 07.06.10, Accepted 30.10.10

Abstract

The Xitiaoxi catchment is one of the most important catchments in the Taihu Basin in southeastern China. It contributes a significant amount of surface runoff and nutrient to Taihu Lake. Understanding the nutrient cycling and identification of critical non-point source pollution in this catchment are therefore of primary importance. In this paper, the Xinanjiang-Nitrogen (XAJ-N) model, a conceptual model of nutrient mobilization and transport is developed by integration of the Xinanjiang rainfall-runoff model, the Integrated Nitrogen CAtchment (INCA) model and the Modified Universal Soil Loss Equation (MUSLE). It is implemented with the environmental modelling language PCRaster and estimates the water fluxes and nutrient loadings on a cell-by-cell basis in daily time step. The model includes the nitrogen cycling processes of mineralization, leaching, fixation, volatilization, nitrification, denitrification and plant uptake. Nitrogen is assumed to be mobilized by surface runoff and groundwater. The model performance was verified by comparing simulated and measured daily discharge and nutrient loadings. The results showed a fairly good relationship between predicted and observed values. Due to the scarce observed data, the simulation results were also validated using an internal mass balance method and values from literature. It showed that the modelling approach can be used as a tool to estimate export of nutrient with daily resolution at a catchment scale.

Key Words: Discharge simulation, Nitrogen, Xinanjiang-Nitrogen (XAJ-N) model, Nitrogen balance, PCRaster

4.1 Introduction

With increasing population and rapid economic development, surface water is heavily polluted due to large amount of municipal sewage, industrial wastewater and non-point source pollution

in China. Especially in the Taihu Basin, water pollution has become a serious environmental problem in view of the fact that algae bloom occurred much more frequently, extending its coverage and simultaneously persisting throughout the summer in recent years (Qin et al., 2007). Since the point source pollution is easily controlled, the diffuse non-point source pollution has received increased attention in recent decades (Edwards and Withers, 2008). Excessive nutrients from intensive agriculture discharged into aquatic systems contribute main pollutants to surface water in the Taihu Basin, thereby causing serious ecological problems such as eutrophication, algal blooms, oxygen depletion and decrease of biodiversity. It is therefore essential to quantify the nutrient load and identify the critical sources in the catchment scale.

In order to improve the water quality and to reduce pollutants, a considerable amount of studies have focused on the estimation of non-point source pollution (Ding et al., 2010). The non-point source pollution is strongly linked to hydro-chemical processes, and thus hydrological models are commonly used to estimate the nutrient loadings and to quantify the effects of agricultural activities on water quality and quantity. A variety of models have been developed to simulate hydrological processes, nutrient transport through surface runoff, soil infiltration, and groundwater flow, as well as in-stream nutrient processes at different scales. Examples include ANSWERS (Beasley et al., 1980), SWRRB (Williams et al., 1985), SWAT (Arnold et al., 1998), HSPF (Donigian et al., 1995), AGNPS (Young et al., 1989), INCA (Whitehead et al., 1998a; Wade et al., 2002a) and LASCAM (Viney et al., 2000). Some of these models provide long-term, daily simulation of nutrient load in large catchments (Arnold and Fohrer, 2005; Viney et al., 2000), whereas others are event-based (e.g. SPNM, SWRRB, AGNPS, ANSWERS) and are clearly unsuitable for long-term continual predictions. Although the long-term continuous nutrient models are capable of providing accurate results, a large number of parameters cannot be obtained from field measurements and must instead be determined through model calibration. An additional constraint to model development and verification is that water quality and hydro-meteorological data are rarely simultaneously collected in a satisfactory resolution. For locations without long-term data collection, estimates based on hindcast model applications might be available (Breuer et al., 2008).

The PCRaster program (http://pcraster.geo.uu.nl) is a dynamic and distributed environmental modelling language (van Deursen, 1995; Wesseling et al., 1996), which provides a raster GIS modelling environment. Since most of the models mentioned above require extensive input and calibration parameters, dynamic modelling language is a powerful tool for development of environmental models. There have been several models developed for nutrient flux estimation using PCRaster in different temporal and spatial scale. The PolFLow model (De Wit, 2000)

calculated average N and P loads for 5-year periods and has been applied to several large catchments (e.g. Rhine, Elbe). The RiNUX model (Loos et al., 2009) was designed to simulate monthly sediment yields and nutrient loads using global datasets. These models obtained satisfying precision but are unsuitable for different spatial-temporal scales.

The study area, Xitiaoxi River catchment, is one of the most important rivers draining into Taihu Lake. Current agricultural practice is a very intensive multi-cropping system with irrigated summer rice - winter wheat (or rapeseed) rotations. The high yields of rice in the catchment are achieved through high nutrient application rates. In recent years, an increasing impact on water quality is attributed to nutrient from intensive agricultural activities transported with surface water to Taihu Lake. A large number of studies investigated the nutrient loading because of the high frequency of algae blooming in Taihu Lake. Lai et al. (2006) and Yu et al. (2007) used the SWAT model to investigate the nutrient transport in the Taihu Basin with long-term annual simulation time step. These studies provided good insights into the spatial and temporal characteristics of the nutrient cycle in the Taihu Basin. However, the nutrient dynamics in soil and water are still not clear. The nutrient simulation at annual scale can not represent the seasonal changes. Furthermore, the missing daily or weekly data sets limit the application of models. Therefore, the objectives of this study are: (a) to develop a simple nutrient transport model named Xinanjiang-Nitrogen (XAJ-N) model by integration of hydrology, soil erosion and nitrogen dynamics at the watershed scale and (b) to apply the XAJ-N model for understanding the characteristics of nitrogen cycle in the Xitiaoxi catchment. In the model, the Xinanjiang rainfall-runoff model was applied in PCRaster for hydrological modelling (Zhao et al., 1980; Zhao, 1992). Nutrient dynamics are simulated based on the Integrated Nitrogen CAtchment (INCA) model (Wade et al., 2002a), and the particulate nitrogen was predicted by soil erosion model using the Modified Universal Soil Loss Equation (MUSLE) (Williams, 1975). Due to limited available data, both the observed data and an internal mass balance method were applied for model validation.

4.2 Model concepts and methods

4.2.1 Model overview

The model framework, as shown in Figure 4.1, includes all the components with the input data, modelling methods and output variables for the XAJ-N model. The forcing variables mainly consist of climate variables, land use/cover, digital elevation model (DEM), social-economic data and agricultural practice. In general, the XAJ-N model is composed of three different

modules for estimating river discharge, sediment yield and nitrogen dynamics. The first module is water fluxes model which assesses amount of surface runoff and groundwater in the catchment based on the Xinanjiang model concept (Zhao et al., 1980; Zhao, 1992) using PCRaster. The second module applies the Modified Universal Soil Loss Equation (MUSLE) (Williams, 1975) to estimate the sediment yield and particulate nitrogen, and the third module uses the data produced by the hydrological model as input data to simulate nitrogen transport based on the Integrated Nitrogen CAtchment (INCA) model (Whitehead et al., 1998a, 1998b; Wade et al., 2002a). The model simulates N transport in a catchment scale at 200 m ×200 m grid with daily temporal resolution by using PCRaster (Wesseling et al., 1996).

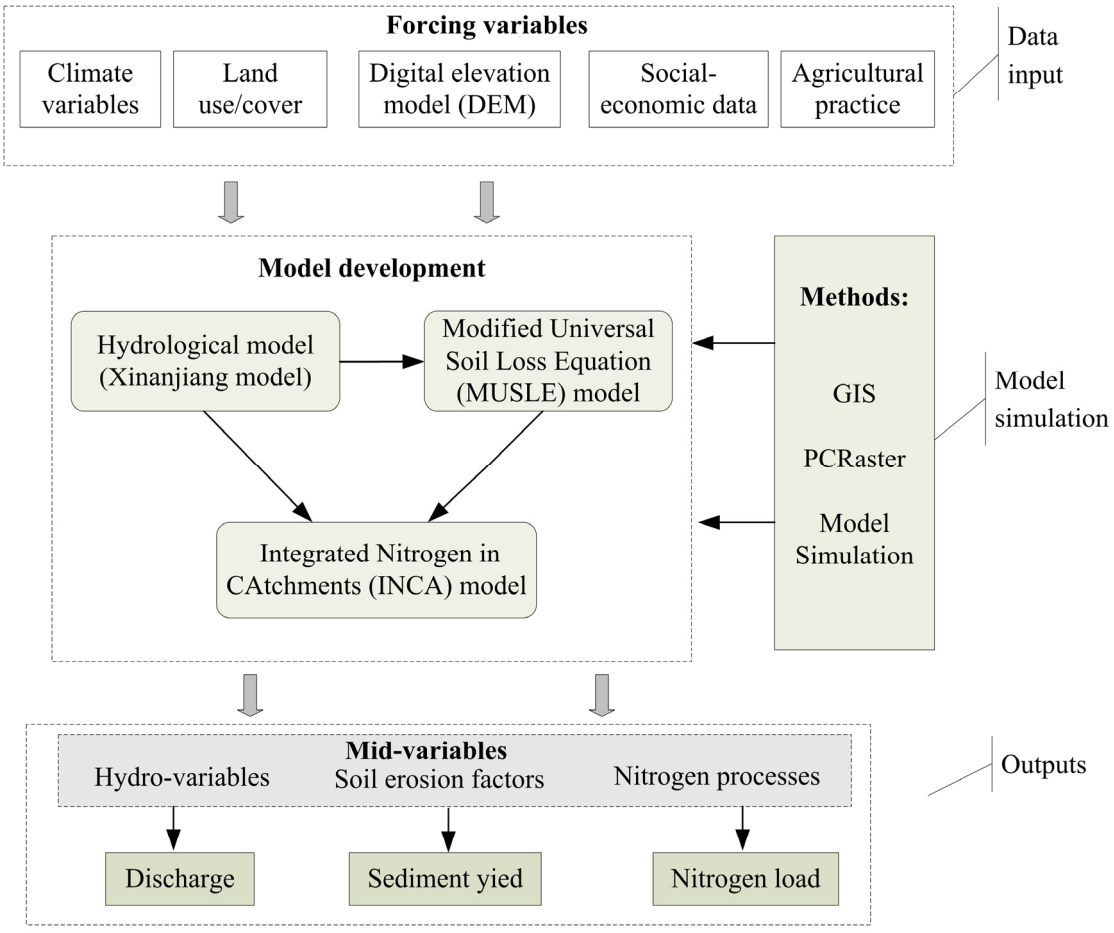

Figure 4.1: The framework of the nitrogen simulation in the XAJ-N model

4.2.2 Hydrological modelling

The water fluxes module, PCRaster-Xinanjiang (PCR-XAJ) model was developed by Zhao et al. (2009, 2011a), which is a simple raster-based hydrological model based on the Xinanjiang

model concept (Zhao et al., 1980; Zhao, 1992), and implemented in PCRaster. The model estimates surface water and groundwater flow based on grid calculation at daily step. The main feature of the PCR-XAJ model is the concept of runoff generation on repletion of storage, which means that runoff is not generated until the soil moisture content of the aeration zone reaches maximum capacity, and thereafter runoff equals the rainfall excess without further loss (Zhao, 1992). As shown in Figure 4.2, watershed heterogeneity is described with a parabolic curve representing the water storage capacity of the soil (Zhao et al., 1980). The mechanism of runoff generation and separation (Figure 4.2) in the Xinanjiang model was employed in the pervious areas (i.e. paddies, forests, arable land, and orchards). The runoff in the water bodies and urban areas is calculated separately. Both the overland flow and channel flow are calculated with one-dimensional kinematic wave equations, available as a built-in function in PCRaster. The groundwater routing is modeled as a simple, linear storage. A more detailed description of the PCR-XAJ model can be found in the developers' publication (Zhao et al., 2009, 2011a).

Water fluxes are the main agents for dissolved nitrogen transport between soil store and groundwater store. As illustrated in nitrogen simulation (Figure 4.2), several key processes (e.g. nitrification, mineralization, and denitrification) are soil moisture dependent. The parameter associated with soil moisture deficit is expressed as:

$$S_{smd} = \frac{SMD_{mx} - SMD}{SMD_{mx}} \tag{1}$$

where SMD is the daily soil moisture deficit (mm) and SMD_{mx} is the maximum soil moisture deficit (mm). The daily outflow from the surface reactive soil zone (RS , m d^{-1}) and deeper groundwater zone (R_{gw} , m d^{-1}) are directly calculated by PCR-XAJ model (Figure 4.2).

4.2.3 Nitrogen processes

The nitrogen simulation is based on the concept of the Integrated Nitrogen in CAtchments (INCA-N) model (Wade et al., 2002a). The INCA-N model is a semi-distributed, dynamic nitrogen model which simulates the nitrogen dynamics in the soil, groundwater stores and streams of large catchments, considering different sources of N (deposition, manure, and fertilizers) in different land use (Wade et al., 2002a).

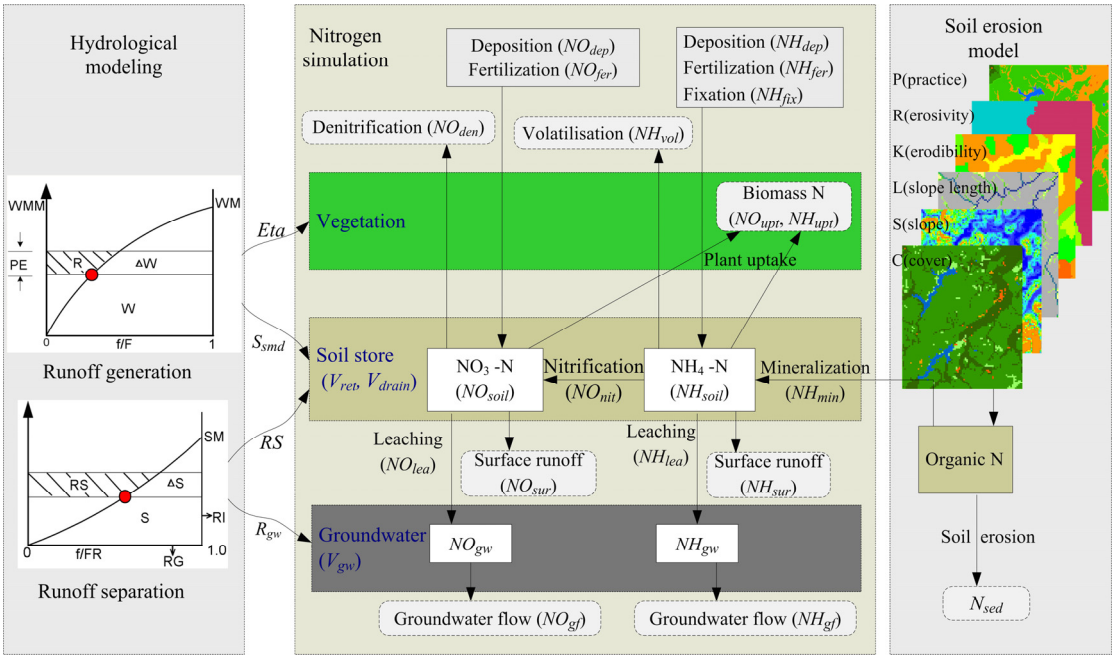

Figure 4.2: Model components integration in the XAJ-N model by using PCRaster

As shown in Figure 4.2, the nitrogen added to each grid cell is stored in the soil store or transported directly or through the groundwater to the surface water which is routed to the river. The key processes and N transformations are assumed to occur in the plant/soil system, comprising of plant uptake, ammonia volatilization, nitrification, denitrification, mineralization, immobilization, and nitrogen fixation (Figure 4.2). The N fertilization is considered as the main input from diffuse sources into the soil store. The nitrogen balance of each grid cell within each land-use type is calculated by adding up the input amounts (inorganic fertilizers, manure excretion by livestock, atmosphere deposition, and biological fixation in the field). Subsequently, the nitrogen is leached to either the groundwater store or transferred directly to the rivers by surface runoff, lost to the atmosphere, or stored in the soil. In the groundwater store, it is assumed that no biogeochemical reactions occur and that a mass balance of ammonia and nitrate is adequate (Wade et al., 2002a).

In the soil store, plant uptake of nitrate nitrogen (NO_3^--N) is assumed to be temperature and soil moisture dependent:

$$NO_{upt} = \frac{C_{upt,no} \cdot S_{smd} \cdot S_{plant} \cdot NO_{soil}}{V_{ret} + V_{drain}} \quad (2)$$

where NO_{soil} is the nitrate nitrogen mass (kg N ha^{-1}) in the soil store, $C_{upt,no}$ is the

nitrate-uptake rate by the plant in kg N ha^{-1} d^{-1}/(kg N ha^{-1} m^{-1}) which simplifies to m d^{-1}, V_{ret} and V_{drain} are the retained and drainable water volumes in the soil (m), respectively, which are calculated in the hydrological module. The drainable water volume represents the water volume stored in the soil that responds more slowly and may make up the majority of water storage in the soil (Wade et al., 2002a). The parameter S_{plant} is a seasonal plant growth index, which simulated an increase and decrease in plant nutrient demand based on the time of year (Wade et al., 2002a).

The daily fluxes of NO_3^--N associated with surface runoff (NO_{sur} , kg N ha^{-1} d^{-1}), and leaching (NO_{lea} , kg N ha^{-1} d^{-1}) are defined as:

$$NO_{sur} = \frac{RS \cdot NO_{soil}}{V_{ret} + V_{drain}} \tag{3}$$

$$NO_{lea} = \frac{\nabla S \cdot NO_{soil}}{V_{ret} + V_{drain}} \tag{4}$$

where ∇S denotes the water infiltrated from soil to groundwater in a fixed day (m d^{-1}).

The amount of daily nitrification can be calculated as:

$$NO_{nit} = \frac{C_{nit} \cdot S_{smd} \cdot NH_{soil}}{V_{ret} + V_{drain}} \tag{5}$$

where NH_{soil} is NH_4^+-N mass in the soil store (kg N ha^{-1}), and C_{nit} is the nitrification rate in kg (NO_3^-) N ha^{-1} d^{-1}/(kg (NH_4^+) N ha^{-1} m^{-1}. In the calculation process, the model only considers the amount of elementary nitrogen, and then the unit of C_{nit} can be simplified to m d^{-1}. Denitrification is the bacterial reduction of nitrate, NO_3^-, to N_2 or N_2O gases under anaerobic (reduced) conditions, and the total amount (NO_{den} , kg N ha^{-1} d^{-1}) equals to:

$$NO_{den} = \frac{C_{den} \cdot S_{smd} \cdot NO_{soil}}{V_{ret} + V_{drain}} \tag{6}$$

Similary, the parameter C_{den} denotes the denitrifcation rate in kg N ha^{-1} d^{-1}/(kg N ha^{-1} m^{-1})

which simplifies to m d^{-1}.

The non-biological fixation is expressed as:

$$NO_{fix} = C_{fix} \tag{7}$$

where C_{fix} is the non-boilogical fixation rate (kg N ha^{-1} d^{-1}).

Thus, the change of nitrate mass in the soil store is calculated as:

$$\Delta NO_{soil} = NO_{fer} + NO_{dep} + NO_{nit} + NO_{fix} - NO_{sur} - NO_{den} - NO_{upt} - NO_{lea} \tag{8}$$

where NO_{fer} and NO_{dep} are the input rates of NO_3^--N for fertilizer application (kg N ha^{-1} d^{-1}) and atmosphere deposition (kg N ha^{-1} d^{-1}), respectively.

In the groundwater store, the change of nitrate nitrogen equals to:

$$\Delta NO_{gw} = NO_{lea} - \frac{R_{gw} \cdot NO_{gw}}{V_{gw}} \tag{9}$$

where NO_{gw} is nitrate nitrogen in the groundwater store (kg N ha^{-1}), and V_{gw} is the groundwater drainage volume (m).

As for NH_4^+-N, the daily fluxes of ammonium associated with surface runoff, plant uptake, leaching, immobilization, and volatilization are, respectively, calculated as:

$$NH_{sur} = \frac{RS \cdot NH_{soil}}{V_{ret} + V_{drain}} \tag{10}$$

$$NH_{upt} = \frac{C_{upt,nh} \cdot S_{smd} \cdot S_{plant} \cdot NH_{soil}}{V_{ret} + V_{drain}} \tag{11}$$

$$NH_{lea} = \frac{\nabla S \cdot NH_{soil}}{V_{ret} + V_{drain}} \tag{12}$$

$$NH_{imb} = \frac{C_{imb} \cdot S_{smd} \cdot NH_{soil}}{V_{ret} + V_{drain}}$$

$$NH_{vol} = \frac{C_{vol} \cdot S_{smd} \cdot NH_{soil}}{V_{ret} + V_{drain}} \quad (13)$$

where $C_{upt,nh}$, C_{imb} and C_{vol} are the rates for NH_4^+-N plant uptake (m d^{-1}) immobilization (m d^{-1}) and volatilization (m d^{-1}), respectively.

The minelization is soil moisture dependent, which is calculated as:

$$NH_{min} = C_{min} \cdot S_{smd} \quad (14)$$

where $C_{upt,nhvol}$ is the mineralization rate (kg N ha^{-1} d^{-1}). The nitrogen cycle in the INCA model is basically a mixture of linear and first order kinetics function (Whitehead and Toms, 1993). N fixation from atmosphere and N mineralization from soil organic pool are described by linear equations and having unit kg N ha^{-1} d^{-1}. The other processes such as denitrifcation or nitrification are described as first order kinetics. Since calculation was undertaken based on nitrogen mass balance (elementary N), the units of the parameters $C_{upt,no}$, $C_{upt,nh}$, C_{den}, C_{nit}, C_{imb} and C_{vol} can be simplified to m d^{-1}.

The change of NH_4^+-N in soil store is calculated as:

$$\begin{aligned} \Delta NH_{soil} &= NH_{fer} + NH_{dep} + NH_{min} \\ &\quad - NH_{sur} - NH_{imb} - NH_{upt} - NH_{lea} - NO_{nit} - NH_{vol} \end{aligned} \quad (15)$$

where NH_{fer} and NH_{dep} are the input rates of NH_4^+-N for fertilizer application (kg N ha^{-1} d^{-1}) and atmosphere deposition (kg N ha^{-1} d^{-1}).

In the groundwater store, the change of NH_4^+-N equals to:

$$\Delta NH_{gw} = NH_{lea} - \frac{R_{gw} \cdot NH_{gw}}{V_{gw}} \quad (16)$$

where NH_{gw} is the ammonium nitrate in the groundwater store (kg N ha^{-1}).

Organic N attached to soil particles is transported by surface runoff to the main channel. This form of nitrogen is associated with the sediment loading from the field. The amount of organic nitrogen is calculated with sediment yield by the soil erosion model, as shown in Figure 4.2. In-stream attenuation is estimated by the method of two retention parameters described in detail in Loos et al. (2009).

4.3 Study area and data input

4.3.1 Study area

The Xitiaoxi catchment, covering more than 2200 km^2, is located in the upstream of Taihu Lake in southeastern China (Fig. 3). The Xitiaoxi River, also known as "Western Tiaoxi River", together with Eastern Tiaoxi River are two of the most important tributaries in the Taihu Basin. The Xitiaoxi River, with its length of 159 km, supplies 27.7% of the water volume of Taihu Lake. High mountainous and hilly area are distributed in the southwest with maximum elevation of 1585 m (above mean sea level), whereas low alluvial plains lie in the northeastern parts with a well developed drainage network. The whole catchment is characterized by a semitropical climate with mean annual rainfall of about 1465 mm.

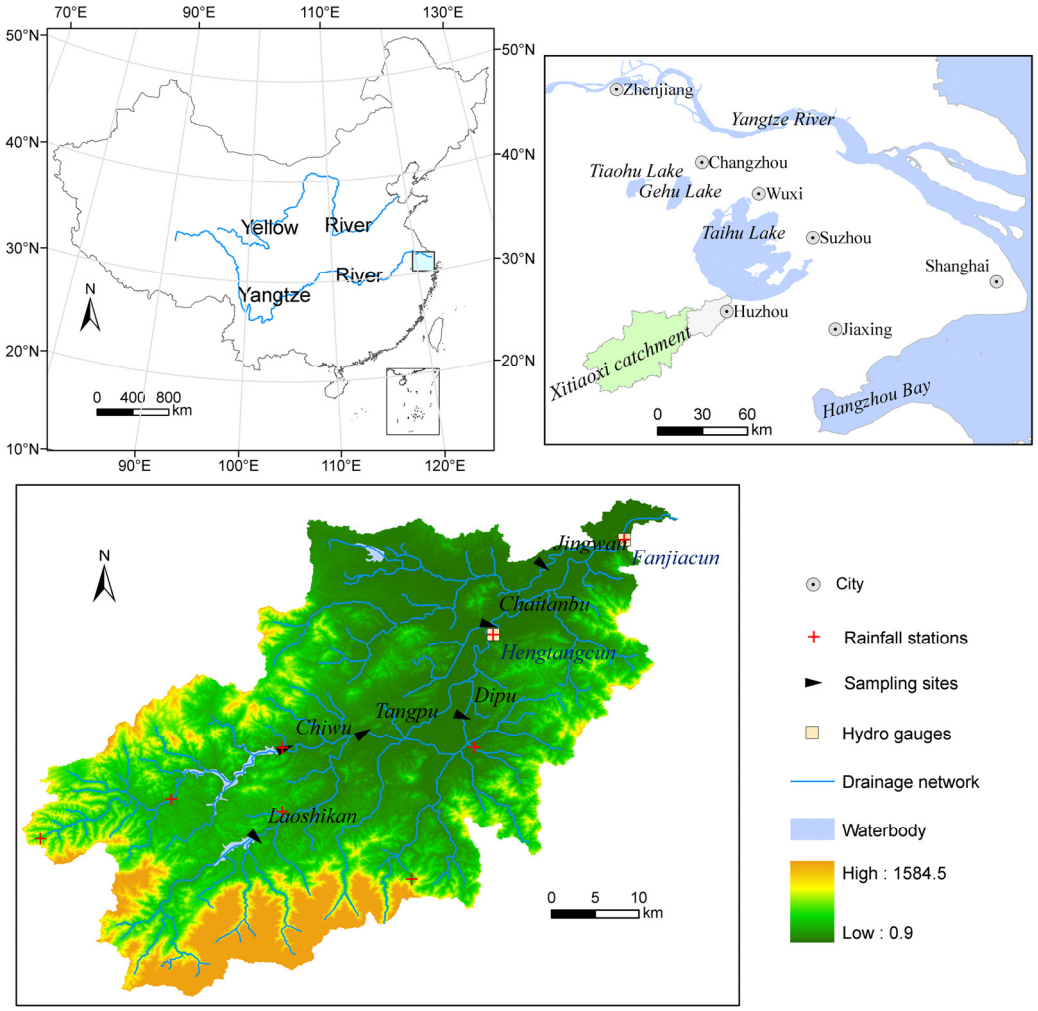

Figure 4.3: Location of the study area and monitoring sites (Li et al., 2004a)

4.3.2 Data input

The satellite images from Landsat 7 Enhanced Thematic Mapper (ETM) sensor acquired on October 11, 2001 (http://glcfapp.umiacs.umd.edu:8080/esdi/index.jsp) were used for extracting the river network and land use maps by using an unsupervised classification method. The land use/cover information was used for runoff generation, nutrient uptake calculation, crop management factors and Manning's roughness coefficients derivation based on the literature (Chow et al., 1988). Figure 4.4 shows the land use in the catchment. About 62.4% of the upper reaches are covered with forest, and three quarters are planted with bamboo. About 25.6% of the catchment is paddy land, which is mostly located in the low alluvial plains. A fraction of about 4.1% is farmland. Other negligible land uses classes are residential area of 1.9% and grassland and surface water area of 6%. Red earth, skeleton soil and paddy soil are the main soil

types (Figure 4.4), contributing about 82.4% of total area (Zhang et al., 2006).

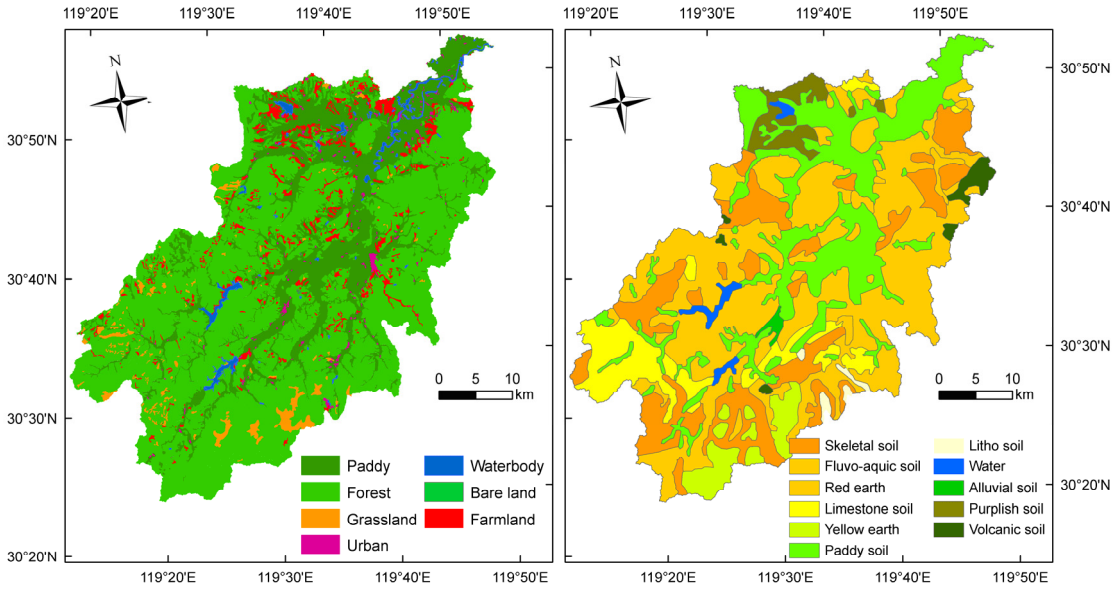

Figure 4.4: Land use and soil classification in the Xitiaoxi catchment

A digital elevation model (DEM) with a resolution of 25m×25m was obtained from the Nanjing Institute of Geography and Limnology (NIGLAS), Chinese Academy of Sciences. The DEM was used to derive the hydrologic parameters of the catchment, i.e. slope, local drainage direction (LDD). To avoid producing a large number of pixels for the catchment and much more model running time, a grid size of 200m×200 m was selected for continuous daily simulation. All the spatial data such as land use, DEM (Figure 4.3) and soil map were resampled to the same resolution. The local government Anji Hydrology Bureau provided long-term continuous hydro-climatic data. Eight rainfall stations (Figure 4.3) with daily precipitation during the period from 1978 to 2007 were available for hydrological simulation. Daily temperature at Anji and pan evaporation of two stations at Anji and Fanjiacun were collected (Table 4.1).

Table 4.1 Overview of data for hydrological modelling and nutrients balance simulation

Data	Year	Resolution	Source
Digital elevation model	--	25m	Nanjing Institute of Geography and Limnology
Land cover	2001	30m	Landsat 7 ETM 2001, Oct, 11.
Soil properties	--	1:100000	Soil database [a]
Daily temperature	1979-2007	1 station	Anji Hydrology Bureau
Precipitation	1979-2007	8 stations	Anji Hydrology Bureau

Evaporation	1978-2007	2 stations	Anji Hydrology Bureau
Streamflow	1978-2007 [b]	2 stations	Anji Hydrology Bureau
Fertilizer application	1999-2007	town level	Huzhou Bureau of statistics [c]
Livestock numbers	2000-2007	town level	Huzhou Bureau of statistics [c]
Population distribution	2000	1km^2	DSIESS [d]
Crop yield (harvest)	1999-2007	county level	Huzhou Bureau of statistics [c]
Water quality data	1999-2007	6 sites	Anji Environmental Monitoring Centre

[a] http://www.soil.csdb.cn

[b] Daily observed discharge: Hengtangcun (1978-2007), Fanjiacun (1978-2001).

[c] http://www.hustats.gov.cn (Visited on 2009, Nov, 12.)

[d] DSIESS: Data Sharing Infrastructure of Earth System Science, www.geodata.cn

The Xitiaoxi catchment has an intensive multi-cropping system with alternating alluvial lowland summer rice - upland winter rapeseed or wheat rotations and integrated livestock breeding, fishery persisting over several centuries. According to annual statistics in 2005 (http://www.hustats.gov.cn), the agricultural crops mainly include rice (16085 ha), rapeseed (5268 ha), vegetables (6034 ha), beans (3224 ha) and sweet potato (2006 ha) etc. The agricultural practices are strongly associated with the local climate conditions (i.e. precipitation and temperature). Rice is planted in mid June, and is harvested in October. Rape is planted in the end of October and harvested between the end of May and the beginning of June in the subsequent year. The diffuse emission data such as fertilizer and manure application, population distribution and livestock number are collected from yearbooks of Zhejiang Provinces (Table 4.1). The N input from the atmospheric deposition and fertilization is shown in Figure 4.5. The amount and date of fertilizer application correspond to common practice in the region (Tian et al., 2001; Roelcke et al., 2002), with amounts near/above 300 kg ha^{-1} per crop, thus attributing to large-scale non-point source agricultural pollution of water bodies.

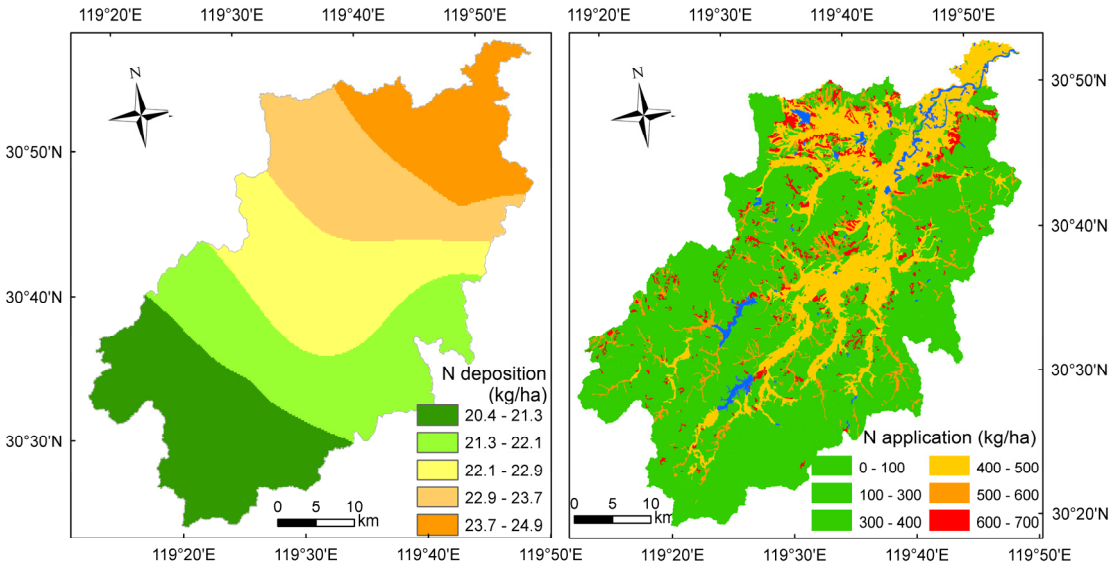

Figure 4.5: N atmospheric deposition and fertilizer application rates in the Xitiaoxi catchment

The sewage from rural areas is regarded as surface point source pollutions because there is no drainage system. Excretion from livestock is considered as animal manure since it is used as fertilizers onto farmland. Previous studies provided similar indices of human and livestock emissions (Pieterse et al., 2003; Lai et al., 2006); so that here the average annual emission rates are used, i.e. total nitrogen 3.5 kg per person, and 0.183 kg per unit weight of livestock. The nutrient loads from the point sources were calculated according to the relationship between nutrient export rates and industrial productions in 1999 for the catchment (Li et al., 2004a).

4.3.3 Model verification

There are 30 years (1978-2007) of continuous daily streamflow records at Hengtangcun (1308 km^2) and 24 years (1978-2001) at Fanjiacun station (1914 km^2) for model calibration and validation. After the initial "warm-up" period, 9 years of continuous daily discharge was used for both calibration and validation. A general description about the discharge prediction is displayed in the present study, since the details have been shown in Zhao et al. (2009, 2011a). The parameters were firstly initialized from the literature (Zhao, 1992; Wade et al., 2002a), and then adjusted by trial-and-error method until model simulations satisfactorily matched the measured data. The detailed description and the values of parameters in the model are displayed in Table 4.2. The parameters values and their sensitivities in the hydrological model have been stated in Zhao et al. (2011a). The parameters in the nitrogen simulation are mainly derived from Wade et al. (2002a), and then calibrated by comparing the simulated with

measured values. The observed nutrient data surveyed bi-monthly at six sites of the catchment (Figure 4.3) from 1999 to 2007 were used for model performance evaluation. Due to the limitation of the available measured data, we divided the six monitoring sites into two parts for model calibration (Laoshikan, Tangpu and Jingwan) and validation (Chiwu, Dipu and Chaitanbu), respectively. The model efficiencies according to the Nash-Sutcliffe efficiency (NE) (Nash and Sutcliffe, 1970) and correlation coefficient (R^2) were calculated at daily resolution as criteria for goodness-of-fit. The objective for each constituent of interests was to maximize the model coefficients NE and R^2.

Table 4.2 Parameters in the hydrological and nutrients processes simulation

Parameter	Description	Value estimation	Value
Hydrology			
K	Ratio of potential evapotranspiration to pan evaporation	0.8-1.2	1.02
b	Exponent of the tension water capacity parabolic curve	0.1-0.4	0.4
WM	Areal mean tension water capacity	80-170 mm	110
SM	Areal mean free water capacity of the surface soil	5-45 mm	40
Ex	Exponent of the free water capacity curve	0.5-2.0	1.4
KG	Outflow coefficient of the free water storage to groundwater	KG + KSS = 0.7-0.8	0.45
KSS	Outflow coefficients of the free water storage to interflow		0.25
KKG	Recession constant of groundwater storage	0.95-0.995	0.98
KKSS	Recession constant of lower interflow storage	0.5-0.9	0.5
Nutrients			
C_{den}	Denitrification rate (m day^{-1})	0.01-19	0.8
C_{fix}	Non-biological fixation rate (kg N ha^{-2} day^{-1})	0.000-0.0001	0.004
$C_{upt,no}$	Plant uptake rate for nitrate (m day^{-1})	0-162	30
C_{nit}	Nitrification rate (m day^{-1})	1-54	1.02
C_{min}	Mineralization rate (kg N ha^{-2} day^{-1})	1-292	2.3
C_{vol}	Volatilization rate (m day^{-1})	0.00-1	0.79
$C_{upt,nh}$	Plant ammonium uptake rate (m day^{-1})	0-162	4.73

4.4 Results and discussion

4.4.1 Hydrological modelling

Figure 4.6 shows the hydrographs of the measured and simulated discharge at Hengtangcun and Fanjiacun stations. Overall, the model performance was satisfactory in both the calibration and the validation periods. The results show a good correlation between measured and simulated daily discharge at Hengtangcun station with NE in a range of 0.77 and 0.81 and R^2 from 0.79 to 0.83 for the studied period. Comparably, the simulated results at Fanjiacun station matched adequately well with the observed discharge. The NE and R^2 efficiencies for daily discharge lie in the similar range with that of Hengtangcun.

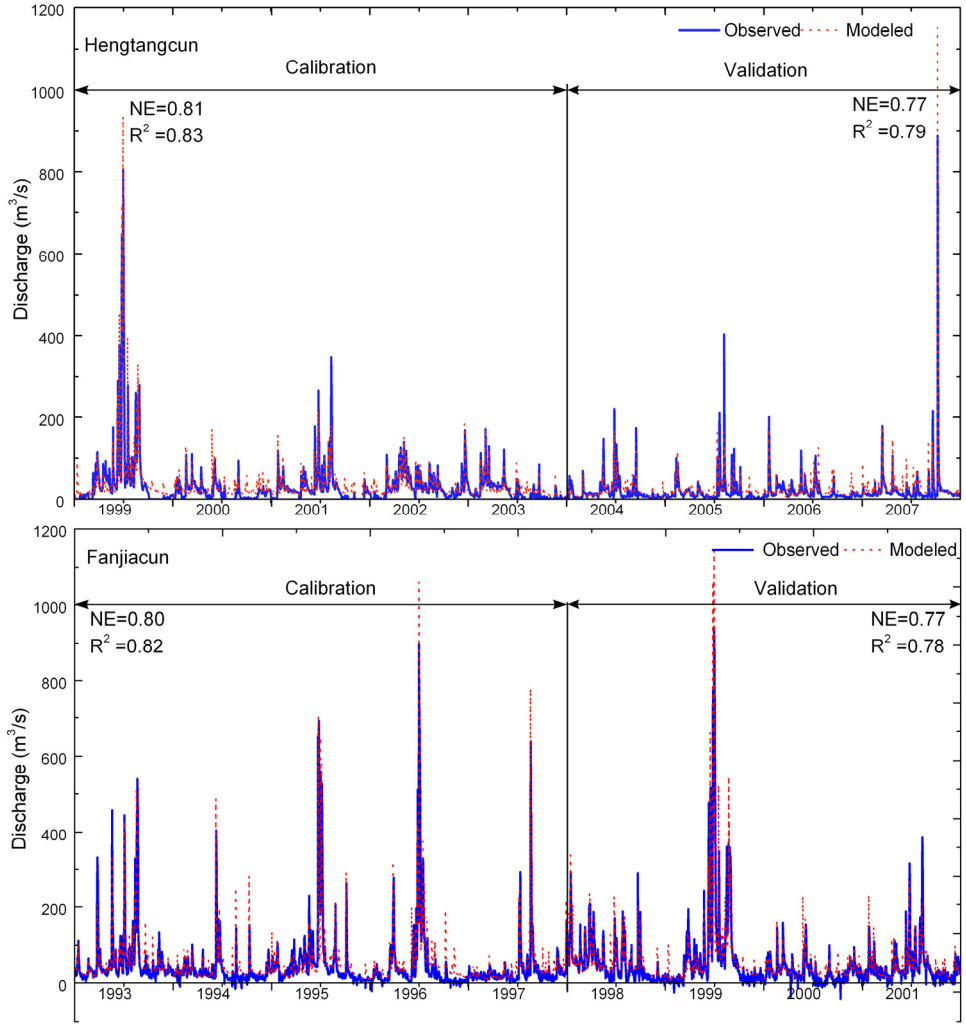

Figure 4.6: Comparison of daily measured and modeled discharge in the Xitiaoxi Catchment

Although the model presented satisfying results between the observed and modelled discharge,

some flood peaks occurring in the summer were overestimated. This may be caused by the two reservoirs located in the upstream of the catchment. The reservoirs are used for irrigation during dry season and flood control in rainy season as well as electricity production. In addition, the return flow from Taihu Lake leads to some negative discharge values at Fanjiacun station, which can not be estimated by the present model.

4.4.2 Nitrogen simulation

Nutrient loads are calculated by multiplying the nutrient concentration at Chaitanbu site with observed discharge at Hengtangcun station. We assumed that these two stations were suitable to calculate nutrient loads since they are almost located in the same place. In addition, nutrient concentrations at six monitoring sites (Figure 4.3) are also used for model performance evaluation.

Total nitrogen

Figure 4.7 presents the simulated and observed TN loads at Chaitanbu from July of 2002 to 2005. It can be clearly seen that the modelled TN loads fit generally well to the observed loads with NE=0.41. Nevertheless, some observed values are extreme lower than the modelled loads due to over-predicted discharge in winter season.

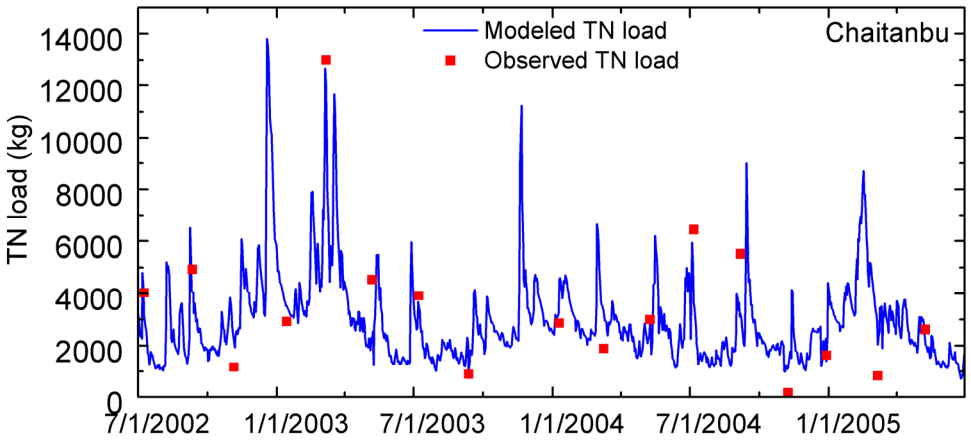

Figure 4.7: Daily observed and simulated TN load at six monitoring sites

The simulation results for TN show a pronounced seasonal variation in line with the observed high TN loads in rainy season (Figure 4.7). Furthermore, the variation of nitrogen loads between wet years and dry years is adequately simulated by the model. In addition, simulated results present seasonal trends with higher TN concentration in summer and winter during the

early growing season of rice, rapeseed and wheat. In the studied catchment, rice is transplanted in early June while rapeseed and wheat are transplanted and sown in late October. It was during these periods that large amount of chemical fertilizer and organic manures were applied as basal or after dressing (Gao et al., 2004). Li et al., (2004a) investigated the relationship between land use patterns and nutrient concentration in the runoff, and assessed nutrient loads using an export coefficients model in the same catchment. They found that annual export of nitrogen was about 1589 t yr^{-1} from diffuse sources and total nitrogen export of the catchment was approximately 2031 t yr^{-1} at Jingwan site. However, our simulation results show a range of 887 to 1475 t yr^{-1} in total nitrogen export at Chaitanbu in the upstream of Jingwan (Figure 4.3), which was a little lower than their estimations. This may be attributed to the estimation based on the different outlets. In addition, the excrement of human and livestock were taken into account in our study, but the industrial point source pollutions can not be estimated accurately in the current model due to limited available dataset.

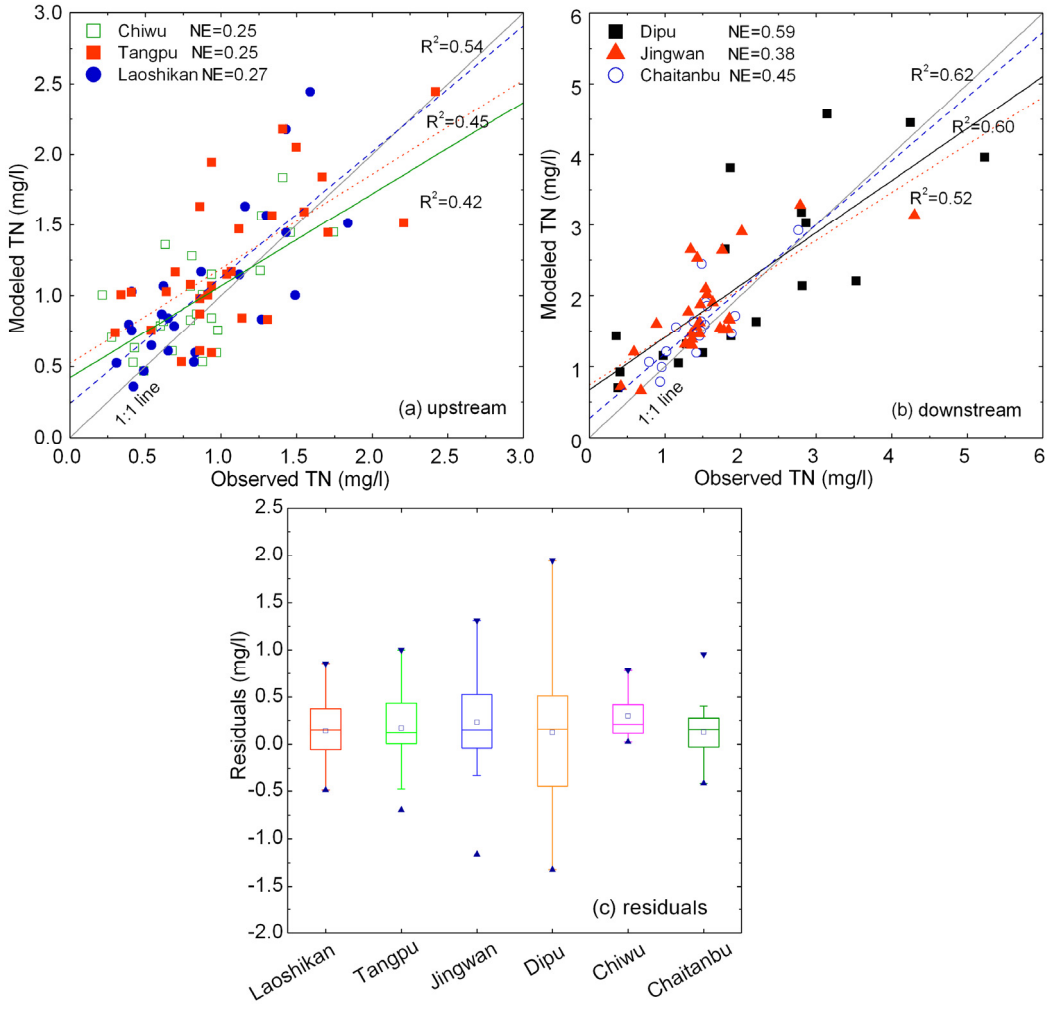

Figure 4.8: Daily observed and simulated TN concentrations at six monitoring sites in the

Xitiaoxi catchment

In order to evaluate the model performance, we additionally compared the simulated TN concentrations at six different sites with discontinuous daily monitoring data in the Xitiaoxi catchment. Figure 8 displays the observed and simulated TN concentrations along with 1:1 line at six monitoring sites along the river. The simulation values match relatively well with the measured values for both calibration and validation at different sites. In contrast, the simulated results display good agreement with observed values in the downstream sites, presenting both higher Nash-Sutcliffe coefficients between 0.38 and 0.59 and R^2 from 0.52 to 0.62 (Fig. 8b). The TN concentrations in the downstream (Dipu, Jingwan, and Chaitanbu) have a broader range of 0.5-5.2 mg/l in observed data and 0.6-4.5 mg/l in the modelled values. However, the simulated results are slightly worse with lower Nash-Sutcliffe coefficients in a range of 0.25 and 0.27 and R^2 between 0.42 and 0.54 in the upstream sites (Chiwu, Tangpu, and Laoshikan) (Figure 4.8a). The residuals present spatial distribution of the simulated results errors (Figure 4.8c), which indicate that the simulated TN concentrations are evidently distinguished from the observed values at Dipu site due to point source emissions from Anji County.

Ammonium nitrogen

Figure 4.9 displays the modelling results of ammonium nitrogen load at Chaitanbu site from 1999 to 2007. Compared with observed values, the ammonium load simulation is moderate satisfactory. Although the model generated the mean long-term ammonium load as well as the seasonal variability, some years do not show a perfect match, which is partly attributed to the discharge simulation that indicates an over/under prediction in peak flow. Additionally, the model slightly overestimates ammonium loads in winter season (from November to January of subsequent year), which is probably largely due to an overestimation of streamflow.

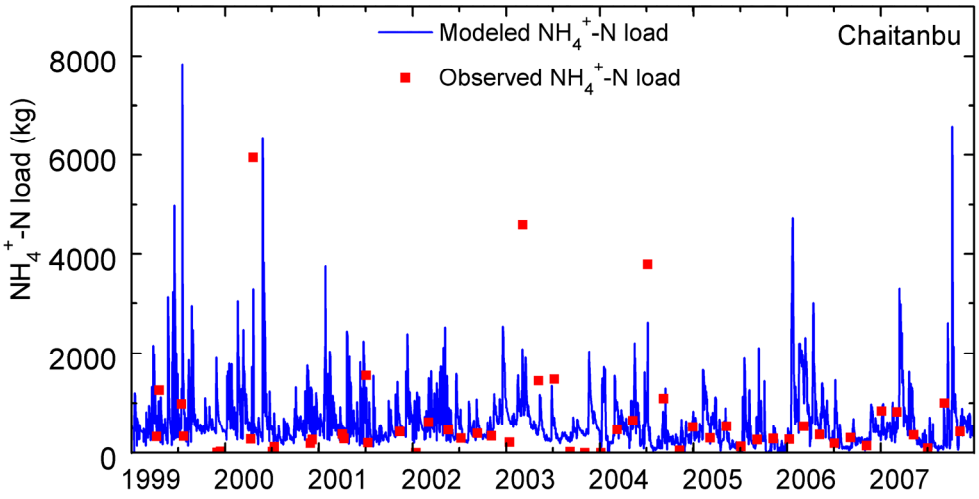

Figure 4.9: Daily observed and simulated ammonium nitrogen load at Chaitanbu

The simulation results shows NH_4^+-N load in a range from 304 t yr^{-1} to 561 t yr^{-1}, which accounts for 38-40% of TN load. Compared with Li et al. (2004a), the results in our study were acceptable and reasonable. Liang et al. (2008) estimated the NH_4^+-N load from 1995 to 2001 (except 1998 and 2000) based on the relationship between land use and concentration of NH_4^+-N in runoff using functions of Geographic Information Systems. The results suggested that the mean annual loads of NH_4^+-N varied between 0.92 and 3.52 kg ha^{-1} yr^{-1} for the whole catchment. This is much higher than our simulation results (0.23-0.43 kg ha^{-1} yr^{-1}). The differences may be caused by the point sources from Huzhou city in the downstream of the catchment.

Figure 4.10 shows scattergram of the observed and measured NH_4^+-N concentrations at six different sites and their distribution along with the 1:1 fit line. The NE values between 0.19 and 0.48 and R^2 from 0.41 to 0.62 indicate an acceptable relationship between the observed and simulated NH_4^+-N concentrations for both calibration and validation at six sites (Figure 4.10a and b). Apparently, the lowest NE and R^2 values were found at Dipu site near Anji County, which probably resulted from the point sources pollution. In contrast, the simulation results at the upstream sites are relatively better than those in the downstream. This may be due to the uniform land use components and rare anthropological activities in the upstream of the catchment.

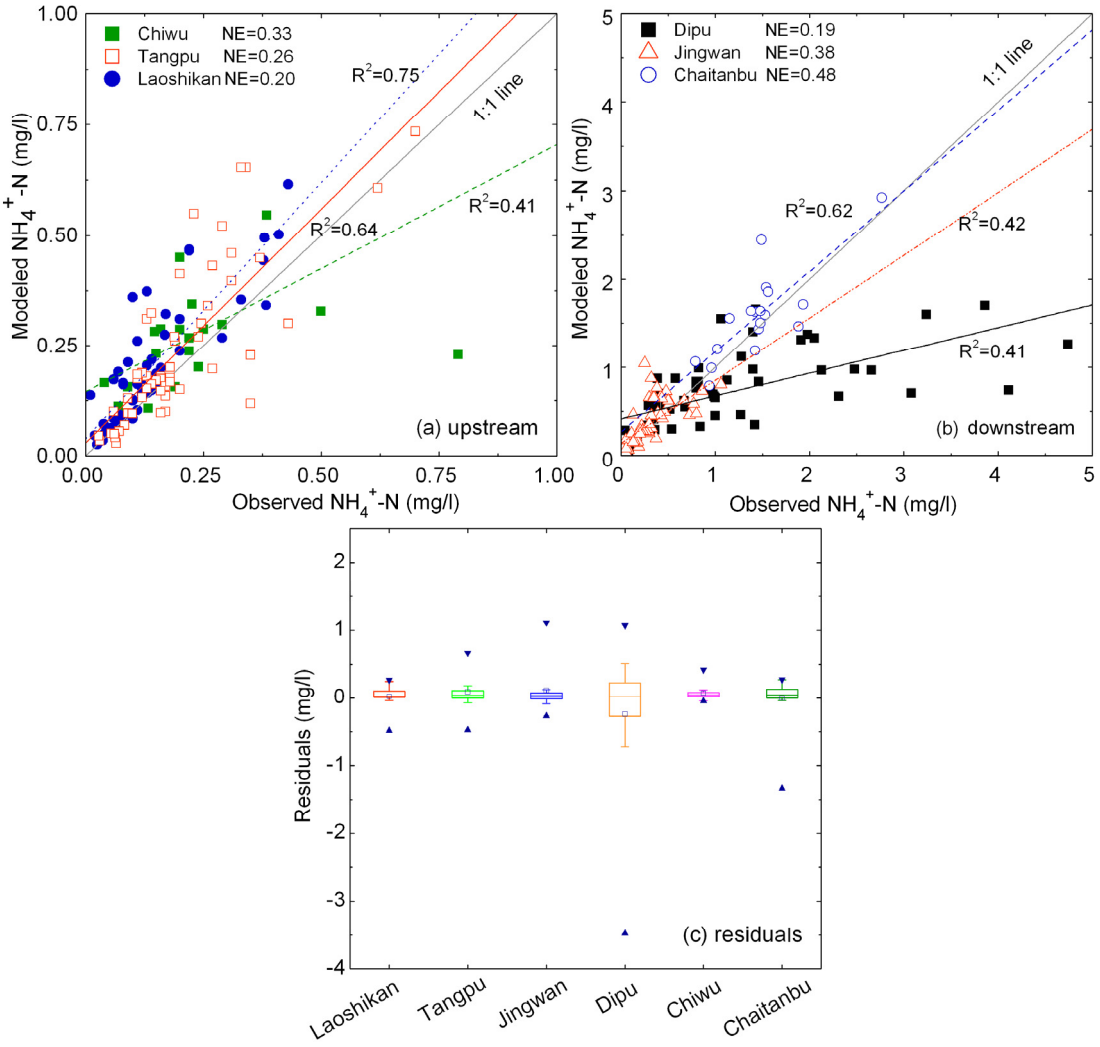

Figure 4.10: Daily observed and modelled ammonium nitrogen concentration at six monitoring sites in the Xitiaoxi catchment

As well, NH_4^+-N concentrations simulation shows large variances in the spatial distribution of the catchment. As shown in Figure 4.10b, NH_4^+-N concentration at Dipu has much wider range from 0.04 mg/l to 4.86 mg/l in observed values, whereas the simulated content of NH_4^+-N is relatively lower, between 0.22 mg/l and 1.67 mg/l. Furthermore, other sites (Chaitanbu and Jingwan), located in close vicinity of the towns, illustrate relatively higher contents of NH_4^+-N. This is also consistent with the spatial distribution of residuals between observed and modelled NH_4^+-N concentrations at these sites (Figure 4.10c).

In the Xitiaoxi catchment, previous study also reported that the NH_4^+-N in the south part was much higher than those in the north part of the catchment (Liang et al., 2008). High concentrations of ammonium nitrogen characterize the point source pollution coming from

domestic sewage and urban waste water. The high content of NH_4^+-N in the waterbody is not likely to come from farmland, because soil has a fairly strong capacity of adsorbing NH_4^+-N, and NH_4^+-N fertilizers applied to paddy fields would only likely flow into rivers with overspill as a result of a heavy storm right after application of the fertilizer. This is, however, a rare case (Xing et al., 2001). For example, higher NH_4^+-N concentration at Dipu was attributed by the point source pollution from Anji County. Municipal sewage and industrial wastewater are discharged into the river by drainage system which may make a great contribution to higher NH_4^+-N concentration.

4.4.3 Nitrogen balance analysis

Nitrogen supply

Due to data limitation, not only the observed nutrient data surveyed bi-monthly at six sites of the catchment were used of evaluated the model performance, but also a hindcast method was introduced to analyze the nutrient balances in the catchment. Table 4.3 shows the simulated nutrient processes compare to the values in published literature.

Fertilizer application

On an annual basis, the total N input in the arable land of the catchment fall in a range of 425-635 kg N ha^{-1}, consistent with application level in the Taihu region. The total N-fertilizer application rates in arable lands in the Taihu Basin at present are 550-650 kg N ha^{-1} yr^{-1} to two crops, much higher than the national average of about 300 kg N ha^{-1} (Zhu et al., 2000). In such a mesoscale catchment, the N inputs flux varied spatially and temporally due to land use components, agricultural practices and human activities. The highest inorganic fertilizers application rate occurred in vegetables land, followed by crops such as paddy, wheat and rapeseed. During the growing season (from April to October), arable lands received the large amount of fertilizers.

Atmospheric deposition

Except for fertilizer application, atmospheric deposition is an important source of total N inputs. The deposition rates are assumed 12.5-14.3 kg NH_4^+-N and 9.2-11.5 kg NO_3^--N in the model, which is the average measured values in this region (Wang et al., 2004c). Compared with other regions, previous studies indicated that intensive agriculture and coal combustion are the main contributors to higher rates of atmospheric nitrogen deposition in the Taihu Basin (Chen and

Mulder, 2007; Luo et al., 2007). Both Wang et al. (2004) and Luo et al. (2007) stated that NH_4^+-N and NO_3^--N were the main components of atmosphere deposition. The average annual NH_4^+-N deposition was about 12.8 kg ha^{-1}, and NO_3^--N was in a range of 8.35-9.48 kg ha^{-1}. The total nitrogen input by wet deposition was between 22.0 and 27.0 kg ha^{-1} (Wang et al., 2004c).

Mineralization

Estimated average N mineralization (74-167.3 kg N ha^{-1} yr^{-1}) contributed less than 25% of the N sources in the arable land. This was relatively higher than the measured values (84 kg N ha^{-1} yr^{-1}) by Roelcke et al. (2002), who investigated the nitrogen mineralization in the paddy land of the Taihu region under aerobic conditions. The present study indicated higher mineralization rates compared to UK (62 kg N ha^{-1} yr^{-1}) (Whitehead et al., 1998a). As for the forests, the estimated mineralization rates lay in the range of 26-35.6 kg N ha^{-1} yr^{-1}. According to the observations in China, the simulation results were acceptable. Torstveit (2000) reported average net N mineralization rates of about 0.4 kg N ha^{-1} d^{-1} in the period April-May in South China. Other studies found N mineralization rates in the tropical rain forest in July of 0.22 kg ha^{-1} d^{-1} (Sha et al., 2000) and 0.29 kg ha^{-1} d^{-1} (Zhou, 2000).

Biological fixation

Comparably, N fixation rate contributed a small proportion of the overall N input due to the small areas of legume crops in the catchment. In most other studies, the biological nitrogen fixation was even ignored since its limited contribution in the nitrogen balance (Roelcke et al., 2002; Wang et al., 2007).

Table 4.3 Comparing simulated nitrogen processes of Xitiaoxi catchment with published literature

Process	Land cover	Present study (kg $ha^{-1}yr^{-1}$)	Values in literatures (kg ha^{-1} yr^{-1})	Literature sources
N uptake	Forest	26.7-58.4	11-44	Zhu, 1997
	Arable	246-375	257-320	Richter and Roelcke, 2000
Fixation	Forest	1.45	0.32, <1-2	Granhall, 1981
	Arable	4.3	2.7	Chen et al., 2008b
Fertilizers	Forest	0; 155(bamboo)	0, 300-600 (intensive managed)	Xu et al., 2008

	Arable	425-635	164-635	Chen et al., 2001
Deposition	Forest	12.5-14.3	22	Luo et al., 2007
	Arable	NH_4^+-N,9.2-11.5 NO_3^--N	27	Wang et al., 2004c
Mineralization	Forest	26-35.6	15-120	Smolander et al., 1998
	Arable	74-167.3	84	Han et al., 2001
			62	Whitehead et al., 1998a
Denitrification	Forest	0.03	2.0	Brumme et al., 1999
			<1	Gundersen and Bashkin, 1994
	Arable	18.4-39.6	16-29.3	Xing, 1998
			32	Han et al., 2001
Volatilization	Forest	1.1-3.05		
	Arable	12.7-37.9	8.4-24.2.	Tian et al., 2001
			42.1	Chen et al., 2008b
Nitrification	Forest	1.65-4.7	0-7	Martikainen, 1984
	Arable	93.2-154.8	124-175	Rankinen et al., 2004
Leaching	Forest	1.16-13.4	1-43	Whitehead et al., 1998a
	Arable	12.4-65.6	19-84	Whitehead et al., 1998a
			34.1	Guo et al., 2004
			8.1-85.6	Ma, 1992; Zhu et al., 2005

Nitrogen output

To analyze nitrogen cycling for different land use components, the nitrogen losses from the catchment through plant uptake, ammonia volatilization, leaching through runoff and denitrification were estimated in the model.

Plant uptake

N crop uptake is one of the most important routes for N loss from the catchment which account for 40-60% of applied N fertilizer. The estimated N uptake rate is about 246-375 kg N ha^{-1} yr^{-1}, 26.7-58.4 kg N ha^{-1} yr^{-1} for arable land and forests, respectively. The crop uptake rate is similar to the results in Richter and Roelcke (2000), with average rates of 89-113 kg N ha^{-1} for wheat and 168-207 kg N ha^{-1} for rice in the Taihu region. However, compared with the fertilizer application rate, the N uptake efficiencies are relatively lower. The accumulated N in the arable land may lead to an imbalance of the nutrient cycle in the agroecosystems, as well high nitrogen losses transported by water flux, and thus resulting in surface water deterioration.

Volatilization

The ammonia volatilization from the catchment takes a large proportion of the total N output. A general range of 12.7 to 37.9 kg N ha^{-1} yr^{-1} was found in the arable land from our simulation, which is consistent with the observation by Tian et al. (2001) in a paddy rice-winter wheat rotation system in the Taihu Basin. In the Xitiaoxi catchment, large amount of ammonia were lost through NH_3 volatilization from arable land, cattle slurry, pig slurry, manure, etc. Especially in the rice fields, the application of urea resulted in considerable NH_3 volatilization (Li et al., 2008).

Leaching

The mean N export rates in leaching were between 12.4 and 65.6 kg N ha^{-1} yr^{-1}, accounted for about 5-10% of the total N inputs. In contrast, the nitrate leaching loss is much higher than that of ammonium nitrogen. Considerable nitrate leaching was attributed to excessive and inappropriate irrigation and nitrogen (N) fertilization in this region, which may result in severe groundwater pollution. Compared with the results of Guo et al. (2004) and Ma (1992) who found TN was from 8.1 to 85.6 kg ha^{-1} yr^{-1} in different years, our results displayed narrower range. Additionally, it was argued that N leaching losses increased with the increasing application of N fertilizer in the Taihu Basin.

Denitrification

The current estimated denitrification rate was 18.4-39.6 kg N ha^{-1} yr^{-1} in the arable land, whereas the N loss by denitrification over the forest region was much less. In contrast, the simulated values in this study are similar to the findings by Chen et al. (2008) and Gundersen and Bashkin (1994), and slightly higher than the large amount of field experimental data elsewhere in China (Xing, 1998).

The average total N input to the Xitiaoxi catchment was 81.3 kg N ha^{-1} yr^{-1} (455.8-490 kg N ha^{-1} yr^{-1} for arable land) of which about 54.1% was for plant uptake, 11.9-17.5% was export through runoff, 1.7% was for denitrification, 6.3-17.1% was lost through ammonia volatilization, and the remaining 9.6-26% accumulated in the landscape.

4.5 Conclusions and perspectives

The paper presented the newly developed XAJ-N model to simulate and predict daily discharge,

N fluxes in the Xitiaoxi catchment in South China. The advantage of the model lies in the fact that it considers different hydrological and hydro-chemical processes in the soil and water stores and evaluates the model performance by both comparing the observed and simulated values and using the mass balance method in such a data scarce catchment. This makes the model a powerful tool to simulate field and in-stream processes and describe the spatial and temporal characteristics of nutrient loads at catchment scale.

The present model took the basic climate, topography, soil, land cover/use and agricultural data as input to simulate both daily discharge and nutrient loads in the Xitiaoxi catchment in south China. Two hydro-gauges, Hengtangcun and Fanjiacun with long-term daily discharge are used to evaluate hydrological model performance. The results of streamflow simulation showed good agreement between simulated and observed daily discharge with NE from 0.77 to 0.81 during the studied period.

Nitrogen simulation presented acceptable and reliable results for both the range and the seasonal dynamic of the nutrient load in general. Nitrogen concentrations at six different sites were also selected for model performance evaluation. The model efficiencies of NE in the range of 0.19 to 0.48 indicated that the model performance were relatively reasonable but need to be improved with long-term continuously observed dataset. On the other hand, nitrogen simulation also displayed that point source pollution lead to large errors in the simulated results at Dipu site. A large amount of domestic waste water and household pollutants from Anji County were directly discharged into surface water resulting in higher measured NH_4^+-N concentrations.

Due to limited availability of measured nutriments data, mass balance method was implemented to compare the simulated nutrient processes with corresponding values published in the literature. The analysis indicated fertilizer and atmospheric deposition were the main input components with input rates of 425-635 kg N $ha^{-1}yr^{-1}$, 22-25.8 kg N $ha^{-1}yr^{-1}$, respectively. As for the N output from the catchment, plant uptake, ammonium volatilization and leaching through the runoff account for large proportion of the total N input. Nitrogen emission rate to the atmosphere through volatilization and denitrification was likely responsible for the higher N loss rate in the catchment.

The simulation results in our study provide a scientific basis for understanding N sources and exports in the catchment scale, as well as good knowledge for identifying the pollution sources and its effective mitigation in areas similar to Xitiaoxi catchment. However, different processes

for each land use components should be considered in detail. Furthermore, the applicability of the model particularly in the paddy land (flooded zone with anaerobic conditions) needs to be validated with measurements data in the future.

Acknowledgements

This study was supported by the programs “Studies and Research in Sustainability” from DAAD (Deutscher Akademischer Austausch Dienst) and “Development and Application of Non-point Source Pollution Model Using Dynamic Environmental Modelling Language” (sklhse-2010-A-01) from the State Key Laboratory of Hydro-Science and Engineering and the Department of Hydraulic Engineering, Tsinghua University, China. The authors would like to express their gratitude to the two reviewers for their valuable comments and suggestions which greatly improved the quality of this paper.

Chapter V Application of a nutrient model for sediment yield and phosphorus load estimation in a data scarce catchment in South China

G.J. Zhao, G. Hörmann, N. Fohrer, J. Kiesel, J.F. Gao, H.P. Li

Journal of Environmental Sciences-China (In printed)
Submitted 08.07.10, Accepted 30.01.11

Abstract

Nutrient transportation from agricultural land to surface water has received much attention throughout the world since it plays an increasingly important role in affecting the water environment. Understanding the nutrient cycle in agricultural systems is essential to reduce non-point pollution for improving water quality. This paper describes the preliminary evaluation of the Xinanjiang-Phosphorus (XAJ-P) model for suspended sediment (SS) and phosphorus (P) estimation in the Xitiaoxi catchment, in southeastern China. The model was implemented in the environmental modelling language PCRaster. It estimates the sediment yields and phosphorus loads on a cell-by-cell basis with a daily time step. The results show that an average of 127.4 t yr^{-1} P was exported to the river and streams in the catchment. Spatial distribution of P loads indicates that the non-point source load from arable land had a dominant contribution with an export rate of 1.63 to 4.92 kg ha^{-1} yr^{-1}. It is also found that an annual average P load of about 63.7 t was exported from point sources to the rivers. P budget analysis indicate that average P input and output were 71.3 kg ha^{-1} yr^{-1} and 46.2 kg ha^{-1} yr^{-1} respectively, while the total P utilization efficiency was 59.3%, leading to an average P surplus of 25.1 kg ha^{-1} yr^{-1} in the arable land of the Xitiaoxi catchment. The application of XAJ-P in the catchment shows that the developed model can be used as a major tool to simulate long-term daily P loads at the catchment scale.

Key Words: Sediment yields, Phosphorus load, Xinanjiang-Phosphorus (XAJ-P) model, PCRaster

5.1 Introduction

Large amounts of nutrient discharge into surface water, and the aquatic ecosystems have been and still are confronted with serious water environmental problems. Eutrophication of water bodies is one of the global environmental problems, which may largely be attributed to the nutrient input from agricultural non-point sources (NPS) (Carpenter, 2005; Sharpley et al., 2001). Phosphorus (P) is mostly the limiting factor of eutrophication in fresh water bodies that have been widely investigated at catchment scales (Neal and Robson, 2000; May et al., 2001). With the identification and reduction of water pollution from many point sources, attention has been turned toward the contribution from diffuse agricultural sources of P, which are now considered as the major source of P in most cases (Sharpley and Rekolainen, 1997; Hart et al., 2004).

The main mechanism by which P is lost from row-cropped agricultural land is by runoff carrying both soluble and particulate forms of P (Quinton et al., 2001). Particulate P is usually the largest fraction of P in runoff from row-crop production systems, due to greater losses of sediment in the farming system. The pathways of P transfer in different land components (e.g. forest, paddy and farmland) are complex, and many processes and parameters are poorly understood or under-investigated (Sharpley et al., 2002). P losses from intensive double or multi-cropped rotated arable land with excessive fertilizer and manure application may account for a substantial portion in both particulate and soluble P. Assessing the relative contribution made by individual sources is necessary for minimizing P losses within the framework of agricultural management and policy decisions.

Many models has been developed and applied to quantify NPS pollution, e.g., SWAT (Arnold et al., 1998), AGNPS (Young et al., 1989) and HSPF (Donigian et al., 1995). These models are capable of simulating the nutrient cycles, however, the input data sets necessary to set up the models are rarely available in most developing countries. In particular, one of the main restraints for the model applications is that associated data sets are extremely sparse and the modeler must get along with data that have been routinely collected for regulatory or monitoring purposes. It is then necessary to adapt the model structure to the database and to develop a model with simpler structure and less data requirements.

Taihu Lake is one of the three most eutrophicated lakes in China (Qin et al., 2007). In recent years, serious water pollution problems have received much attention due to the fact that algae blooms occurred more frequently, and extended its coverage and persisted throughout the summer (Qin et al., 2007). NPS pollution was confirmed to be one of the major sources of P contributing to the eutrophication of the lake (Zhang et al., 2001). The Xitiaoxi River is one of

the main tributaries draining into Taihu Lake, and contributes a large amount of water and nutrient (Li et al., 2004a). A better understanding of the P cycle in the catchment and identification of the critical sources of P export are essential and necessary to improve the aquatic ecosystem and to control the eutrophication of Taihu Lake.

There have been several studies concerning the estimation of nutrient loads by using continuous large-scale NPS models in Taihu Basin. Lai et al. (2006) and Yu et al. (2007) used the SWAT model to investigate the annual nutrient loads for the whole Taihu Basin. Li et al. (2004a, 2009) and Liang et al. (2008) estimated the nutrient loads using the export coefficients model in the Xitiaoxi catchment. These studies presented the spatial and temporal characteristics of annual nutrient loads in the Taihu Basin, however, the studies on the nutrient dynamics in soil and water and nutrient loads from different land use components are still limited at catchment scale in this region. Thus, the objectives of this study are: a) to develop a simple soil erosion and phosphorus transport model (XAJ-P model) based on the Xinanjiang rainfall-runoff model (Zhao et al. 1980; Zhao, 1992); b) to apply the XAJ-P model to understand the characteristics of P flows in the agricultural cycle and c) to assess various contributions of P fluxes to the water in the Xitiaoxi catchment.

5.2 Methodologies

The Xinanjiang-Phosphorus (XAJ-P) model is a hybrid model implemented in PCRaster (http://pcraster.geo.uu.nl/) consisting of three different modules (Figure 5.1). The first module is a water flux model, which analyses the quantity of surface and groundwater in the catchment using the PCR-XAJ model (Zhao et al., 2009; 2011a). As shown in Figure 5.1, the hydrological model applies the Xinanjiang model concept for runoff generation and separation (Zhao et al., 1980; Zhao, 1992). The second module uses the data generated by the first module as input data to estimate nutrient transport (phosphorus) based on the Integrated CAtchments model of Phosphorus dynamics (INCA-P) (Wade et al., 2002), and the third module applies the Modified Universal Soil Loss Equation (MUSLE) (Williams, 1975) to estimate the sediment yield and particulate phosphorus.

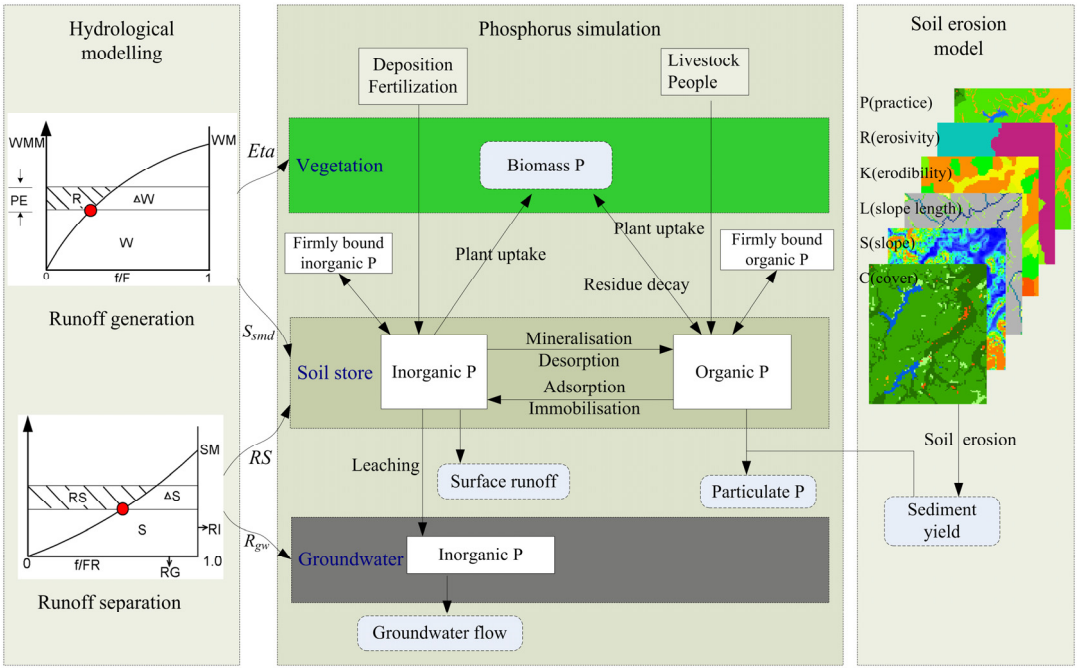

Figure 5.1: Framework of the Xinanjiang-Phosphorus (XAJ-P) model in PCRaster

The XAJ-P model simulates P transport at the catchment scale with a 200×200 m grid and daily resolution. The model simulates several key processes by which suspended solids (SS), particulate phosphorus (PP) and dissolved phosphorus (DP) are mobilized in the soil store and/or groundwater store, and transported via different pathways and drains to watercourses. The model has been implemented in the PCRaster environmental modelling language (Wesseling et al., 1996). It requires input data of hydro-climatic time series, soil types, slope, land use and P input from inorganic and organic fertilizers in each grid cell. Sediment yields are calculated using the Modified Universal Soil Loss Equation (Williams, 1975), which was redesigned for application to large river basins (Figure 5.1). Although the model was developed primarily to predict diffuse pollution at catchment scale, point sources are also taken into account based on industrial production and the number of people and livestock in each grid cell.

5.2.1 Sediment yield and transport

Mostly, soil erosion is a hydrologically driven process and plays an important role in the PP transport from fields to rivers. In this study, a simple conceptual sediment modelling approach, the Modified Universal Soil Loss Equation (MUSLE) is coupled to the Xinanjiang model to predict daily soil erosion (Figure 5.1). The in-stream processes consist mainly of sediment deposition and degradation. MUSLE has a comparably improved accuracy of soil erosion estimation over the Universal Soil Loss Equation (USLE) and the Revised Universal Soil Loss

Equation (RUSLE) by including the runoff as an independent factor in erosion simulation (Williams, 1975; Neitsch et al., 2005). In general, the sediment yields in each grid can be calculated as follows:

$$Sed = 11.8\left(Q_{sur} q_{peak} A\right)^{0.56} \cdot K_{usle} \cdot C_{usle} \cdot P_{usle} \cdot LS_{usle} \cdot CFRG \quad (1)$$

where, Sed is the sediment yield (tons), Q_{sur} is the surface runoff volume (m^3), q_{peak} is the peak runoff rate (m^3 s^{-1}), A is the area of the grid (ha), K_{usle}, C_{usle}, P_{usle}, LS_{usle} and $CFRG$ are respectively, the soil erodibility factor (Mg MJ^{-1} mm^{-1}), the crop management factor, the erosion control practice factor, the topographic factor and the coarse fragment factor. The details of the USLE factors and the descriptions of peak runoff rate calculation can be found in Neitsch et al. (2005).

The in-stream processes of sediment transport consist of two components operating simultaneously: deposition and degradation. To determine whether deposition or degradation occurs, the maximum concentration of sediment (transport capacity) is calculated by:

$$S_{mx} = \partial \cdot v_{mx}{}^{\lambda} / 1000 \quad (2)$$

where, S_{mx} is the transport capacity (kg m^{-3}), ∂ is a user defined coefficient, λ is an exponent parameter for calculating sediment reentrained in channel sediment routing (Neitsch et al., 2005).

The peak velocity v_{mx} (m s^{-1}) in a reach segment/grid at each time step can be calculated from Manning's equation (Chow et al., 1988):

$$v_{mx} = \frac{\alpha}{n} \cdot R_{ch}{}^{2/3} \cdot S_{ch}{}^{1/2} \quad (3)$$

where, α is the peak rate adjustment factor, n is Manning's roughness coefficients in the channel, R_{ch} is the hydraulic radius (m), and S_{ch} is the channel invert slope (m m^{-1}). If sediment load in a channel segment is larger than its sediment transport capacity, channel deposition will be the dominant process, and the net amount of sediment deposited Sed_{dep} (kg) equals to:

$$Sed_{dep} = \begin{cases} (S_i - S_{mx}) \cdot V_{ch} & S_i > S_{mx} \\ 0 & S_i \le S_{mx} \end{cases} \quad (4)$$

where, S_i is the initial sediment concentration in the channel (kg m^{-3}), and V_{ch} is the volume of water in the channel segment (m^3), calculated in the hydrological model.

Otherwise, channel degradation occurs in the channel segment, and the net amount of sediment degradation Sed_{deg} (kg) is calculated by:

$$Sed_{deg} = \begin{cases} 0 & S_i \ge S_{mx} \\ (S_{mx} - S_i) \cdot V_{ch} \cdot K_{ch} \cdot C_{ch} & S_i < S_{mx} \end{cases} \quad (5)$$

where, K_{ch} is the channel erodibility factor (cm/h/Pa), and C_{ch} is the channel cover factor (Arabi et al., 2008).

The final amount of sediment in the reach is determined by:

$$Sed_{i+1} = Sed_i - Sed_{dep} + Sed_{deg} \quad (6)$$

where, Sed_{i+1} and Sed_i are the in-stream sediment at time $i+1$ and i respectively.

5.2.2 Phosphorus processes

The XAJ-P model integrates the Xinanjiang rainfall-runoff model and the Integrated CAtchments model of Phosphorus dynamics model (INCA-P) (Wade et al., 2002b) using the environmental modelling language PCRaster. The INCA-P model is a semi-distributed, dynamic nutrient model, which simulates the phosphorous dynamics in soils, groundwater stores and streams of large catchments, considering different sources of P (deposition, manure, fertilizers) and different land use components (Wade et al., 2002b).

Firstly, some hydrologic variables are presented as following to better understand the integration of Xinanjiang rainfall runoff model and the INCA-P model. The drainage volume in the soil V_{soil}, representing the water volume stored in the soil that responds rapidly to water inflow, is calculated as:

$$V_{\text{soil}} = \text{HER} - R_{\text{sr}} \quad (7)$$

where, R_{sr} (mm) is surface runoff and calculated in the Xinanjiang rainfall-runoff model (Zhao et al., 2009). Hydrologically effective rainfall HER, defined as that part of total incident precipitation which reaches river channels, is used to drive the water flow and nutrient fluxes (Wade et al., 2002b). In the hydrological model, it is expressed as:

$$\mathrm{HER} = \left(\mathrm{Pr} + M\right) - ET - \Delta S \tag{8}$$

where, Pr (mm) is liquid precipitation, M (mm) is snowmelt, ET (mm) is evapotranspiration and ΔS (mm) denotes the water infiltrated from surface soil to groundwater in a fixed day.

The soil retention volume V_{soil} (mm) represents the water volume stored in the soil that responds more slowly and may make up the majority of water storage in the soil, which is linearly dependent on the soil moisture deficit. The calculation has completely described by Wade et al. (2002a).

As shown in Figure 5.1, different processes of P mobilization and transport in the soil store are considered, whereas in the groundwater, it is assumed that no biogeochemical reactions occur due to low mobility of P (Wade et al., 2002b).

In the soil, organic P by plant uptake $P_{up,org}$ (kg P ha^{-1}) is assumed to be temperature and soil moisture dependent (Wade et al., 2002b):

$$P_{up,org} = \frac{C_{up,org} \cdot S_{smd} \cdot S_{plant} \cdot P_{soil,org}}{V_{ret} + V_{soil}} \tag{9}$$

where, $P_{soil,org}$ is the organic P mass (kg P ha^{-1}) in the soil store, $C_{up,org}$ (m day^{-1}) is the plant uptake rate, which has seasonal relationship dependent on air temperature. The soil moisture factor S_{smd}, is calculated by the soil moisture deficit in the Xinanjiang-Nitrogen model (Zhao et al., 2011b), and the parameter S_{plant} is a seasonal plant growth index, which simulates an increase and decrease in plant nutrient demand based on the time of year (Wade et al., 2002b).

The fluxes of P associated with leaching $P_{leach,org}$ (kg P ha^{-1}), mineralization $P_{mir,org}$ (kg P ha^{-1}) and immobilization $P_{imb,org}$ (kg P ha^{-1}) are defined as (Wade et al., 2002b):

$$P_{leach,org} = \frac{R_{sr} \cdot P_{soil,org}}{V_{ret} + V_{soil}} \tag{10}$$

$$P_{mir,org} = \frac{C_{mir} \cdot S_{smd} \cdot P_{soil,org}}{V_{ret} + V_{soil}} \tag{11}$$

$$P_{imb,org} = \frac{C_{imb} \cdot S_{smd} \cdot P_{soil,inog}}{V_{ret} + V_{soil}} \tag{12}$$

where, $P_{soil,inog}$ (kg P ha^{-1}) is inorganic P mass in the soil store. The constants, C_{mir} and C_{imb}, are the rates of mineralization and immobilization, respectively.

Thus, the change in readily available organic P mass $\Delta P_{soil,org}$ (kg P ha^{-1}) in the soil becomes:

$$\Delta P_{soil,org} = P_{ip,org} - P_{leach,org} - P_{up,org} - P_{imb,org} + P_{mir,org} - \Delta P_{fb,org} \tag{13}$$

where, $P_{ip,org}$ is the input of organic P (kg P ha^{-1}), $\Delta P_{fb,org}$ denotes the change of firmly bound organic P mass (kg ha^{-1}), and can be calculated as follows:

$$\Delta P_{fb,org} = \frac{C_{tr,org} \cdot P_{soil,org}}{V_{ret} + V_{soil}} - \frac{C_{tr,forg} \cdot P_{fb,org}}{V_{ret} + V_{soil}} \tag{14}$$

where, $C_{tr,org}$ and $C_{tr,forg}$ are the transfer rates between organic P and firmly bound organic P. $P_{fb,org}$ denotes firmly bound P mass (kg P ha^{-1}) in the soil store.

The change of organic P in the groundwater store $\Delta P_{gw,org}$ (kg P ha^{-1}) is calculated by:

$$\Delta P_{gw,org} = \frac{\Delta S \cdot P_{soil,org}}{V_{ret} + V_{soil}} - \frac{R_{gw} \cdot P_{gw,org}}{V_{gw}} \tag{15}$$

where, R_{gw} is the groundwater flow (mm), which is estimated in the Xinanjiang model (Zhao et al., 2009; 2011a). $P_{gw,org}$ is organic P mass in the groundwater store (kg P ha^{-1}), and V_{gw} (mm) is the groundwater volume.

As for the inorganic P, the fluxes of P associated with leaching $P_{leach,inog}$ (kg P ha^{-1}) and plant uptake $P_{up,inog}$ (kg P ha^{-1}) are respectively calculated as (Wade et al., 2002b):

$$P_{up,inog} = \frac{C_{up,inog} \cdot S_{smd} \cdot S_{plant} \cdot P_{soil,inog}}{V_{ret} + V_{soil}} \tag{16}$$

$$P_{leach,inog} = \frac{R_{sr} \cdot P_{soil,inog}}{V_{ret} + V_{soil}} \tag{17}$$

And the change in readily available inorganic P mass in the soil store $\Delta P_{soil,inog}$ (kg P ha^{-1}) is:

$$\Delta P_{soil,inog} = P_{ip,inog} - P_{leach,inog} - P_{up,inog} + P_{imb,org} - P_{mir,org} - \Delta P_{fb,inog} \tag{18}$$

where, $P_{ip,inog}$ is the input of inorganic P (kg P ha^{-1}), and $\Delta P_{fb,inog}$ is the change of firmly bound inorganic P mass (kg P ha^{-1}) in the soil, which can be calculated as:

$$\Delta P_{fb,inog} = \frac{C_{tr,in} \cdot P_{soil,inog}}{V_{ret} + V_{soil}} - \frac{C_{tr,fin} \cdot P_{fb,inog}}{V_{ret} + V_{soil}} \tag{19}$$

where, $C_{tr,in}$ and $C_{tr,fin}$ are the transfer rates between inorganic P and firmly bound inorganic P. $P_{fb,inog}$ denotes firmly bound P mass (kg P ha^{-1}) in soil store.

The changes of inorganic P in the groundwater store $\Delta P_{gw,inog}$ (kg P ha^{-1}) is:

$$\Delta P_{gw,inog} = \frac{\Delta S \cdot P_{soil,inog}}{V_{ret} + V_{soil}} - \frac{R_{gw} \cdot P_{gw,inog}}{V_{gw}} \tag{20}$$

where, $P_{gw,inog}$ (kg P ha^{-1}) is inorganic P mass in the groundwater store.

Particulate P attached to soil particles is transported by surface runoff from fields to the main channel. This form of phosphorus is associated with the sediment load from the field. Koo et al. (2005) indicate that only PP in the top 10 mm of the soil can be transported attached with soil particles. Thus, the amount of P transported in particulate form by surface runoff is estimated by:

$$P_{psr} = 1000 \cdot Sed \cdot C_{pp,top} \cdot \varepsilon_p \quad (21)$$

where, $C_{pp,top}$ is the concentration of PP in the top 10 mm of the soil (kg kg^{-1}), which is estimated based on soil texture (Liang et al, 2004), and ε_p is the enrichment ratio of P. The enrichment ratio of P in sediment decreases markedly with the amount of eroded sediment and a logarithmic relationship suggested by Menzel (1980) is used in the model:

$$\varepsilon_p = exp\left(2 - 0.2 \cdot lnSed\right) \quad (22)$$

A two retention parameters method was used for modelling in-stream attenuation, which is described in more detail in Loos et al. (2009).

5.3 Data input and model initialization

5.3.1 Study area

The Xitiaoxi catchment, covering about 2271 km^2, is located in the upstream of Taihu Lake in southeastern China (Figure 5.2). The Xitiaoxi River, with its length of 157 km, supplies 27.7% of the inflowing water volume of Taihu Lake. The annual average rainfall is approximately 1465 mm. As shown in Figure 5.2, high mountainous and hilly areas occur in the southwest, whereas low alluvial plains lie in the northeastern parts with a well-developed drainage network. A detailed description of the Xitiaoxi catchment is available in Zhao et al. (2009; 2011a).

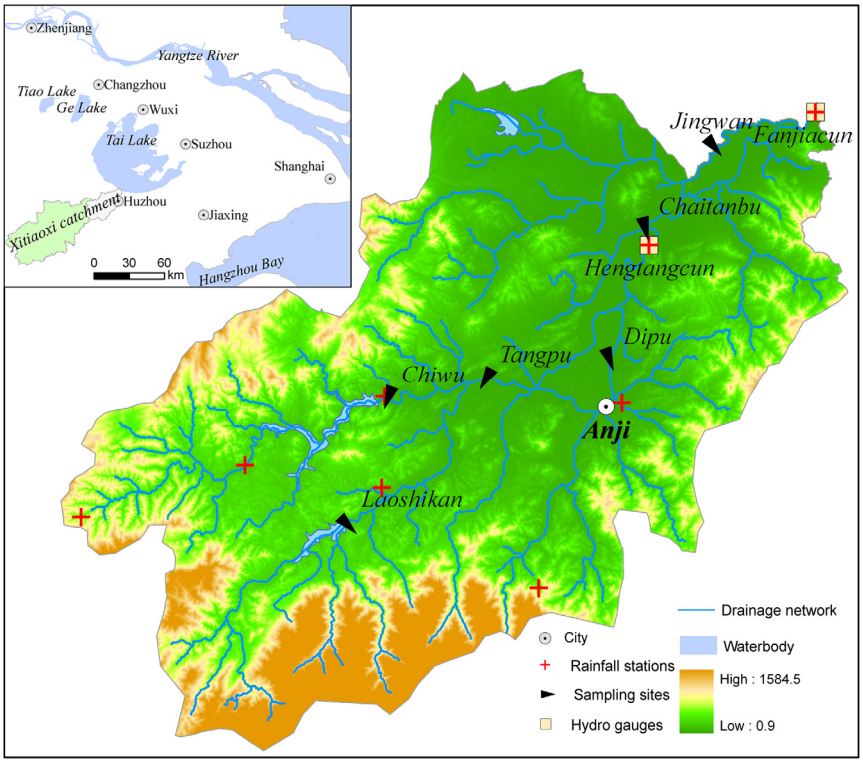

Figure 5.2: Location of the study area and monitoring sites (Li et al., 2004a)

5.3.2 Available database

The details of basic input data including land use maps, digital elevation model (DEM), hydro-meteorological data (e.g. rainfall, evaporation) have been described in Zhao et al. (2011b).

The current agricultural practice in the study area is an intensive double-cropping system with irrigated summer rice and uplands winter wheat, occasionally rapeseed. In addition, bamboo production, tea garden, fruits and vegetables cover small area in the upland of the catchment. Diffuse emission data such as fertilizer and manure application, population distribution and livestock number are collected from yearbooks of Zhejiang Provinces (2005). The amount and date of fertilizer application are in conformance with the conventional cultivation (Guo et al., 2004). Typically, about 75-140 kg P ha^{-1} is applied as fertilizer on arable lands (Tian et al., 2001; Roelcke et al., 2002). In contrast, P fertilizer application rates are much higher in most areas producing economic crops, such as flowers and vegetables, especially in the suburban areas of big cities and can amount to 400-600 kg P ha^{-1} yr^{-1} (Chen et al., 2008a). Atmospheric deposition of P was estimated from the observed data by Luo et al. (2007) and reconstructed according to the annual precipitation. Figure 5.3 shows the spatial distribution of P input from the

atmospheric deposition and fertilizer application.

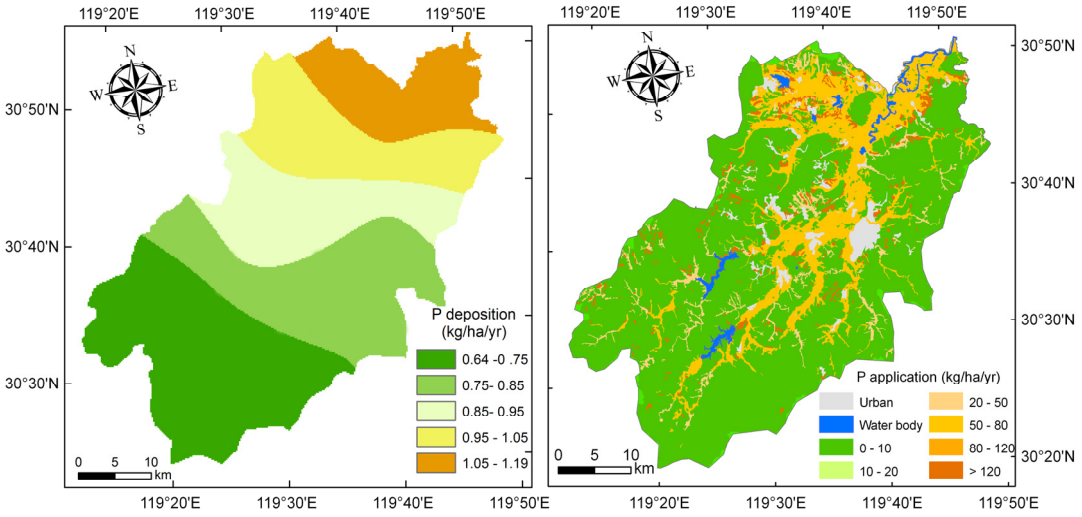

Figure 5.3: Spatial distribution of average annual P application and deposition rates in the Xitiaoxi catchment

The sewage from rural areas is regarded as surface point source pollution, because there is no drainage system. Human sewage load to the catchment is calculated by multiplying the resident population in each grid by typical excretion rates for humans (0.6-1.2 kg P person^{-1} yr^{-1}) (Johnes 1996; Lai et al., 2006; Ding et al., 2010). The P load from livestock mainly includes big cattle, pigs, sheep and poultry (chickens and ducks). The annual livestock export rates are shown in Table 1. The P load from point sources was calculated according to the relationship between P export rates and industrial productions in 1999 for the catchment (Li et al., 2004a), and then spread up to the grids in the correspondingly region.

Table 5.1 TP export rates from livestock excretion per year

Livestock	Values in this study (kg P head^{-1} yr^{-1})	Values in references (kg P head^{-1} yr^{-1})	References
Big livestock	10.2	9.20-11	Johnes, 1996; Ding et al., 2010
Sheep	2.0	1.9-2.22	Loos et al., 2009
Pigs	3.2	3.12, 3.5	Ding et al., 2010
Poultry	0.2	0.2-0.24	Chen et al., 2008b; Loos et al., 2009

5.3.3 Model initialization and calibration

The model outlined in methodologies section involves a total of 20 parameters (Table 5.2). The parameters were firstly initialized with literature values (Table 5.2), and then adjusted by trial-and-error methods until model simulations satisfactorily matched the measured data. Furthermore, a hindcast method based on mass balance was applied to control the main processes of P transport and mobilization (Breuer et al., 2008). In the present study, the XAJ-P model mainly considers six land use types (i.e. forest, paddy, grassland, farmland, water body, urban area). Most parameters for P transportation are land use dependent, which are initialized from Wade et al. (2002b) and Dean et al. (2009).

Table 5.2 Parameters in the sediment yields and P transportations modelling

Parameter	Definition (unit)	Values ranges	Calibrated values	References
Sediment				
K_{usle}	Soil erodibility factor	0-1	0.01-0.13	Arabi et al., 2008; Wang et al., 2009
C_{usle}	Crop management factor	0-1	0.001-0.47	
P_{usle}	Erosion control practice factor	0.2-1	0.3-0.9	
∂	Coefficient for in-stream sediment transport	1-1.5	1.35	
λ	Flow velocity coefficient	0.0001-0.01	0.0046	
K_{ch}	Channel erodibility factor (cm/h/Pa)	0-1.0	0.035-0.3	Setegn et al., 2010
C_{ch}	Channel cover factor	0.001-0.6	0.21-0.35	
α	Peak rate adjustment factor	0-1	0.8-1	
n	Channel Manning's roughness coefficients	0.008-0.3	0.002-0.3	Chow et al., 1988
In-stream attenuation				
p	Temperature attenuation relationship	1-3	2	de Wit, 2000; Loos et al., 2009
ps_1	Parameter for overall loss within stream	50	45	
ps_2	Exponent coefficient for headwater loss	3	3	
Phosphorus				
$C_{up,org}$	Organic P plant uptake rate (m day^{-1})	0-2	0.03-1.8	

$C_{up,inog}$	Inorganic P plant uptake rate (m day^{-1})	0-6	0.01-3.5
C_{imb}	Immobilization rate (m day^{-1})	0-0.1	0.0001-0.05
C_{mir}	Mineralization rate (m day^{-1})	0-0.25	0.0001-0.19
$C_{tr,org}$	Transfer rate of organic P to firmly bound P (m day^{-1})	0-5	0.001-0.2
$C_{tr,forg}$	Transfer rate of firmly bound P to organic P (m day^{-1})	0-5	0.001-0.05
$C_{tr,in}$	Transfer rate of inorganic P to firmly bound P (m day^{-1})	0-0.1	0.001-0.1
$C_{tr,fin}$	Transfer rate of firmly bound P to inorganic P (m day^{-1})	0-0.1	0.001-0.1

Model calibration attempts to fit simulated to measured values at the main gauging stations. Streamflow calibration was done with daily values and the results have been shown in Zhao et al. (2009, 2011a, 2011b). The observed suspended solid concentration (SSC) and nutrient data surveyed bi-monthly at six sites of the catchment (Figure 5.2) from 1999 to 2007 were used for model performance evaluation. Due to the limitation of the available measured data, we divided the six monitoring sites into two parts for model calibration (Laoshikan, Tangpu and Jingwan) and validation (Chiwu, Dipu and Chaitanbu), respectively.

The simulation results were evaluated by visual inspection of plots of the range between observed and simulated values. The Nash-Sutcliffe efficiency (NE) (Nash and Sutcliffe, 1970) and correlation coefficient R^2 were both computed as criteria for goodness-of-fit.

The model efficiency, NE, is expressed as:

$$NE = 1 - \frac{\sum_{i=1}^{n}\left(O_i - P_i\right)^2}{\sum_{i=1}^{n}\left(O_i - \bar{O}_i\right)^2} \tag{23}$$

Where, O_i and P_i are the observed and predicted values for the ith pair, n is the total number of observations, and $\bar{O}_i$ is the mean of observed values. The range of NE values is from 1.0 to negative infinity. The closer the NE is to 1.0, the better the model results are. The objective for both calibration and validation was to maximize the coefficients NE and R^2.

5.4 Results and discussion

5.4.1 Sediment simulation

Sediment yields are associated with the overland soil erosion in the whole catchment, which reflects the integrated response of sediment generation processes in the field and in-stream processes at the catchment scale.

Figure 5.4 shows the observed and modeled suspended solid concentration along with 1:1 line at six monitoring sites along the river. The simulation values match consistently well with the measured values for both calibration and validation at different sites. The high coefficients (Figure 5.4) indicated a positive relationship between the simulated and measured sediment concentration. Relatively high NE and R^2 showed that the model performed satisfactorily. However, the daily sediment simulation indicates that modeled SSC are comparably lower than the measurements at Jingwan and Chaitanbu in the downstream parts of the catchment. The observed daily SSC during the period for which measured data was available (1999-2000 and 2003) ranged between 4.1 and 100 mg/l at these two sites, whereas the modeled SSC for the same period had a slightly narrower range of 3.5 mg/l to 61mg/l.

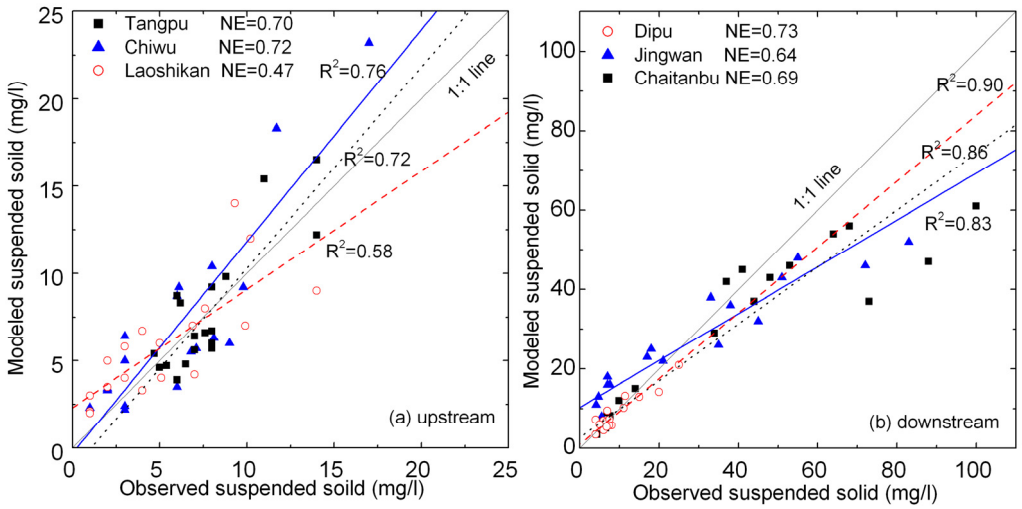

Figure 5.4: Daily observed and simulated suspended solid concentration at six monitoring sites

Generally, the simulation results for SSC in the downstream sites showed broader range compared with the sites in the upper reaches, and the SSC are underestimated in the downstream parts. The slope in the lower alluvial plain is featureless and the dominant in-stream process for sediment is deposition, but the observed SSC at Chaitanbu and Jiangwan are much higher. Previous studies concluded that the average sediment concentration should decrease in the downstream direction, that is, sediment discharge would increase less than

water discharge (Pistocchi, 2008). This can not explain the phenomenon in the Xitiaoxi catchment, one possible reason is the frequent sand mining activities in the downstream reaches of the catchment, which may lead to more sediment re-suspension.

5.4.2 Phosphorous modelling

Figure 5.5 shows the modeled and observed TP loads at Chaitanbu from 2002 to 2007. The model simulates reasonably for both the range and the dynamics of the TP load with a model efficiency NE of 0.43, and the seasonal variation of TP load is in agreement with the observed values. At the annual scale, TP loads estimated from XAJ-P model are in a range of 97.3 to 152.4 t yr^{-1} at Chaitanbu from 1999 to 2007 (with an average of 127.4 t yr^{-1}), which is consistent with the results found by Li et al. (2004a).

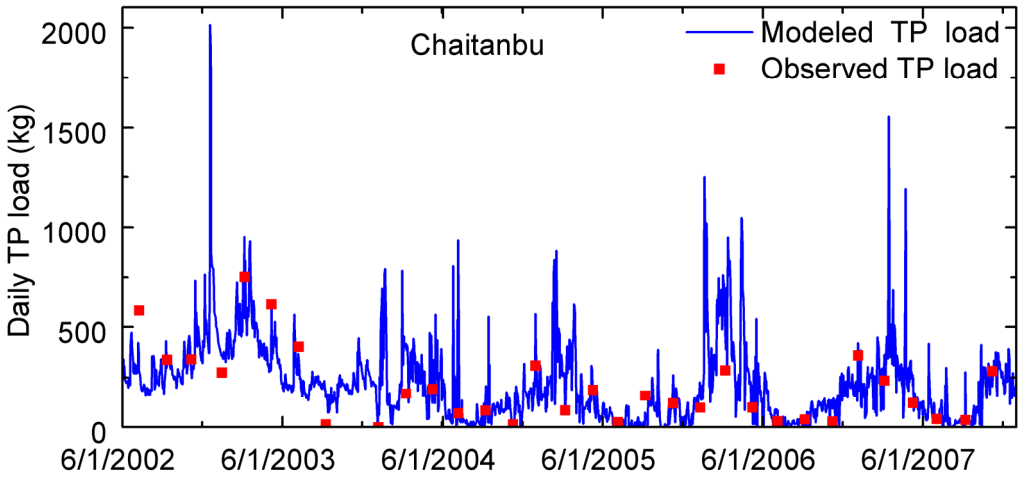

Figure 5.5: Daily observed and modeled TP load at Chaitanbu station

The daily observed TP load shows a range of 0 to 751.8 kg P day^{-1}, while the simulation illustrates a broader range from 2.4 to 2013.2 kg P day^{-1}. The significant discrepancies between the measurements and simulation are partly attributed to the over/under prediction in streamflow. In general, phosphorus movement in soils is present in both dissolved and particulate forms (Haygarth and Sharpley, 2000). Particle P is eroded during heavy rainfall events and constitutes a significant proportion of P transported from most cultivated lands (He et al., 2006). This may lead to a large amount of particulate P washed off by surface runoff and being discharged into the river. However, it is not possible to compare extreme TP load events/peaks with the observed values due to limited available measurement data.

Figure 5.6 illustrates the observed and simulated TP concentrations along with 1:1 line at six

sites. During calibration (Laoshikan, Tangpu and Jiangwan) the NE and R^2 values are in a range of 0.29 to 0.41 and 0.29 to 0.52, respectively. In contrast, model efficiencies for both NE and R^2 show similar range during validation (Chiwu, Dipu and Chaitanbu). The simulation results indicate that the model performed acceptable but need further improvement.

Phosphorus concentrations display spatial variances of nutrient export in different river sections in the catchment. Both modeled and observed P concentrations present narrow ranges in the upstream sites (Chiwu, Tangpu and Laoshikan), especially at Laoshikan site (Figure 5.6a), since this region is mostly covered by forests. In contrast, higher P concentration at Dipu, Jingwan and Chaitanbu indicates that a large amount of P flux is coming from upstream croplands and domestic wastewater (Figure 5.6b). For example, the observed values at Dipu have a much wider range from 0.025 to 0.543 mg/l for TP, which is largely attributed to the point source pollution from Anji County (Figure 5.2). The broader concentration ranges also indicate a high degree of variability in surface runoff losses since particulate P is highly dependent on rainfall events. It means that the P concentration is much higher in drainage water if rainfall occurs shortly after P fertilizer application. Thus, an abnormal rise of P concentration can be recorded for unexpected rainfall occurrence in the tillage period (Guo et al., 2004).

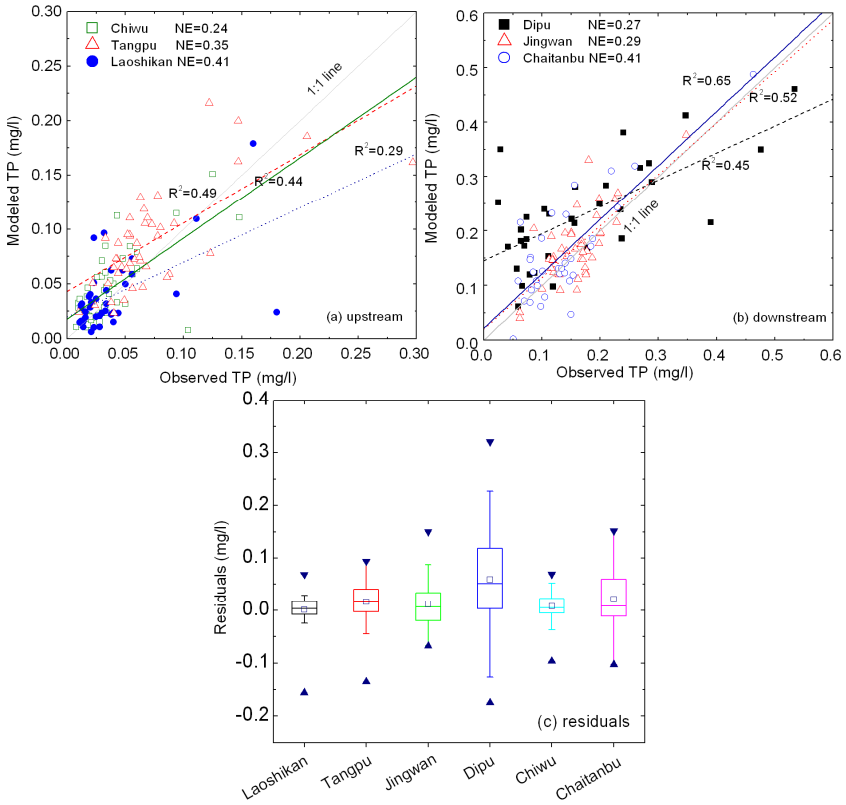

Figure 5.6: Daily observed and simulated TP concentration at six monitoring sites in the

Xitiaoxi catchment (a) TP simulation at upstream sites, (b) TP simulation at downstream sites, (c) spatial distribution of residuals between observed and modeled TP concentration

5.4.3 Spatial distribution of nutrient loads

Figure 5.7a shows the simulated spatial distributions of diffuse P loads in the catchment. The TP loads vary significantly among different land-use types, especially between forests and arable lands. The TP export of the dominating paddy land in the lowland of the Xitiaoxi catchment varies from 1.63 to 4.92 kg ha^{-1} yr^{-1} and is a function of the considerable amount of inorganic P fertilizer input. Similar results were also found in previous studies: Guo et al. (2004) addressed that the TP load from agricultural land is 1.75 kg ha^{-1} yr^{-1} in the Taihu Basin. Lai et al. (2006) assessed the nutrient transport in the whole Taihu Basin based on SWAT modelling, and found that the highest TP load rate occurred in paddy land (2.94 kg ha^{-1} yr^{-1}), and the lowest in forest areas with an export rate of 0.65 kg ha^{-1} yr^{-1}. In the Xitiaoxi catchment, the double-rotation of rice/wheat or rice/rapeseed is the dominant agriculture practice in the broad alluvial plain (Liang et al., 2008). In order to obtain large crop yields, excessive application of fertilizer in the arable land has significantly increased the nutrient accumulation in the soil (Ju et al., 2004).

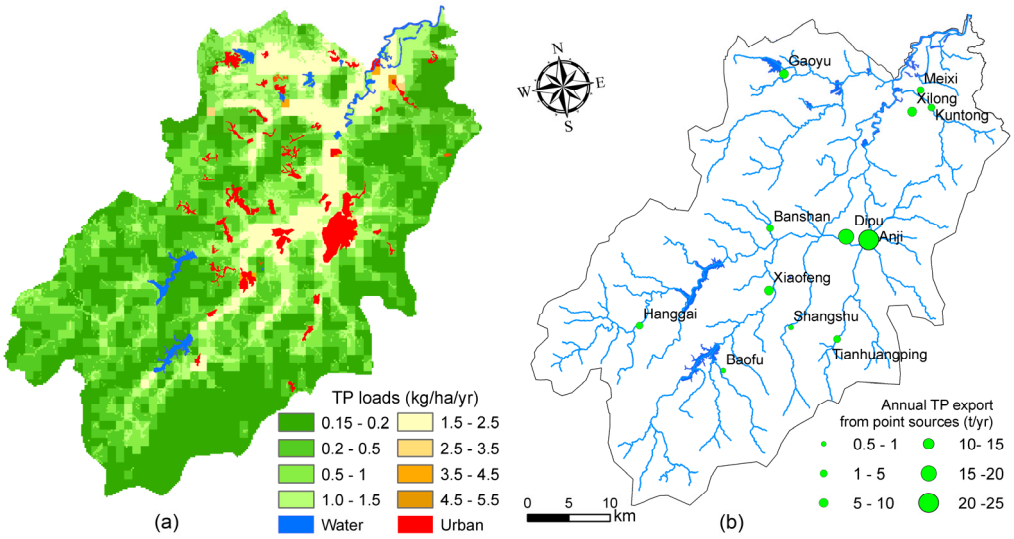

Figure 5.7: Spatial distribution of P loads from different sources

Figure 5.7b shows the spatial distribution of TP loads from point source pollution in the Xitiaoxi catchment. In total, approximately 63.7 t yr^{-1} P drained into the river from point source pollution in the Xitiaoxi catchment. From Figure 5.7b, it can be found that most point sources are located in the downstream parts of the catchment, which is consistent to the findings of

Liang et al. (2008). In contrast, the TP load from Anji and Dipu County make a large contribution of more than 50% P to the total point source pollution with an annual output of 23.5 t and 13.7 t into the surface water. This also explains the extremely high observed TP concentration at the Dipu site.

5.4.4 Phosphorus budget analysis

The P budget for the Xitiaoxi catchment is positive, with inputs exceeding outputs by 25.1 kg P ha^{-1} in the arable land. The accumulation of P in the landscape is due to the high fertilizer application rates. As shown in Fig. 8, mineral fertilizers are the dominating P input, which accounts for 71.6% of diffuse P input, followed by livestock manure (15.4%) and rural sewage (10.7%). Input from atmospheric deposition is only 1.8% of the total input. Anthropogenic activities, therefore, have exerted the greatest influence on P fluxes, which implies that P release into waters is mainly driven by agricultural activities, especially mineral fertilizer application (Guo et al., 2004).

As for the output, the P losses from the catchment are mainly due to crop removal, which accounts for 59.3% of the diffuse inputs, river loads make up 4.5%, and 36.2% of the total inputs to the catchment are unaccounted from (probably stored in catchment soils or vegetation). On the national level, the total P utilization efficiency (plant uptake P/P input) in Chinese agriculture is 45.7%, leading to an average surplus of 14.7 kg ha^{-1} yr^{-1} (Chen et al., 2008a). These values are slightly lower than in our study, which may be caused by the excessive fertilization in the Xitiaoxi catchment.

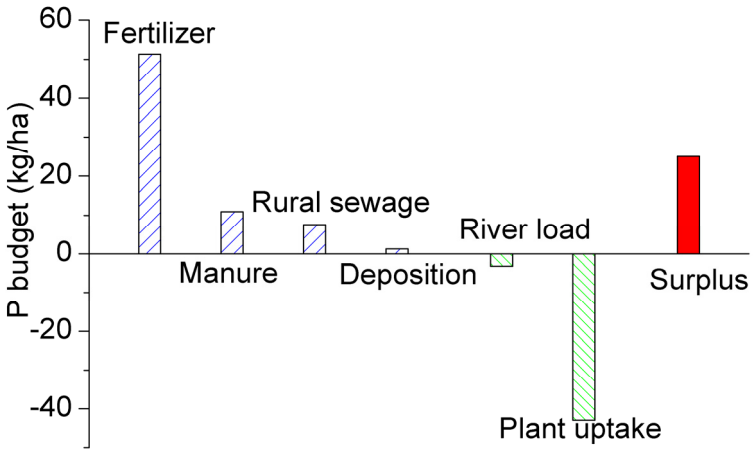

Figure 5.8: P input and output in the arable land of the Xitiaoxi catchment

5.5 Conclusions

The paper presents the newly developed XAJ-P model to simulate and predict daily sediment yields and P fluxes in the Xitiaoxi catchment. The model was implemented in PCRaster by integrating the Xinanjiang rainfall runoff model, INCA-P and MUSLE modules and applied to estimate field and in-stream processes of P and identify the critical sources of P load in a data scarce catchment.

The XAJ-P model presents acceptable and reliable results for both the range and seasonal dynamics of the sediment yield and P load. P concentrations at six different sites were also selected for model performance evaluation, which shows a good agreement between observed and simulated values. Spatial distribution of P loads indicates that the non-point source load, especially from arable land, is the major contributor. The phosphorus budget analysis shows relatively low phosphorus utilization efficiency about 59.3% in arable land. Excessive P application through inorganic fertilizer in the arable farming system has resulted in the accumulation of soil P and degraded surface water quality.

The successful application of XAJ-P in the Xitiaoxi catchment indicates that the model is a useful tool to describe the spatial and temporal characteristics of P load at the catchment scale with a long-term simulation. It is necessary to further apply the developed model in other catchments with high sampling frequencies of water quality components to verify the proposed methodology.

Acknowledgements

This study was supported by the program “Studies and Research in Sustainability” from Deutscher Akademischer Austausch Dienst (DAAD), and was jointly funded by the program “Development and application of non-point source pollution model using dynamic environmental modelling language (No. sklhse-2010-A-01) and the Knowledge Innovation of Chinese Academy of Sciences (No. KZCX2-YW-Q10-3). The authors would express their gratitude to the local government for providing the data. Great thanks are also extended to the anonymous reviewers for their very helpful comments and valuable suggestions.

Chapter VI Discussion and conclusion

6.1 Summary of achievements

The methodology developed in this thesis, ranges from the assimilation of the hydro-climatic, water quality and agricultural data to the final application of a catchment scale non-point sources pollution model. The main findings are summarized as follows:

6.1.1 Application of a raster-based hydrological model for streamflow prediction

The PCR-XAJ model was developed by integrating the Xinanjiang rainfall runoff model and flood polder operation by using PCRaster for discharge simulation in the Xitiaoxi catchment (chapter II). Model performance was assessed by comparing the observation with simulated values. A good agreement between observed data and the simulated values indicates that the developed model can produce reseasonable and reliable accuracy for runoff simulation. In addition, a simplified polder operation method was introduced to calculate the outflow from the polders. The results imply that the polder operation can reduce the flood peaks to some extent. Model sensitivity analysis indicated that the ratio of potential evapotranspiration to pan evaporation (K), the outflow coefficients of the freewater storage to groundwater (KG) and interflow (KSS) and the areal mean tension water capacity (WM) were the most sensitive parameters.

6.1.2 Impacts of spatial data resolution on discharge simulation

There are numerous factors influencing the hydrological processes simulation results, suitable spatial resolution should be considered carefully due to model running time and the work for data collection and processing. The impact of grid size of spatial input data (including land use and DEM) on the discharge simulation is evalulated by the PCR-XAJ model in Chapter III. The results show that spatial input data with higher resolution leads better simulation results (Blöschl, 2001; Bormann, 2006; Wu et al., 2008). The aggregation of input data does not lead to significant errors up to a grid of 1 km. Model efficiencies decrease slightly with cell size increasing, and more significantly up to the grid size of 1 km. Additionally, the increasing grid size affects the characteristics of the slope and land use and causes important information loss, which may lead to a large deviation in water balance simulation.

6.1.3 Development of a nitrogen model in a data scarce catchment

Chapter IV presented the integration of hydrology, soil erosion and nitrogen dynamics at the watershed scale and the application of the XAJ-N model for understanding the characteristics of nitrogen cycle in the Xitiaoxi catchment. The simple structure and the mechanism of mass balance based Integrated Nitrogen CAtchment (INCA) model allowed taking advantage of its concept and integrating with the conceptual hydrological model at catchment scale. The water flux module of the PCR-XAJ model was successfully coupled with the INCA-N model, as well as with a two parameter approach describing the in-stream process. Nitrogen simulation presented acceptable and reliable results for both the range and the seasonal dynamic of the nutrient load in general. However, point source pollution may lead to large errors in the nutrient loading esimation. In the Xitiaoxi catchment, fertilizer and atmospheric deposition were found to be the main input components with input rates of 425-635 kg N ha^{-1} yr^{-1}, 22-25.8 kg N ha^{-1} yr^{-1}, respectively. As for the N output from the catchment, plant uptake, ammonium volatilization and leaching through the runoff account for large proportion of the total N input. Nitrogen emission rate to the atmosphere through volatilization and denitrification was likely responsible for the higher N loss rate in the catchment.

6.1.4 Development and application of a phosphorus model in Xitiaoxi catchment

The new developed Xinanjiang-Phosphorus (XAJ-P) model consists of three sub-modules i.e. water flux module, soil erosion module and phosphorus module. The first module is a water flux model, which analyses surface water and groundwater quantity in the catchment using the PCR-XAJ model (Zhao et al., 2009; 2011a). The second module uses the data generated by the first module as input data to estimate phosphorus transport based on the INCA-P (Wade et al., 2002b), and the third module applies the Modified Universal Soil Loss Equation (MUSLE) (Williams, 1975) to estimate the sediment yield and particulate phosphorus. The Nash-Sutcliffe efficiencies (NS in Chapter II and III, and NE in Chapter IV and V) in the range of 0.24 to 0.41 indicate that the model performance is relatively reasonable but should be improved using a long-term continuously observed dataset. Spatial distribution of P loads indicates that the non-point source load, especially from arable land, is the major contributor. The average P input and output are 71.3 kg ha^{-1} yr^{-1} and 46.2 kg ha^{-1} yr^{-1} respectively in the arable land of the Xitiaoxi catchment, while the total P utilization efficiency in agriculture is 59.3%, leading to an average P surplus of 25.1 kg ha^{-1} yr^{-1}.

6.2 Discussion

The understanding of the hydrological and nutrient related processes in a catchment is important and necessary for finding a reasonable solution of regional hydro-geochemical problems associated with water resources planning, optimal allocation and agricultural practice management and fertilizer application in the agricultural catchment. In general, long term continuous monitoring is usually expensive and time consuming. Furthermore, it is hard to collect necessary data in a satisfactory resolution in the same period. Thus, modelling can be considered an attempt to integrate the current knowledge and available data set, which can produce scientific results for decision making.

The XAJ-NP model proved to be a powerful model that can reproduce relative acceptable results for estimating water and nutrient fluxes in a humid catchment. Errors arising from the model structure are generally the most poorly understood but are potentially the most influential. They result from unknown or unrepresented processes, inappropriate approximations and simplifications, and numerical effects introduced by the mathematical implementation of the conceptual model and its spatio- temporal discretisation (Liu and Gupta, 2007). The hydrological model of XAJ-NP represents the processes dominating runoff-response in humid region. Nevertheless, hydrological processes in the Xitiaoxi catchment are highly influenced by human activities, as already mentioned in Chapter II and III. The reservoirs operations reduced extreme flood peaks during rainy seasons, and regulated the low flow in the dry season, thus observed discharge with zero value occurred very frequently. On the other hand, the return flow from the Taihu Lake also contributes simulation errors at downstream sites. In addition, the polders located in the downstream of the catchment as well affect the runoff generation and accumulation. Although the model applied a simple method to estimate the polders operation, the impacts of reservoirs are very significant due to their high volumes. The results of the model applications conducted in this thesis suggest that some of these are partly responsible for model shortcomings.

In the hydrological processes simulation, the routing of the overland flow and channel flow was calculated by using the kinematic wave equation. In fact, it is reasonable to applied the kinematic wave equation in the upper reaches of the hilly region with higher surface (and the channel) slope. However, it is not applicable in the flat alluvial plain. An alternative option should be developed for the routing of overland flow and channel flow in the flat region in the future.

As for nutrient simulation, the XAJ-NP model applied the concept of INCA model for daily nutrient processes in each cell. The INCA model separates the runoff into surface flow in the

active soil zone and groundwater flow; however, this is comparably simplified for runoff simulation. The combination of the Xinanjiang model and INCA model proved that the model can estimate the total amount of nutrient loads and seasonal dynamics (Chapter IV, section 4 and Chapter V, section 4). Furthermore, model calibration and validation were undertaken by the comparison between the modeled and observed water quality data at different sites along the river, and an internal mass balanced approach was applied for model verification. However, the main limitation for the model calibration in such a data scarce area is that the extreme peaks and low events can not be represented without continuous long-term observation. Thus, for an extensive evaluation of the nutrient model performance is more data needed.

In the INCA model, the nutrient processes are assumed land use independent (Wade et al., 2002a), and the original INCA model considers six different land use classes i.e. forest, short vegetation (ungrazed), short vegetation (grazed, but not fertilized), short vegetation (fertilized), arable and urban. However, paddy land is the dominant arable land in the Xitiaoxi catchment, and the applicability of the model particularly in paddy land (flooded zone with anaerobic conditions) needs to be reconsidered.

The estimation of sediment yield is very important for the phosphorus simulation, since particle-bound phosphorus is eroded during heavy rainfall events and constitutes a significant proportion of phosphorus transported from most cultivated lands (He et al., 2006). However, it is not possible to compare extreme total phosphorus load events/peaks with the observed values due to limited available measurement data. Significant discrepances may result from over/underestimation of soil erosion simulation. Moreover, design and application of the erosion model (namely MUSLE) rarely extend to the paddy land, thus limitations have to be expected in this context.

6.3 Conclusions and outlook

This thesis presents the results in measurement and modelling of water and nutrient (nitrogen and phosphorus) load at a catchment scale. It mainly provided insight into the dynamics of water, nutrient load and sediment yield of the Xitiaoxi catchment in south China. A raster based hydrological model was developed with polder operation, which considers both the land use information and hydraulic projects in the flooded plain for discharge simulation at the catchment scale. A hybrid model for the integrated assessment of water flux, nutrient loads and sediment yields is available. The model produces acceptable results for both seasonal trends and magnitude of runoff and nutrient load. The derived information has significantly updated

the knowledge about the hydrological processes and nutrient dynamics in the Xitiaoxi catchment. The current results will provide the base for any further planning approach for the agriculture management, irrigation projects and flood control for the water and nutrient management in large scale catchment.

Although the study provides a basic tool for water resources management and agricultural practice at the catchment scale, further assessments based on considerable measurement data would be important for improving the model applicability. The accuracy of hydrological processes simulation can be improved by obtaining more information on hydraulic projects (e.g. reservoirs operation). Detailed knowledge and mechanism of nutrient dynamics in the paddy land should be reconsidered in the model. Long-term continuous water quality measurement data is necessary to further evaluate the model performance.

Bibliography

Abbott, M.B., Bathurst, J.C., Cunge, J.A., O'Connell, P.E., Rasmussen, J., 1986. An introduction to the European Hydrological System-Systeme Hydrologique European, "SHE", 2, Structure of a physically-based, distributed modeling system. J. Hydrol. 87, 61-77.

Arabi, M., Frankenberger, J.R., Engel B.A., Arnold, J.G., 2008. Representation of agricultural conservation practices with SWAT. Hydrol. Process. 22, 3042-3055.

Arnold, J.G., Fohrer, N., 2005. SWAT2000: current capabilities and research opportunities in applied watershed modeling. Hydrol. Process. 19, 563-572.

Arnold, J.G., Srinivasan, R., Muttiah, R.S. Williams, J.R., 1998. Large area hydrologic modeling and assessment, Part I.: Model development. J. Am. Water Resour. Assoc. 34(1), 73-88.

Bates, P.D., Lane, S.N., Ferguson, R.I., 2005. Computational Fluid Dynamics: Applications in Envrionmental Hydraulics. John Wiley & Sons Ltd.

Bates, P.D., De Roo, A.P.J., 2000. A simple raster-based model for flood inundation simulation. J. Hydrol. 236, 54-77.

Beasley, D.B., Huggins, L.F., Monke, E.J., 1980. ANSWERS: a model for watershed planning. Trans. ASAE 23, 938-944.

Bergström, S., 1976. Development and application of a conceptual runoff model for Scandinavian catchments. Department of Water Resources Engineering, Lund Institute of Technology, Bulletin Series A-52, Swedish Meteorological and Hydrological Institute, Norrköping, Sweden.

Beven, K.J., Kirkby, M.J., 1979. A physically based, variable contributing area model of catchment hydrology. Hydrol. Sci. J. 24, 43-69,

Beven, K.J., 2001. Rainfall-runoff Modeling: A Primer. Wiley, West Sussex, pp. 217-254.

Blöschl, G., Sivapalan, M., Gupta, V.K., Beven, K.J., 1997. Scale Problems in Hydrology. Water Resour. Res. 33 (12), 2881-2999.

Blöschl, G., 2001. Scaling in hydrology, Hydrol. Process. 15, 709-711.

Booij, M.J., 2005. Impact of climate change on river flooding assessed with different spatial model resolutions. J. Hydrol. 303, 176-198.

Bormann, H., 2006. Impact of spatial data resolution on simulated catchment water balances and mode performance of the multi-scale TOPLATS model. Hydrol. Earth Syst. Sci. 10, 165-179.

Breuer, L., Vaché, K.B., Julich, S., Frede, H.G., 2008. Current concepts in nitrogen dynamics for mesoscale catchment. Hydrol. Sci. J. 53, 1059-1074.

Brumme, R., Borken, W., Finke, S., 1999. Hierarchical control on nitrous oxide emission in forest ecosystems. Global Biogeochem. Cy. 13 (4), 1137-1148.

Canale, R.P.; Effler, S.W., 1989. Stochastic phosphorous model for Onondaga Lake. Water Res., 23, 1009-1016.

Carpenter, S.R., 2005. Eutrophication of aquatic ecosystems: biostability and soil phosphorus. Proceeding of the National Academy of Sciences of the United States of America, 102, 10002-10005.

Chaplot, V., 2005. Impact of DEM mesh size and soil map scale on SWAT runoff, sediment, and NO3-N loads predictions. J. Hydrol. 312, 207-222.

Chaubey, I., Cotter, A.S., Costello, T.A., Soerens, T.S., 2005. Effect of DEM data resolution on SWAT output uncertainty. Hydrol. Process. 19, 621-628.

Chen, F., Peng, B.Z., Bao, H.S., 2001. Responses of soil nutrient to driving mechanism in Taihu Lake basin in last 20 years. J. Geogr. Sci. 11 (1), 92-98.

Chen, M., Chen, J., Sun, F., 2008a. Agricultural phosphorus flow and its environmental impacts in China. Sci. Total Environ. 405(1-3): 140-152.

Chen, N.W., Hong, H.S., Zhang, L.P., Cao, W.Z., 2008b. Nitrogen sources and exports in an agricultural watershed in Southeast China. Biogeochemistry 87, 169-179.

Chen, X., Chen, Y.D., Xu, C.Y., 2007. A distributed monthly hydrological model for integerating spatial variations of basin topography and rainfall. Hydrol. Process. 21, 42-252.

Chen, X.Y., Mulder, J., 2007. Atmospheric deposition of nitrogen at five subtropical forested sites in South China. Sci. Total Environ. 378, 317-330.

Chow, V.T., Maidment, D.R., Mays, L.W., 1988. Applied hydrology McGraw-Hill, New York.

Ciarapica, L., Todini, E., 2002. TOPKAPI: a model for the representation of the rainfall-runoff process at different scales. Hydrol. Process. 16, 207-229.

De Roo, A.P.J., Offermans, R.J.E., Cremers, N.H.D.T., 1996. LISEM: a single event

physically-based hydrologic and soil erosion model for drainage Basins. II: sensitivity analysis, validation and application. Hydrol. Process. 10, 1118-1127.

De Roo, A.P.J., Wesseling, C.G., Van Deursen, W.P.A., 2000. Physically-based river basin modelling within a GIS: The LISFLOOD model. Hydrol. Process. 14, 1981-1992.

De Roo A.P.J., 2003. The simulation of two polders for flood protection in the German part of the Oder catchment. European Communities, EUR 20739 EN, Joint Research Centre, Ispra, Italy.

De Wit, M., 2000. Modelling nutrient fluxes from source to river load: a macroscopic analysis applied to the Rhine and Elbe basins. Hydrobiologia 410, 123-130.

Dean, S., Freer, J., Beven, K., Wade, A.J., Butterfield, D., 2009. Uncertainty assessment of a process-based integrated catchment model of phosphorus. Stoch. Environ. Res. Risk Assess. 23, 991-1010.

Ding, X.W., Shen, Z.Y., Hong, Q., Yang, Z.F., Wu, X., Liu, R.M., 2010. Development and test of the Export Coefficient Model in the Upper Reach of the Yangtze River. J. Hydrol. 383, 233-244.

Donigian, A.S., Bicknell B.R., Imhoff, J.C., 1995. Hydrological simulation program—Fortran (HSPF). In: V.P. Singh, Editor, Computer Models of Watershed Hydrology, WRP, Highlands Ranch, CO, USA, 395-442.

Donoso, G., Cancino, J., Magri, A., 1999. Effects of agricultural activities on water pollution with nitrates and pesticides in the central valley of Chile. Water Sci. Technol. 39(3), 49-60.

Du, J.K., Xie, S.P., Xu, Y.P., Xu, C.Y., Singh, V.P., 2007. Development and testing of a simple physically-based distributed rainfall-runoff model for storm runoff simulation in humid forested basins. J. Hydrol. 336, 334-346.

Eagleson, P.S., 1970. Dynamic Hydrology. McGraw Hill: New York.

Edwards, A.C., Withers, P.J.A., 2008. Transport and delivery of suspended solids, nitrogen and phosphorus from various sources to freshwaters in the UK. J. Hydrol. 350, 144-153.

Ellis, E.C., Wang, S.M., 1997. Sustainable traditional agriculture in the Taihu Lake Region of China. Agric. Ecosyst. Environ. 61, 177-193

Gao, C., Zhu, J.G., Zhu, J.Y., Gao, X., Dou, Y.J., Hosen, Y., 2004. Nitrogen export from an agriculture watershed in the Taihu Lake area, China. Environ. Geochem. Health 26, 199-207.

Gao, J.F., Lv, G.N., 2005. Hydrological modeling based on cartographical modelling: a case study on the Xitiaoxi watershed, upper reaches of Taihu Basin. J. Lake Sci. 17(4), 305-310.

Gao, J.F., Gao, Y.N., Zhao, G.J., Hörmann, G., 2010. Minimum ecological water depth of a typical stream in Taihu Lake Basin, China. Quatern. Int. 226, 136-142.

Granhall, U., 1981. Biological nitrogen fixation in relation to environmental factors and functioning of natural ecosystems, in P. Clark and T. Rosswall (eds), Terrestial Nitrogen Cycles, Vol. 33, Ecological Bulletin (Stockholm), pp. 131-144.

Grayson, R.B., Blöschl, G., 2000. (Eds) Spatial Patterns in Catchment Hydrology: Observations and Modelling. Cambridge University Press, Cambridge, UK, 404 pp.

Gundersen, P. Bashkin, V.N., 1994. (Eds) Nitrogen Cycling, John Wiley & Sons Ltd., Chichester, pp. 255-283.

Guo, H.Y., Wang, X.R. Zhu, J.G., 2004. Quantification and index of non-point source pollution in Lake Taihu region with GIS. Environ. Geochem. Health 26, 147-156.

Farenga, S.J., Daniel, N., 2007. Making a community information guide about nonpoint source pollution, Science Scope 30, 12-15.

Fohrer, N., Haverkamp, S., Frede, H.G., 2005. Assessment of the effects of land use patterns on hydrologic landscape functions: development of sustainable land use concepts for low mountain range areas. Hydrol. Process. 19, 659-672.

Förster, S., Kuhlmann, B., Lindenschmidt, K.E., Bronstert, A., 2008. Assessing flood risk for a rural detention area. Nat. Hazards Earth Syst. Sci. 8, 311-322.

Han, Y., Roelcke, M., Cai, Z.C., Richter, J., 2001. Development of an advisory model to reduce nitrogen losses in double cropping systems in the Taihu Region of China. In: Stoecker, B., Grosse, W., Li, W.H. (Eds) Ecosystem Service and Sustainable Watershed Management Towards Flood Prevention, Pollution Control, and Socio-Economic Development in North China. Proceedings of International Conference in China, Beijing, PR China, 23-25 August 2000. pp 411-419. Cologne, Germany.

Hart, R.H., Quin, B.F., Nguyen, M.L., 2004. Phosphorus runoff from agricultural land and direct fertilizer effects: a review. J. Environ. Qual. 33, 1954-1972.

Haverkamp, S., Fohrer, N., Frede, H.G., 2005. Assessment of the effect of land use patterns on hydrologic landscape functions: a comprehensive GIS-based tool to minimize model uncertainty resulting from spatial aggregation. Hydrol. Process. 19, 715-727.

Haygarth, P.M., Sharpley, A.N., 2000. Terminology for phosphorus transfer. J. Environ. Qual. 29, 10-15.

He, Z.L., Zhang, M.K., Stoffella, P.J., Yang, X.E., Banks, D.J., 2006. Phosphorus concentrations and loads in runoff water under crop production. Soil Sci. Soc. Am. J. 70, 1807-1816.

Hessel, R., Jetten, V., Liu, B.Y., Zhang, Y., Stolte, J., 2003. Calibration of the LISEM model for a small loess Plateau catchment. Catena 54, 235-254.

Hesselink, A.W., Stelling, G.S., Kwadijk, J.C.J., Middelkoop, H., 2003. Inundation of a Dutch river polder, sensitivity analysis of a physically based inundation model using historic data. Water Resour. Res. 39 (9), 1234.

Hu, Q.F., Wang, Y.T., 2009. Impact assessment of climate change and human activities on annual highest water level of Taihu Lake. Water Sci. Eng. 2 (1), 1-15.

Huang, S., Rauberg, J., Apel, H., Lindenschmidt, K.E., 2007. The effectiveness of polder systems on peak discharge capping of floods along the middle reaches of the Elbe River in Germany. Hydrol. Earth Syst. Sci. 11, 1391-1401.

Johnes, P.J., 1996. Evaluation and management of the impact of land use change to the nitrogen and phosphorus load delivered to surface waters: the export coefficient modelling approach. J. Hydrol. 183, 323-349.

Ju, X.T., Liu, X.J., Zhang, F.S., Roelcke, M., 2004. Nitrogen fertilization, soil nitrate accumulation, and policy recommendations in several agricultural regions of China. AMBIO 33(6), 300-305.

Koo, B.K., Dunn, S.M., Ferrier, R.C., 2005. A distributed continuous simulation model to identify critical source areas of phosphorus at the catchment scale: model description. Hydrol. Earth Syst. Sci. Discuss. 2, 1359-1404.

Koren, V., Reed, S., Smith, M., Zhang, Z., 2003. “Combining physically based and conceptual approaches in the development and parameterization of a distributed system.” Information from Weather Radar and Distributed Hydrological Modelling (Proceedings of symposium HS03 held during IUGG2003 at Sapporo, Japan, July 2003) IAHS publication, No. 282, 101-108.

Lai, G.Y., Yu, G., Gui, F., 2006. Preliminary study on assessment of nutrient transport in the Taihu Basin based on SWAT modelling. Sci. in China Ser. D Earth Sci. 49, 135-145.

Lenhart, T., Eckhardt, K., Fohrer, N., Frede, H.G., 2002. Comparison of two different

approaches of sensitivity analysis. Phys. Chem. Earth. 27, 645-654.

Li, H., Liang, X.Q., Cheng, Y.X., Tian, G.M., Zhang, Z.J., 2008. Ammonia volatilization from urea in rice fields with zero-drainage water management. Agric. Water Manage. 95, 887-894.

Li, H.P., Liu, X.M., Yang, G.S., 2004a. Nutrient pollutant load analysis of Xitiaoxi watershed in Taihu region. J. Lake Sci. 16, 89-98 (in Chinese with English abstract).

Li, Z.F., Yang, G.S., Li, H.P., 2009. Estimated nutrient export loads based on improved export coefficient model in Xitiaoxi watershed. Environ. Sci. 30(3), 668-672 (in Chinese with English abstract).

Li, Z.J., Ge, W.Z., Liu, J.T., Zhao, K., 2004b. Coupling between weather radar rainfall data and a distributed hydrological model for real-time flood forecasting. Hydrol. Sci. J. 49, 945-958.

Liang, T., Wang H., Rung H.T., Zhang C.S, 2004. Agriculture land-use effects on nutrient losses in West Tiaoxi Watershed, China. J. Am. Water Resour. Assoc. 40(6), 1499-1510.

Liang, T., Wang, S.N., Cao, H.Y., Zhang, C.S., Li, H.T., Li, H.P., Song, W.C., Chong, Z.Y., 2008. Estimation of ammonia nitrogen load from nonpoint sources in the Xitiao River catchment, China. J. Environ. Sci. 20, 1195-1201.

Liu, J.T., Chen, X., Zhang, J.B., Flury, M., 2009. Coupling the Xinanjiang model to a kinematic flow model based on digital drainage networks for flood forecasting. Hydrol. Process. 23, 1337-1348.

Liu, Y., Gupta, H.V., 2007. Uncertainty in hydrologic modelling: Toward in integrated data assimilation framework. Water Resour. Res. 43, w07401.

Liu, Z.Y., Martina, M.L.V., Todini, E., 2005. Flood forecasting using a fully distributed model: application of the TOPKAPI model to the Upper Xixian Catchment. Hydrol. Earth. Syst. Sci. 9(4), 347-364.

Loos, S., Middelkoop, H., van der Perk, M., van Beek, R., 2009. Large scale nutrient modelling using globally available datasets: A test for the Rhine basin. J. Hydrol. 369 (3-4), 403-415

Lu, G.H., Wu, Z.Y., Wen, L., Lin, C.A., Zhang, J.Y., Yang, Y., 2008. Real-time flood forecast and flood alert map over the Huaihe River Basin in China using a coupled hydro-meteorological modeling system. Sci. China Ser. E-Technol. Sci. 51, 1049-1063.

Luo, L.C., Qin, B.Q., Yang, L.Y., Song, Y.Z., 2007. Total inputs of phosphorus and nitrogen by

wet deposition into Lake Taihu, China. Hydrobiologia 581, 63-70.

Moore, I.D., Lewis, A., Gallant, J.C., 1993. Terrain attributes: Estimation methods and scale effects, in: Modeling change in environmental systems, edited by: Jakeman, A. J., Beck, M. B., McAleer, M. Wiley, New York, 189-214.

Ma, L., 1992. Pollution from agricultural non-point sources and its control in river system of Taihu Lake, Jiangsu. Chin. J. Appl. Ecol. 3(4), 346-354. (in Chinese with English abstract).

Martikainen, P.J., 1984. Nitrification in two coniferous forest soils after different fertilization treatments. Soil Biol. Biochem. 16, 577-582.

May, L., House, W.A., Bowes, M., McEvoy, J., 2001. Seasonal export of phosphorus from a lowland catchment: upper River Cherwell in Oxfordshire England. Sci. Total Environ. 269, 117-130.

Menzel, R.G., 1980. Enrichment ratios for water quality modeling. In: CREAMS - A field scale model for chemicals, runoff, and erosion from agricultural management systems, edited by: Knisel W G, USDA Conservation Research Report, No. 26, 486-492.

Nash, J.E., Sutcliffe, J.V., 1970. River flow forecasting through conceptual models, part I: A discussion of principles. J. Hydrol. 10(3), 282-290.

Neal, C., Robson, A.G., 2000. A summary of river water quality data collected within the Land-Ocean Interaction Study: core data for eastern UK rivers draining to the North Sea. Sci. Total Environ. 251/252, 585-665.

Neitsch, S.L., Arnold, J.G., Kiniry, J.R., Williams, J.R., King, K.W., 2002. Soil and Water Assessment Tool Theoretical Documentation. Version 2000. Texas Water Resources Institute, College Station, Texas. TWRI Report, TR-191.

Neitsch, S.L., Arnold, J.G., Kiniry, J.R., Srinivasan, R., Williams, J.R., 2005. Soil and Water Assessment Tool, Theoretical Documentation: Version 2005. USDA Agricultural Research Service and Texas A&M Blackland Research Center: Temple.

O'Callaghan, J.F., Mark, D.M., 1984. The extraction of drainage networks from digital elevation data, Comput. Vis. Graph. Image Process. 28, 323-344.

Pieterse, N.M., Bleuten, W., Jørgensen, S.E., 2003. Contribution of point sources and diffuse sources to nitrogen and phosphorus loads in lowland river tributaries. J. Hydrol. 271, 213-225.

Pistocchi, A., 2008. An assessment of soil erosion and freshwater suspended solid estimates for continental-scale environmental modelling. Hydrol. process. 22, 2292-2314.

Potter, K.M., Cubbage, F.W., Blank, G.B., Schaberg, R.H., 2004. A watershed-scale model for predicting nonpoint pollution risk in North Carolina. Environ. Manage. 34, 62-74.

Pullar, D., Springer, D., 2000. Towards integrating GIS and catchment models. Environ. Modell. Softw. 15, 451-459.

Qin, B.Q., Xu, P.Z., Wu, Q.L., Luo, L.C., Zhang, Y.L., 2007. Environmental issues of Lake Taihu, China. Hydrobiologia 581, 3-14.

Quinn, P., Beven, K., Chevallier, P., and Planchon, O., 1991. The prediction of hillslope flow paths for distributed hydrological modelling using digital terrain models, Hydrol. Process. 5, 59-79.

Quinton, J.N., Catt, J.A., Hess, T.M., 2001. The selective removal of phosphorus from soil: Is event size important? J. Environ. Qual. 30, 538-545.

Rankinen, K., Lepistö, A., Granlund, K., 2004. Integrated nitrogen and flow modelling (INCA) in a boreal river basin dominated by forestry: scenarios of environmental change. Water Air Soil Pollut. 4, 167-174.

Richter, J., Roelcke, M., 2000. The N-cycle as determined by intensive agriculture - examples from central Europe and China. Nutr. Cycl. Agroecosyst. 57, 33-46.

Roelcke, M., Han, Y., Cai, Z.C., Richter, J., 2002. Nitrogen mineralization in paddy soils of the Chinese Taihu Region under aerobic conditions. Nutr. Cycl. Agroecosyst. 63, 255-266.

Robinson, J.S., Sivapalan, M., 1995. “Catchment-scale runoff generation model by aggregation and similarity analysis.” Scale Issues in Hydrological Modeling, Kalma, J.D. and Sivapalan, M. eds., Wiley, New York, 311-330.

Santhi, C., Arnold, J.G., Williams J.R., Dugas, W.A., Srinivasan, R., Hauck, L.M., 2001. Validation of the SWAT Model on a Large River Basin With Point and Nonpoint Sources, J. Am. Water Resour. Assoc. 37, 1169-1188.

Schuol, J., Abbaspour, K.C., Srinivasan, R., Yang, H., 2008. Estimation of freshwater availability in the West African sub-continent using the SWAT hydrologic model. J. Hydrol. 352(1-2), 30-49.

Setegn, S.G., Dargahi, B., Srinivasan, R., Melesse, A.M., 2010. Modeling of sediment yield from Anjeni-gauged watershed, Ethiopia using SWAT model. J. Am. Water Resour. Assoc.

46(3), 514-526.

Sha, L., Meng, Y., Feng, Z., Zheng, Z., Cao, M., Liu, H., 2000. Studies of nitrogen mineralization and nitrification in different tropical forest soils in Xishuangbanna. Acta Ecol. Sinica 24, 152-156 (in Chinese with English abstract).

Sharpley, A.N., Rekolainen, S., 1997. Phosphorus in agriculture and its environmental implications. In Tunney, H., et al. (ed.) Phosphorus loss from soil to water. CABI Publ., Wallingford, UK. 1-53.

Sharpley, A.N., McDowell, R.W., Jennifer, L.W., Kleinman, J.A., 2001. Assessing site vulnerability to phosphorus loss in an agricultural watershed. J. Environ. Qual. 30, 2026-2036.

Sharpley, A.N., Kleinman, J.A., McDowell, R.W., Gitau, M., Bryant, R.B., 2002. Modelling phosphorus transport in agricultural watersheds: Processes and possibilities. J. Soil Water Conserv. 57, 425-439.

Sheikh, V., Visser, S., Stroosnijder, L., 2009. A simple model to predict soil moisture: Bridging Event and Continuous Hydrological (BEACH) modelling. Environ. Modell. Softw. 24, 542-556.

Singh, V.P., Woolhiser, D.A., 1996. A nonlinear kinematic wave model for watershed surface runoff. J. Hydrol. 31, 221-243.

Smith, R.E., Goodrich, D.C., Woolhiser, D.A., Unkrich, C.L., 1995. KINEROS - A KINematic Runoff and EROSion Model. In Singh, V.P., (Ed.), Computer Models of Watershed Hydrology, Water Resources Publications, Highlands Ranch, CO, USA; 697-732.

Smolander, A., Priha, O., Paavolainen, L., Steer, J., Mälkönen, E., 1998. Nitrogen and carbon transformations before and after clear-cutting in repeatedly N-fertilized and limed forest soil. Soil Biol. Biochem. 30, 477-490.

Su, B.L., Kazama, S., Lu, M.J., Sawamoto, M., 2003. Development of a distributed hydrological model and its application to soil erosion simulation in a forested catchment during storm period, Hydrol. Process. 17, 2811-2823.

Thorburn, P.J., Biggs, J.S., Weier, K.L., Keating, B.A., 2003. Nitrate in groundwater of intensive agricultural areas in coastal Northeastern Australia. Agric. Ecosyst. Environ. 94 (1), 49-58.

Tian, G.M., Cai, Z.C., Gao, J.L., Li, X.P., 2001. Factors affecting ammonia volatilisation from a rice-wheat rotation system. Chemosphere 42, 123-129.

Todini, E., 1996. The ARNO rainfall-runoff model. J. Hydrol. 175, 339-382.

Todini, E., Ciarapica, L., 2001. The TOPKAPI model. In Mathematical models of large watershed hydrology, Chapter 12, Singh, V.P. (Ed.). Water Resources Publications: Colorado, USA.

Torstveit, G., 2000. In situ nitrogen mineralization in sub-tropical forest soil near Guiyang City, China. Master thesis, Department of Soil and Water Sciences, Agricultural University of Norway.

Uhlenbrook, S., Roser, S., Tilch, N., 2004. Hydrological process representation at the meso-scale: the potential of a distributed, conceptual catchment model. J. Hydrol. 291, 278-296.

Van Deursen, W.P.A., 1995. Geographical information systems and dynamic models: development and application of a prototype spatial modelling language. PhD Thesis, Netherlands Geographical Studies. 190p.

Viney, N.R., Sivapalan, M., Deeley, D., 2000. A conceptual model of nutrient mobilisation and transport applicable at large catchment scales. J. Hydrol. 240, 23-44.

Van der Knijff, J., De Roo, A.P.J., 2008. LISFLOOD Distributed Water Balance and Flood Simulation Model, Revised user manual, Office for Official Publications of the European Communities, Luxembourg, EUR 22166 EN/2.

Van Deursen, W.P.A., 1995. Geographical Information Systems and Dynamic Models: development and application of a prototype spatial modelling language. Netherlands Geographic Studies, Issue 190.

Vieux, B., Needham, H., 1993. Nonpoint pollution model sensitivity to grid cell size, J. Water Resour. Planning Manage. 119(2), 141-157.

Wade, A.J., Durand, P., Beaujouan, V., Wessel, W.W., Raat, K.J., Whitehead, P.G., Butterfield, D., Rankinen, K., Lepisto, A., 2002a. A nitrogen model for European catchments: INCA, new model structure and equations. Hydrol. Earth Syst. Sci. 6, 559-582.

Wade, A.J., Whitehead, P.G., Butterfield, D., 2002b. The Integrated Catchment model of Phosphorus dynamics (INCA-P), a new approach for multiple source assessment in heterogeneous river systems: model structure and equations. Hydrol. Earth Syst. Sci. 6, 583-606.

Wang, G.Q., Hapuarachchi, P., Ishidaira, H., Kiem, A.S., 2009. Estimation of soil erosion and sediment yield during individual rainstorms at catchment scale. Water Resour. Manage. 23,

1447-1465.

Wang, J.Q., Zhang, X.Y., Lu, Z.H., 2004a. Digital hydrological model of Qinhuai River basin and its application. Shuili Xuebao 4, 1-7 (in Chinese).

Wang, X.L., Lu, Y.L., Han, J.Y., He, G.Z., Wang, T.Y., 2007. Identification of anthropogenic influences on water quality of rivers in Taihu watershed. J. Environ. Sci. 19, 475-481.

Wang, X.J., Zhang, W., Huang, Y.N., Li, S.J., 2004b. Modeling and simulation of point-non-point source effluent trading in Taihu Lake area: perspective of non-point sources control in China. Sci. Total Environ. 325, 39-50.

Wang, X.Z., Zhu, J.G., Gao, R., Hosen, Y., 2004c. Danamics and ecological significance of nitrogen wet-deposition in Taihu Lake region-taking Changshu agroecological experiment station as an example. Chin. J. Appl. Ecol. 15, 1616-1620 (in Chinese with English abstract).

Wechsler, S. P.: Uncertainties associated with digital elevation models for hydrologic applications: a review, Hydrol. Earth Syst. Sci, 11, 1481-1500, 2007.

Wesseling, C.G., Karssenberg, D.J., Burrough, P.A., Van Deursen, W.P.A., 1996. Integrated dynamic environmental models in GIS: the development of a dynamic Modelling language. Transactions in GIS 1-1, 40-48.

Whitehead, P.G., Toms, I.P., 1993. Dynamic modelling of nitrate in reservoirs and lakes. Water Res. 27, 1377-1384.

Whitehead, P.G., Wilson, E.J., Butterfield, D., 1998a. A semi-distributed Integrated Nitrogen Model for Multiple source assessment in Catchments (INCA): Part I - model structure andprocess equations. Sci. Total Environ. 210/211, 547-558.

Whitehead, P.G., Wilson, E.J., Butterfield, D., Seed, K., 1998b. A Semi-distributed Integrated Nitrogen Model for Multiple source assessment in Catchments (INCA): Part II - Application to large River Basins in South Wales and Eastern England. Sci. Total Environ. 210/211, 559-583.

Williams, J.R., 1975. Sediment-yield prediction with universal equation using runoff energy factor. In Present and Prospective Technology for Predicting Sediment Yield and Sources. Proceedings of the Sediment Yield Workshop, Oxford, MS, 244-252.

Williams, J.R., Nicks, A.D., Arnold, J.G., 1985. Simulator for water resources in rural basins. J. Hydrol. Eng. 111, 970-986.

Wu, S., Li, J., Huang, G.H., 2008. Characterization and Evaluation of Elevation Data Uncertainty in Water Resources Modeling with GIS, Water Resour. Manage. 22, 959-972.

Xing, G.X., 1998. N_2O emission from cropland in China. Nutr. Cycl. Agroecosyst. 52(2-3), 249-254

Xing, G.X., Cao, Y.C., Shi, S.L., Sun, G.Q., Du, L.J., Zhu, J.G., 2001. N pollution sources and denitrification in waterbodies in Taihu Lake region. Sci. China Ser. B 44, 304-314.

Xu, L.G., Zhang, Q., Li, H.P., Viney, N.R., Xu, J.T., Liu, J., 2007. Modeling of surface runoff in Xitiaoxi catchment, China. Water Resour. Manage. 21(8), 1313-1323.

Xu, Q.F., Jiang, P.K., Xu, Z.H., 2008. Soil microbial functional diversity under intensively managed bamboo plantations in southern China. J. Soils Sediments 8, 177-183.

Yao, C, Li, Z.J., Bao, H.J., Yu, Z.B., 2009. Application of developed Grid-Xinanjiang model to Chinese watersheds for flood forecasting purpose. J. Hydrol. Eng. Doi:10.1061/(ASCE) HE. 1943-5584. 0000067.

Young, R.A., Onstad, C.A., Bosch D.D., Anderson, W.P., 1989. Agricultural non-point source pollution model for evaluating agricultural watersheds, J. Soil Water Conserv. 44 (2), 168-173.

Yu, G., Xue, B., Lai, G.Y., Gui, F., Liu, X.M., 2007. A 200-year historical modelling of catchment nutrients changes in Taihu basin, China. Hydrobiologia 581, 79-87.

Young, R.A, Onstad, C.A., Bosch, D.D., Anderson, W.P., 1989. Agricultural non-point source pollution model for evaluating agricultural watersheds. J. Soil Water Conserv. 44(2), 168-173.

Yu, G., Xue, B., Lai, G.Y., Gui, F., Liu, X.M., 2007. A 200-year historical modelling of catchment nutrients changes in Taihu basin, China. Hydrobiologia 581, 79-87.

Zalidis, G., Stamatiadis, S., Takavakoglou, V., Eskridge, K., Misopolinos, N., 2002. Impacts of agricultural practices on soil and water quality in the Mediterranean region and proposed assessment methodology. Agric. Ecosyst. Environ. 88 (2), 137-146.

Zhang, Q., Li, H.P., Xu, L.G., 2006. Surface runoff modelling for Xitiaoxi catchment, Taihu Basin, J. Lake Sci. 18 (4), 401-406 (in Chinese with English abstract).

Zhang, Q., Werner, A.D., 2009. Integrated surface-subsurface modeling of Fuxianhu Lake catchment, southwest China. Water Resour. Manage. 23, 2189-2204.

Zhang, W, Wang X J, Jiang Y C, Zhou X W, 2001. Effect of emission control on water quality of

the Taihu Lake. Rural Ecol-Environment 17, 44-47.

Zhao, G.J., Hörmann, G., Fohrer, N., Gao, J.F., 2009. Impacts of spatial data resolution on simulated discharge, a case study of Xitiaoxi catchment in South China. Adv. Geosci. 21, 131-137.

Zhao, G.J., Hörmann, G., Fohrer, N., Gao, J.F., Li, H.P., Tian, P., 2011a. Application of a simple raster-based hydrological model for streamflow prediction in a humid catchment with polder systems. Water Resour. Manage. 25, 661-676.

Zhao, G.J., Hörmann, G., Fohrer, N., Li, H.P, Gao, J.F., 2011b. Development and application of a nitrogen simulation model in a data scarce catchment in South China. Agric. Water Manage. 98, 619-631.

Zhao, R.J., Zhuang, Y.L., Fang, L.R., Liu, X.R., Zhang, Q.S., 1980. The Xinanjiang model. Hydological Forescasting. IAHS publication 129. IAHS press, Wallingford, 351-356.

Zhao, R.J., 1984. Water Hydrological Modelling - Xinanjiang Model and Shanbei Model. China Water Resources and Hydropower Press: Beijing, China (in Chinese).

Zhao, R.J., 1992. The Xinanjiang model applied in China. J. Hydrol. 135, 371-381.

Zhou, C., 2000. Regional Nitrogen Cycling of Forest Ecosystems in China. Ph.D. thesis, Institute of Geographic Science and Natural Resources, Chinese Academy of Sciences (in Chinese with English abstract).

Zhu, J.G., Han, Y., Liu, G., Zhang, Y.L., Shao, X.H., 2000. Nitrogen in percolation water in paddy fields with a rice/wheat rotation. Nutr. Cycl. Agroecosyst. 57, 75-82.

Zhu, Z.L., 1997. Nitrogen balance and cycling in agroecosystems of China. In: Zhu Z.L. et al. (eds) Nitrogen in soil of China. Kluwer Academic Publishers, Dordrecht/Boston/London, pp. 323-330.

Zhu, Z.L., Wen, Q.X., 1992. Nitrogen in soils of China. Jiangsu Science and Technology Publishing House, Nanjing, China (in Chinese)

Zhu, A.N., Zhang, J.B., Zhao, B.Z., Cheng, Z.H., Li, L.P., 2005. Water balance and nitrate leaching losses under intensive crop production with Ochric Aquic Cambossols in North China Plain. Environ. Int. 31, 904-912.

Acknowledgements

This dissertation summarizes more than three years of my work in the field of numerical simulation in hydrological processes and nutrient dynamics in the Department of Hydrology and Water Resources Management, Institute for the Conservation of Natural Resources, Christian-Albrechts-Universität zu Kiel

During my PhD, I had a pleasant experience and lots of support from many different people, all of which deserve my gratitude. First of all, I would like to thank my supervisors Professor Dr. Nicola Fohrer and Dr. Georg Hörmann for giving me the opportunity to work on an inspiring subject with all the scientific freedom and support one could wish for.

The discussions with my colleagues in Kiel contributed to a big extent to the progress of this work. Their helpfulness, qualifications and collaboration as well as the good working atmosphere will always remain in my mind. Especially thanks should be given to Jens Kiesel who translated the summary of the thesis to German, and always patiently discussed the questions I met.

My utmost gratitude goes to Deutscher Akademischer Austausch Dienst (DAAD) for providing the opportunity to work in the project “Studies and Research in Sustainability” and funding me studying in Kiel for more than three years.

I would also like to thank several Chinese professors, Junfeng Gao, Hengpeng Li, Tong Jiang and Qinghua Cai, who as well discussed the questions about the thesis with me and provided sufficient support for my field campaign and data collection.

Finally, I am most grateful for the support of my family for all the support they have given me over the years. I especially thank my wife Peng Tian for her understanding and support, particularly in the last few months, when I was occupied too much with finalizing my thesis.

Kiel, 2011 Guangju Zhao

Erklärung

Hiermit erkläre ich, dass ich die vorliegende Dissertation, abgesehen von der Beratung durch meine akademischen Lehrer, selbstständig verfasst habe under keine weiteren Quellen und Hilfsmittel als die hier angegebenen verwendet habe. Diese Arbeit hat weder ganz, noch in Teilen, bereits an anderer Stelle einer Prüfungskommission zur Erlangung des Doktorgrades vorgelegen. Ich erkläre, dass die vorliegende Arbeit gemäß der Grundsätze zur Sicherung guter wissenschaftlicher Praxis der Deutschen Forschungsgemeinschaft erstellt wurde.

Kiel, 3 January, 2011

(Guangju Zhao)